UNIVERSIDADE DE ÉVORA

SCHOOL OF SCIENCE AND TECHNOLOGY

DEPARTAMENT OF PHYSICS

Modelization and Characterization of Photovoltaic Panels

Md Tofael Ahmed

Supervisor: Mouhaydine Tlemçani, Ph.D.

Co-supervisor: Teresa Cristina de Freitas Gonçalves, Ph.D.

Masters in Solar Energy Engineering

Dissertation

Évora, 2017

Modelização e Caracterização de Panéis Fotovoltaicos

Dissertação realizada em regime de coorientação sob orientação do

Doutor Mouhaydine Tlemçani

e sob orientação do

Doutora Teresa Cristina de Freitas Gonçalves

Respetivamente, Professor Auxiliar

e

Professor Auxiliar

Departamento de Física

Escola de Ciências e Tecnologia

UNIVERSIDADE DE ÉVORA

ABSTRACT

This work presents the characterization and modelization of photovoltaic panels in order to study their behaviors. Its purpose is to obtain an enhanced and more efficient parameters model of PV. It describes and implements their physical modeling and mathematical modeling. The effects of external and internal parameters variation on the panel is analyzed and briefly discussed. The produced model can be used for measuring and understanding the actions of photovoltaic cells for certain changes and parameters extraction. The white noise effect and its related output characteristics are explained. The curve fitting approximation with different polynomial method is shown. A non-iterative MPPT algorithm is proposed and implemented also. The simulation is achieved by using MATLAB and SIMULINK programming. An experimental work is also done in order to get the closure and insight about the produced model and to decide upon the validity of the discussed model and algorithm.

Keywords: Photovoltaic, DSP, instrumentation, noise, MPPT.

RESUMO

O presente trabalho consiste na modelação e caracterização de painéis fotovoltaicos para estudar os seus comportamentos. Neste trabalho, propõe-se obter uma estimativo eficiente dos parâmetros que caracterizam o painel fotovoltaico. A modelação física e matemática do painel é descrita e implementada. O efeito que a variação dos parâmetros internos e externos apresenta é analisado e discutido. O modelo construído poderá ser utilizado para obter e compreender a descrição das células fotovoltaicas para determinadas variações, e para a obtenção de parâmetros. O efeito do ruído branco gaussiano e a potência resultante que lhe está associada são analisados. É implementado um ajuste da curva característica com diferentes métodos polinomiais. As simulações são realizadas recorrendo a programação em MATLAB e SIMULINK. É realizada uma experiência laboratorial como forma de conclusão da aplicação do modelo, de forma a poder analisar a validação do modelo e do algoritmo estudados.

Palavras-chave: Fotovoltaico, DSP, instrumentação, ruído, MPPT.

ACKNOWLEDGMENTS

I would like to sincerely thank all of the people who directly or indirectly contributed to make this dissertation.

Foremost, I would like to express my sincere gratitude and thanks to my supervisor Professor Dr. Mouhaydine Tlemçani for his continuous support by providing great contribution, suggestion and motivation which are the main pillars of making the dissertation successful. His guidance helped me in all the time of research and writing of this thesis. I could not have imagined having a better advisor and mentor for my research. I also like to express my gratitude to my co-supervisor Professor Drª. Teresa Gonçalves for the continuous support of my masters study and research, for her patience, motivation, enthusiasm and immense knowledge. It is a great pleasure working with her.

A very special thanks goes to Professor Dr. António Heitor Reis for all of his unforgettable help in every steps of my masters study.

I also gratefully thank to the Erasmus Mundus 'LEADER' project for the funding of the work, ICT (Institute of Earth Sciences) of University of Évora for the help and space provided to enable the work. I am very thankful to André Albino, Masud R. Rashel, Ana Foles, Germilly Barreto, Isaias Gomes, Fahad Israr, Sergio Aranha and all other friends and colleagues who have motivated and supported me during the work.

Finally, my deepest gratitude goes to my parents, my wife Tania Tanzin Hoque and all of the family members for their extraordinary support and constant encouragement.

CONTENTS

LIST OF FIGURES

LIST OF TABLES

NOMENCLATURE

CO_2	Carbon dioxide [ppm]
GaAs	Gallium arsenide [g/cm^3]
HgTe	Mercury Telluride [g/cm^3]
Ge	Germanium [g/cm^3]
ZnS	Zinc Sulfide [g/cm^3]
Cu_2O	Cuprous Oxide [g/cm^3]
N_A	Acceptor atoms [-]
N_D	Donor atoms [-]
D	Diffusion coefficient [-]
L	Length [m]
E_G	Band gap energy [eV]
n	Refractive index [-]
E_v	Valence band [-]
E_c	Conduction band [-]
E_g	Energy gap [eV]
T	Lifetime [s]
n_i	Intrinsic semiconductor
K	Boltzmann constant [JK^{-1}]
E_F	Fermy energy [eV]
h	Planck´s constant [J.s]
m_h	Effective mass of a hole [kg]
m_e	Effective mass of na electron [kg]
V_t	Thermal voltage [V]
I_s	Saturation current [A]
I_{ph}	Photo Current [A]
I_r	Irradiance [Wm^{-2}]
$I_{ph,ref}$	Referred photo current [A]
T_{amb}	Ambient temperature [ºC]
R_s	Series Resistance [Ω]
V_{oc}	Open circuit voltage [V]
I_{sc}	Short circuit current [A]

R_{sh}	Shunt Resistance [Ω]
I_{mp}	Current at maximum point [A]
V_{mp}	Voltage at maximum point [V]
N	Diode ideality factor [-]
P_{mp}	Power at maximum point [W]
K_i	Temperature coefficient [A/ºC]
T_{nom}	Nominal temperature [ºC]
4^{th}	Fourth [-]

GREEK LETTERS

μ	Diffusion mobility [-]
$h\nu$	Photon energy [J]
α	Absorption coefficient [-]
α'_T	Relative temperature coefficient [$ºC^{-1}$]
α_T	Absolute temperature coefficient [A/ºC]

ACRONYMS

PV	Photovoltaic
P&O	Perturb and Observe
MPPT	Maximum Power Point Tracking
MPP	Maximum Power Point
NOCT	Nominal Operating Cell Temperature
FF	Fill Factor
DAQ	Data Acquisition
DC	Direct Current
NI	National Instrument
USB	Universal Serial Bus
GPIB	General Purpose Interface Bus

Chapter 1. INTRODUCTION

1.1 INTRODUCTION

The capacity of a physical or biological system for change in a quantity is termed as Energy. The forms of energy can be mechanical energy, electrical energy, chemical energy, light energy etc. For every human activity it is required energy. For the growth of new industries and latest technologies the demand of energy is increasing. The dominant source of today's energy is coal, oil and gas which are known as fossil fuels. Those sources of fossil fuels are being used traditionally from ancient time. Due to the increasing demand, after the World War II the nuclear energy started as an alternative and new source of energy [1].

The total primary energy production by 2015 is presented on Figure 1.1; it is found that the global primary production increases by 2015 is 0.8 % [2]. If we look at the figure we see that the energy production has an increasing tendency from the year 2000 to 2015. Nonetheless, the consumption is also increasing day by day.

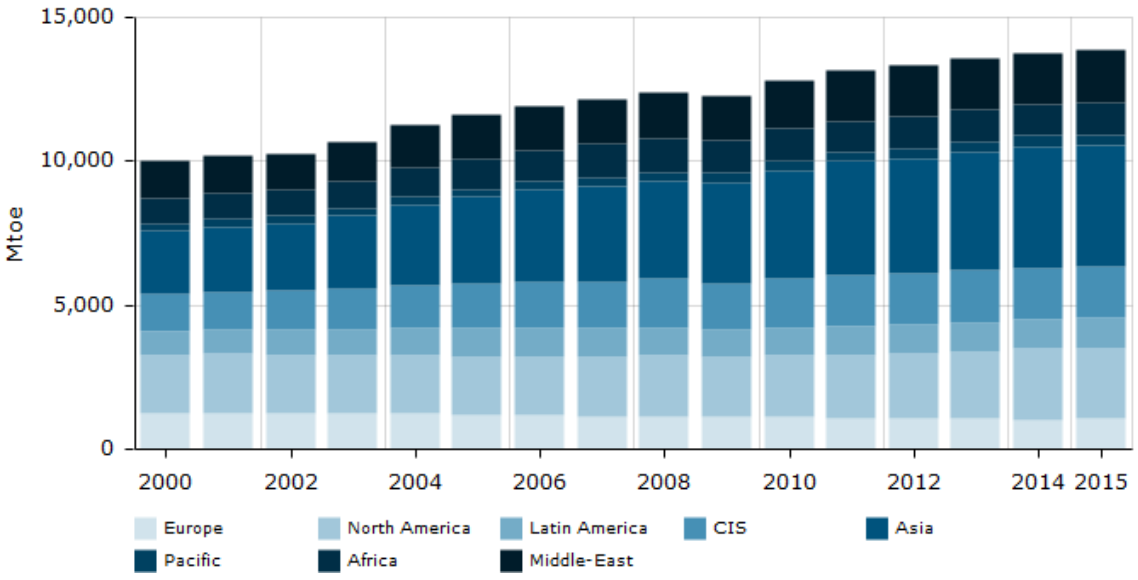

Figure 1.1: Total energy production by 2015 statistics. **[2]**

In a statistics it is found that the world population will reach up to 10 billion in 2050 [1]. It is important to assure the high living standard by economical growth of the world growing population. For that we have to produce more energy by creating other sources. Now a days the major issues in the world are energy crisis and climate change. The change in climate and other environmental issues are occurring due to the use of fossil fuels in the industry mainly.

In order to reduce those problems we have to look for the renewable and sustainable energy production systems. Introducing and developing new energy producing systems can overcome the ongoing and upcoming problems. These sources of energy are very clean, abundant, and economical and they do not have any harmful impact on the environment as those sources do not emit CO2 gases [3].

The renewable energy sources are solar, wind, hydro geothermal, tidal and biomass energies. They are contributing with 22% to the total energy production in the world [1]. The important issues like global warming, environmental pollution, energy crisis and reduction of fossil fuels as energy can be solved through the development of sustainable energy systems. These energy sources are considered green, environment friendly and inexhaustible from the point of view of human civilization.

The main advantages of these energy sources over the traditional ones are reflected in a healthy effect on climate, no carbon emission and creation of new employment for the people. That's why these sources of energy are growing rapidly. The energy production by this way can provide security of energy supply as consumers do not have to be dependent on any other source rather than natural resources [1].

Figure 1.2 shows the map of solar energy of the world. It indicates the sunlight intensity of the countries and continents in the world. Currently, China is considered the best country currently among all renewable energy investment ones. On the other side, because of the available sunlight, India has a great potential in the solar energy production. Some other countries are also on the top are Sweden, Denmark, Philippines, Brazil and the United States of America [4]. In a research it is found that the light amount the sun emits to the Earth is equivalent to the total energy consumed by us in a year [3]. The sun delivers 1.2×10^{14} kW power on Earth which is about 10000 times more than the present energy consumption.

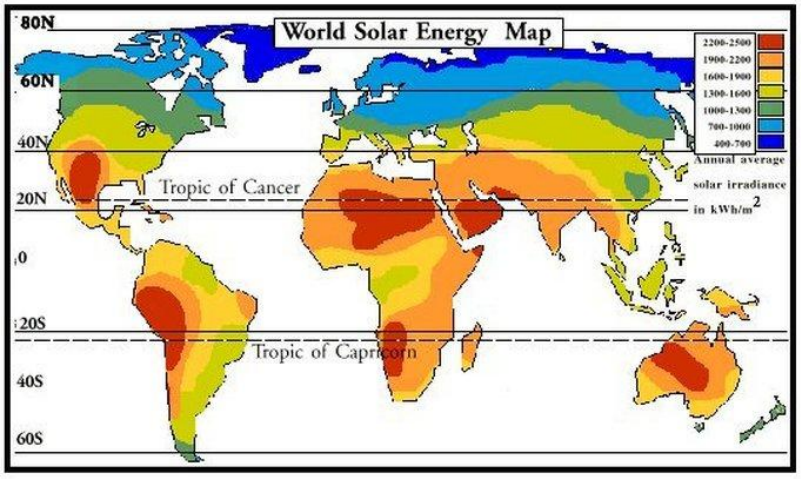

Figure 1.2: Map of the World solar energy. [5]

The main benefit of the solar energy production is that it can occur without any consumption of fossil fuels, harmful noise and without any negative impact to the environment.

To ensure future carbon emission reduction and a sustainable environment for humankind we need to use the solar energy in electricity production. It also can be used for cooling, heating, lighting, transportation and environmental cleaning. It can also be used for drying of food, rice, green house production, etc. It is found that the global average solar radiation, per m^2/year can produce the same amount of energy as 200 kg of coal, 140 m^3 of natural gas or a barrel of oil.

By the end of 2015, global installed capacity of solar-powered electricity reached around 227 GWe. The solar-powered electricity installed capacity is increasing exponentially. The solar-powered electricity production is 1% of the all electricity used globally. The leading countries in solar energy technologies are Germany, China, Italy and the United States. There are two main types of solar energy technologies: photovoltaic energy and thermal energy [5].

Solar energy electricity production can be obtained by two processes:

- Direct electricity conversion from sunlight by using semiconductor devices named solar cells.
- Heat accumulation in solar collectors.

Nonetheless, the electricity production and use of solar energy depends on the availability of solar resource and solar installed capacity.

Figure 1.3 shows the Solar installed capacity by region. The top value is from Europe with 43.7%, then East-asian countries with 35.2%. The next regions are North America, south East Asia and pacific, south and central Asia, Africa, Latin America & the Caribbean and Middle East and North Africa.

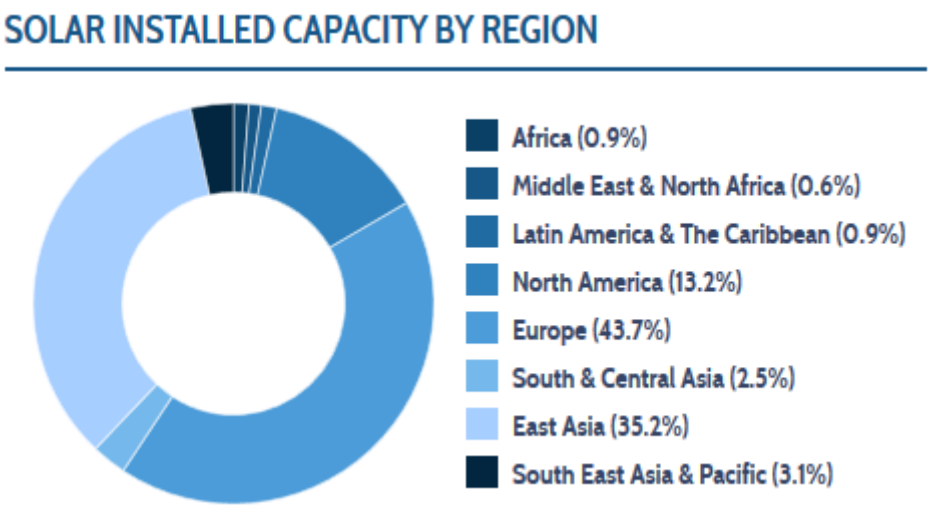

Figure 1.3: Solar installed capacity by region. **[5]**

Photovoltaic technology has been developed in recent years. The reason for the rapid growth of solar photovoltaic technology is that it is long lasting, maintenance free and environment friendly. Even though there is variability in solar radiation and environmental parameters which causes random power output, it is becoming more and more popular due to its flexibility [6]. The technological and environmental benefits are a blessing for the humankind. A photovoltaic (PV) system converts electricity using PV cells. The grouping of cells may be from panels or arrays in the system. The main unit of a PV system is the photovoltaic cell.

There are three types of solar photovoltaic cells in the market today. They are monocrystalline silicon, polycrystalline silicon and thin film technology. The monocrystalline silicon cell is the traditional technology in the solar PV system; monocrystalline modules are formed by assembled cells and those are produced by cutting a piece of continuous crystal.

The composition of polycrystalline solar cell is almost the same as monocrystalline except that instead being grown into a single crystal, it is melted and poured into a mold.

The thin films cells are known as amorphous silicon, which means they are not crystalline. The active material can be silicon or may be a more exotic material like cadmium telluride for example. By using plastic glazing it can be more lightweight and flexible. The commercial production of solar cells is shown in the figure 1.4. From the chart we can see that monocrystalline and polycrystalline are the most produced solar cells.

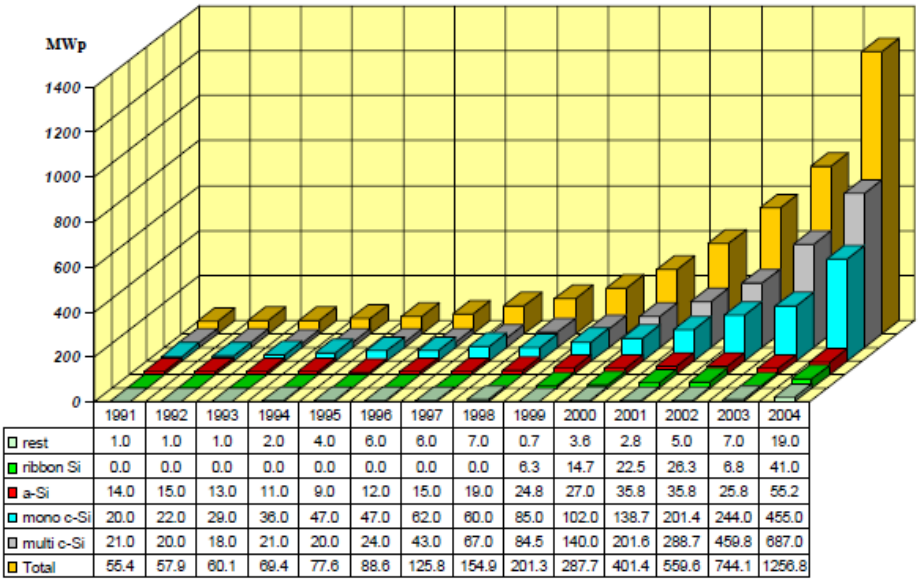

	1991	1992	1993	1994	1995	1996	1997	1998	1999	2000	2001	2002	2003	2004
rest	1.0	1.0	1.0	2.0	4.0	6.0	6.0	7.0	0.7	3.6	2.8	5.0	7.0	19.0
ribbon Si	0.0	0.0	0.0	0.0	0.0	0.0	0.0	0.0	6.3	14.7	22.5	26.3	6.8	41.0
a-Si	14.0	15.0	13.0	11.0	9.0	12.0	15.0	19.0	24.8	27.0	35.8	35.8	25.8	55.2
mono c-Si	20.0	22.0	29.0	36.0	47.0	47.0	62.0	60.0	85.0	102.0	138.7	201.4	244.0	455.0
multi c-Si	21.0	20.0	18.0	21.0	20.0	24.0	43.0	67.0	84.5	140.0	201.6	288.7	459.8	687.0
Total	55.4	57.9	60.1	69.4	77.6	88.6	125.8	154.9	201.3	287.7	401.4	559.6	744.1	1256.8

Figure 1.4: Solar cell commercial production per technology. **[1]**

1.2 LITERATURE REVIEW

Energy is a basic need for civilization and for the development of the society. In the book of Zeman [1] the increasing demand of energy, the primary and traditional source of energy, the prediction of upcoming renewable energy demand and the vast usefulness of the energy are explained clearly.

In order to have a clear idea about the current situation of energy production we studied the report from Enerdata [2]. The advantages of using renewable energy sources and disadvantages of using fossil fuels are stated in the work of Pranahita et al [3]. They [3]- [7] also discussed about the huge scope of solar energy in the Earth. The report of 'International Energy Partnership' [4] mentions the top countries with potential solar energy production. Before

starting the study and characterization of PV cell it is important to have wide idea about different types of cell. The types are explained in the report of REN 21 [5].

In chapter 2 we analyse and discuss mainly photovoltaic systems & technology, the PV system classification and modelling and solar PV characteristics. Sera [8], Tarek et al [9]and, Ma et al [7] describe different types of cell models like, for example, single diode model and double diode model.

We discuss semiconductor and its properties also in chapter 2. In NCERT report [10] semiconductor is discussed and in Zeman's book [11] they mention the typical structure of a solar cell. In the paper of Hu [12] they explain electrons and holes in semiconductor and in William et al [13] they clarify the p-n junction of solar cells. In the paper of Lu [14] various types of diodes, its applications and relationship with I-V and P-V characteristics are described.

After analyzing the different types of models we discuss the various external and internal parameters of the PV cell. All parameters are explained briefly in the paper of Tian et al [15], Masters and Gilbert [16] and Soto et al [17]. For PV cell modeling purpose it is necessary to know the parameters and its characteristics. In the paper of Rodrigues et al [18] they analyze the PV cell ideal model, several parameters variation effects and also the single diode simple model. Before starting the characterization we started to analyse different types of PV cell models. In this paper of Dolara [19] the single diode simple model is characterized, I-V characteristics of that model are presented and different physical models are compared.

In chapter 3 we discuss the PV system modelling, PV cell characterization, parameters extraction, and parameters variation effect with simulated and measured data. In the paper of Ahmed et al [20], Salmi et al [21], Ahmed et al [22] the single diode model of PV cell is used to characterize the solar photovoltaic cell. We explain the reason for using a numerical solution for modelling we start with the mathematical model and then figure out the parameters extraction from five parameters model. A vast parameters extraction process is discussed in this paper of Sera et al [23].

Then, we describe the parameters variation effects on solar photovoltaic cell. Firstly, we considered the external parameters for simulation purpose like variation of solar radiation and temperature. The external parameters variation effects are specifically stated in the paper of Mostafa and Naderi [24] , in Salim et al [25] and Islam et al [26] paper. We present a brief study and simulation of internal parameters variation effects on a PV cell also. Chenni et al [27],

Longatt and Francisco [28], Kachiya and Lokhande [29], Ahmed et al [20], Salmi et al [21] discuss in detailed the MATLAB modeling for various external parameters. We consider two numerical solution and its characteristics for the model. In the paper of Ana et al [30] the various characteristics for convergence speed optimization of iterative methods are described.

In order to obtain the I-V and P-V curve from measured data, we worked with a Data Acquisition System (DAQ) (using signal generator) and a General Purpose Interface Bus (GPIB). We took two samples in order to have more accuracy on measuring. We obtained related output figures characteristics using MATLAB from measured data.

In chapter 4, we discuss noise analysis for different situations of a PV cell, curve fitting approximation by more than one polynomial fitting method and, more importantly, we discuss and use a non-iterative MPPT algorithm method. Ahmed et al [31] describe the noise data approximation on various conditions and curve fitting of different order of a PV cell. Esram and Chapman [32] discuss different Maximum Power Point Tracking (MPPT) techniques. All the techniques are taken by reviewing the earliest literature.

In the paper of Hamidon et al [33] perturb and observe (P&O) MPPT algorithm in MATLAB with photovoltaic array modelling is described. Ahmed et al [34] describe a non-iterative algorithm for MPPT finding of a PV cell. MPPT finding by positioning the points on power-voltage curve is also discussed.

1.3 AIM OF THE DISSERTATION

The aim of this dissertation is to contribute to the research and development of the solar photovoltaic system technology. The main purpose is to increase the effective efficiency of PV panels by adding new features and making significant changes in the solar photovoltaic technology. The characterization and modelization of PV modules, important to increase the effectiveness of their devices, is the main motivation of the dissertation. A proposal and implementation of maximum power point tracking (MPPT) algorithm is discussed in order to track the maximum power point (MPP) for having an efficient PV technology.

1.4 OUTLINE OF THE DISSERTATION

The dissertation is structured in five chapters organized as follows:

In **Chapter 1**, a general introduction of renewable energy and specifically solar photovoltaic system are presented with statistical data. A brief literature review is given and explained.

Chapter 2 presents an overview of PV systems and technologies with its modelling and cell characteristics. Semiconductor properties, the PV effects with solar cell technology and several mathematical and physical model of PV cell are discussed here.

Chapter 3 gives the outline of measurement and characterization of PV panels. PV system modelling with description of characterization is described here. Parameters variation effect for several parameters like solar radiation, temperature, series resistance, shunt resistance and diode ideality factor is shown. Measurement with data acquisition and an experimental test results are considered for the characterization.

Chapter 4 is composed of noise analysis, curve fitting method and MPPT algorithm. Noise effects on I-V and P-V curves are analysed. A curve fitting algorithm with several polynomial methods is used. A non-iterative MPPT method is proposed and implemented here.

In **Chapter 5** the main conclusions are presented. Future research and improvement with suggestions are proposed.

Chapter 2. PHYSICAL & MATHEMATICAL MODEL ANALYSIS OF PV PANEL

2.1 PHOTOVOLTAIC SYSTEMS & TECHNOLOGIES

Photovoltaic systems are the composition of several interconnected components. They are designed to fulfill specific purposes like powering small devices in off-grid solar system where electricity (grid line) is difficult to access. Also, they are used to feed the electricity into the main distribution grid [35]. According to the use of solar photovoltaic system, they can be classified into two different types: grid-connected solar PV system and stand-alone solar PV system.

The other general subtypes are described and classified in the figure 2.1. The significant difference between the two types is that in a stand-alone system the photovoltaic energy and load demand are in phase but in a grid-connected one they are not in phase. Grid-connected systems are divided into direct and indirect systems; stand-alone systems are divided into with storage, without storage and hybrid system. In stand-alone systems, batteries are used for storage mostly; hybrid systems use other power sources like wind or diesel generator in combination with photovoltaic system.

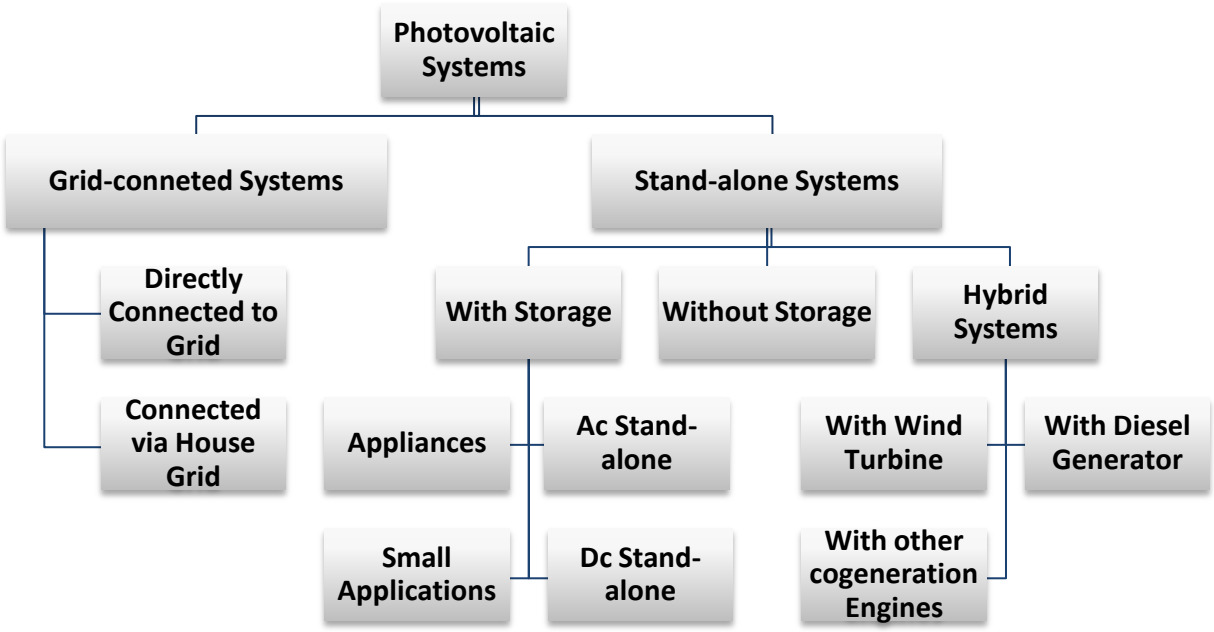

Figure 2.1: Classification of Photovoltaic Systems Technology.

2.1.1 Modeling of PV Systems

To predict the behavior and power output of a PV cell, modeling is mostly necessary and greatly important. The prediction is required in a PV system for various internal and external parameters conditions [8]. The environmental parameters like irradiance and temperature are considered external parameters.

Wind, humidity, dust can also be considered as environmental parameters in a greater context. Attention is given mostly on the behavior of the current-voltage (I-V) and power-voltage (P-V) curve in order to achieve the maximum output power. The main purpose of modelling is to produce I-V and P-V curves, obtaining maximum power output using a generalized model, module effectiveness on a PV system, its characterization and analysis of the performance under different PV panel behaviors.

2.1.2 Solar PV Cell Characteristics

The basic unit of an electrical energy production system using solar energy is termed as solar cell. It produces electrical energy without using any intermediate process. The working procedure of a solar cell depends on the photovoltaic effect. Hence, a solar cell is also known as photovoltaic cell. The electricity production procedure of PV cell relies on the photoelectric effect and the key ingredient of a solar cell is the semiconductor. The mostly used semiconductor for PV cell is silicon.

The basic properties of silicon that makes it the main component of a solar cell are the metal properties and some of those of an electrical insulator. Now a-days, almost all the solar cells electricity production mechanism; like absorption of photons that results in the generation of the charge carriers, and subsequent separation of the photo-generated charge carriers depend on the semiconductors materials.

All the semiconductors materials used to convert photon energy into electrical energy have advantages and drawbacks. The most important parts of the solar cell are discussed in the next part.

2.2 SEMICONDUCTOR & ITS PROPERTIES

The materials whose electrical properties lie between conductors and insulators are known as semiconductors. Silicon and Germanium are the best examples of semiconductor. A semiconductor can be defined in terms of energy bands. In semiconductor materials have almost an empty band and almost filled valence band with a very narrow energy gap separating the two bands [10] .

2.2.1 Types of Semiconductors

The best-known semiconductors types are explained next:

2.2.1.1 Elemental Semiconductors

The element silicon (Si) is the best known semiconductor. It is the prototype of a large class of semiconductors with similar crystal structures like the Germanium (Ge). It is surrounded by four nearest neighbor atoms (each atom is said to be four-fold coordinated) resulting in a tetrahedron form. The mainstay of the electronics industry and the cornerstone of modern technology are formed by the tetrahedral bonded semiconductors [36].

2.2.1.2 Binary Compounds

Elements from the groups III and V of the periodic table (such as GaAs) are responsible for forming compounds and have similar properties to their group IV counter-parts. From the group IV elements to the III-V compounds, the bonding becomes partly ionic due to the transfer of electronic charge from the group III atom to the group V atom [36]. There are significant changes in the semiconductor properties due to ionicity causes. The effects of the ionicity are mainly that it increases the Coulomb interaction between the ions and also the energy of the fundamental gap in the electronic band structure. In the II-VI compounds (for example ZnS) the ionicity becomes even larger and more important; as a consequence of the larger ionicity, most of the II-VI compound semiconductors have bandgap larger than 1 eV. Mercury telluride (HgTe) is an exceptional compound semiconductor, which has actually a zero bandgap (or semimetal) similar to gray tin. For the potential application of displays and lasers the large band gap like II-VI compound semiconductors are used. Among the I-VII compounds semiconductors many of them are regarded as insulators rather than semiconductors.

2.2.1.3 Oxides

Most oxides are found as good insulators but some like CuO and Cu_2O are very well known semiconductors. Though cuprous oxide (Cu_2O) is considered as mineral (cuprite) it is also a classic semiconductor with extensive semiconductor properties. As oxide semiconductors are not well understood with regard to their growth process, they have a very limited scope of applications now a-days [36]. With the exception in the II-VI compound zinc oxide (ZnO), their main application is as a transducer or as an ingredient of adhesive tapes and sticking plasters. With the discovery of superconductivity in many oxides of copper the situation has changed.

2.2.1.4 Layered Semiconductors

Many semiconductors like lead iodide (PbI_2), molybdenum disulfide (MoS_2) and gallium selenide (GaSe) are classified according to their layered crystal structures. Typically there is a covalent bonding within the layers much stronger than the van der Waals forces between the layers. These layered semiconductors are very important and interesting due to the quasi-two-dimensional behavior of electrons in the layers [36]. With the process of intercalation the interaction between layers can be modified; the intercalation states by incorporating foreign atoms between the layers in a process.

2.2.1.5 Organic Semiconductors

There are many organic compounds which are considered semiconductors like, for example, polyacetylene [$(CH_2)_n$] and polydiacetylene. Though organic semiconductors are not yet used in electronic devices, but they have great possibilities for future applications. The main comparison between organic and inorganic semiconductor is that the organic can be easily fitted to the applications. For example, some compounds that contains conjugate bonds, such as –C=C-C=, have large optical nonlinearities and therefore may have important applications in optoelectronics [36]. Another advantage is that, by changing their chemical formulas, the band gap of these compounds can be changed more easily than the inorganic semiconductors to suit the application.

2.2.1.6 Magnetic Semiconductors

There are many compound semiconductors which contain both semiconducting and magnetic properties like, for example, europium (Eu) and Manganese (Mn). They contain magnetic properties due to their magnetic ions. These magnetic semiconductors include EuS and alloys.

The latter compounds exhibit different magnetic properties like ferromagnetism and antiferromagnetism. The magnetic alloys semiconductors which contain lower concentrations of magnetic ions are known as dilute magnetic semiconductors [36]. Because of the alloys potential applications they recently became attract and were given much attention. The Faraday rotations of these alloys are larger than those of the nonmagnetic semiconductors and it can be up to six orders; as a result of those properties these materials can be used as optical modulators based on their large magneto-optical effects.

2.2.1.7 Other Miscellaneous Semiconductors

There are some other semiconductors that cannot be classified in accordance with the above-explained ones. SbSI can be a good example of it; it exhibits Ferro-electricity at low temperatures [36].

There are compounds with the general formula I-III-VI_2 and II-IV-V_2 crystalline in the chalcopyrite structure. For example $AgGaS_2$ is interesting for its nonlinear properties, $CuInSe_2$, useful for solar cells. Other groups of compound semiconductors have many interesting properties but they were not given much attention due to their limited applications. The existence of those semiconductors with interesting properties shows that the future of the field of semiconductor physics has plenty of room for growth and expansion. Table 2.1 shows the physical properties of the c-Si solar cells.

Table 2.1: Physical properties of a c-Si solar cell.

Name	Description	Unit
Doping Type	p-type	N/A
Thickness	300	[μm]
Area	10 × 10 or 12.5 × 12.5	[cm^2]
Top side doping	n^+ type	N/A
Back side doping	p^+ type	N/A
Reduced thickness	250	[μm]
Reduced Area	20 × 20	[cm^2]

The most important and used semiconductor for a solar cell is the crystalline (c-Si) cell, and, presently, it is dominating the PV market. It is preferred over others due to its simple structure and it is a good example of a typical solar cell structure [11].

Figure 2.2 it explains the physical properties of a c-Si solar cell. On the top which has front contact of metal grid, there are serial connections to the back contact of the next cell. Then there is an antireflection coating which is in blue color. There are n-type and p-type layer which consists of p-n junction in contact with the back contact.

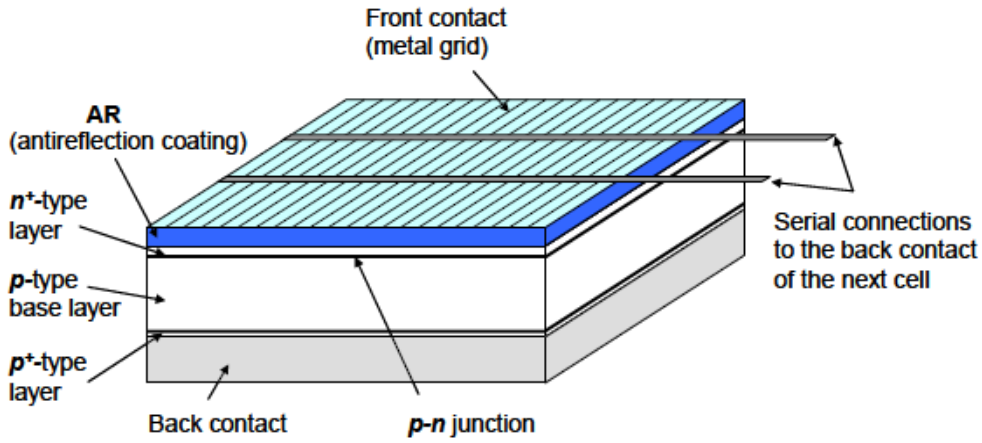

Figure 2.2: A typical structure of a c-Si solar cell [11].

Solar cells consist of two layers and they are top and bottom metallic grid. The bottom metallic grid can be an electrical contact which is responsible for the collection of the separated charge carriers and make a connection with the cell to a load. In order decrease the reflection of sunlight from the cell, usually a thin layer is used as an antireflective coating which covers the topside of the cell. With the purpose of protecting the cell from the effects of the external environment while operating it is required to attach material in the both side of the cell. The material can be a glass sheet or other type of transparent material for encapsulating.

For the thin film solar cells the deposited layers for constituting the cell are on a substrate carrier. A large range of low-cost substrates for example glass sheet like, for example, metal or polymer foil are used when the processing temperature is low during the deposition of the layers.

As already mentioned, the most widely used PV material is the c-Si solar cell and it is the first successful solar cell made. In order to explain the semiconductor properties that are related to basic solar cell operation it is important to use c-Si. The purpose of explaining is to have

knowledge and basic understanding of how solar cells based on other semiconductor materials work. The main semiconductors parameters that are responsible for the design, objectives, performance and efficiency of the solar cell are [1]:

(i) The concentrations of doping atoms determine the width of the space-charge region of a junction. The concentrations of doping atoms are classified into two different types: that one; that donates free electrons is called donor atoms, $N_{D,}$ and that one that accepts electrons is known as acceptor atoms, N_A.

(ii) Transport carriers characterization of charge carriers due to drift and diffusion is caused due to mobility, μ, and diffusion coefficient, D respectively.

(iii) The characterization of the recombination-generation processes happen due to the lifetime, τ, and diffusion length, L, of the excess carriers.

(iv) The absorption ability for visible and other types of solar radiation of a semiconductor is characterized by the band gap energy, E_G, absorption coefficient, α, and refractive index, n.

Semiconductor bandgap and solar cell efficiency figure is presented on Figure 2.3:

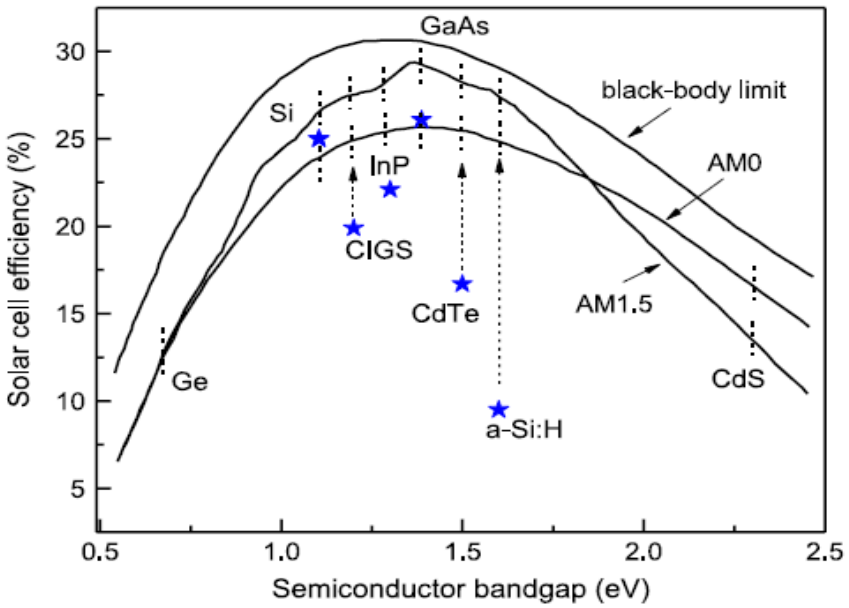

Figure 2.3: Power conversion efficiency as a function of semiconductor band gap [37].

The conductivity of a material depends on the value of band gap energy. The concept of energy bands is important to describe the conductivity, semi-conductivity and non-conductivity of a material. Generally, the electrons have the tendency to fill up the low energy bands first. The more completely a band is filled, the lower energy they have. Most of the energy band in a semiconductor will be totally filled at absolute zero but, the energy bands at higher level are totally empty basically [38]. Close to the totally empty and totally filled part there are two bands that are nearly empty and nearly filled.

The top nearly filled is known as valence band, the lowest nearly empty band is known as conduction band. The gap between the two bands is known as band gap. In the totally filled band there is no flow of current because there is no net velocity. On the other side, the totally empty band does not contribute to current conduction. So, these are the reasons for the contribution of current flows in a semiconductor between valence band and conduction band. Figure 2.4 presents the energy band diagram, where E_v is the valence band, E_c is the conduction band and E_g is the energy gap.

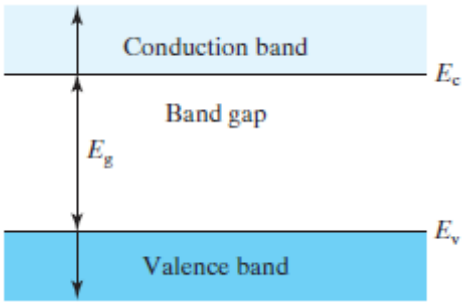

Figure 2.4: The energy band diagram of a semiconductor [12].

The band gap energy is defined by the difference between the conduction band and the valence band as shown in equation 2.1:

$$E_g = E_c - E_v \quad (\mathbf{2.1})$$

The band gap energy is important for semiconductor materials. For the silicon it is about 1.1 eV. The electrons in the conduction band are conduction or mobile electrons and the electrons in the valence band are in covalent bonds. The band gap energy has strong influence and hold on the characteristics of the semiconductor devices. It can be shown with measurement of the absorption of light by the semiconductor as a function of the photon energy, hv. The absorption

of light depends on the difference between photon energy and band gap energy. The light is tightly absorbed when photon energy is larger than band gap energy. Electron-hole pair is created by the consumption of the absorbed photon [12].

The semiconductors have two types usually. Those are:

(1) Intrinsic or pure semiconductors.
(2) Extrinsic or impure semiconductors.

Extrinsic semiconductors are classified into two parts:

(i) N-Type Semiconductor.
(ii) P-Type Semiconductor.

(1) Intrinsic Semiconductor

The semiconductors that do not contain impurities are intrinsic semiconductors. It means that an intrinsic semiconductor is one that is in its extremely pure form. This type of semiconductor is chemically pure, meaning that it's free of impurities and undoped. They do not contain electrons and holes as well. It is also known as i-type semiconductor. In this type of semiconductor, no electron is available at absolute zero temperature. Examples of such semiconductors are: pure germanium and silicon that have forbidden energy gaps of 0.72 eV and 1.1 eV, respectively.

Due to the very small energy gap many electrons that gains sufficient energy can jump across the small gap between the valence and conduction bands in room temperature. The identification symbol of intrinsic semiconductor is n_i which refers it as the intrinsic carrier density.

Figure 2.5 describes the energy band diagram of an intrinsic semiconductor at room temperature. The two levels are the conduction band and the valence band. There is a level between these two levels called Fermi level.

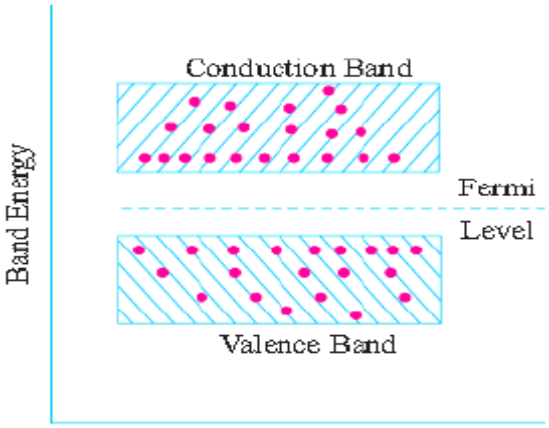

Figure 2.5: Intrinsic Semiconductor energy band diagram.

Figure 2.6 describes the energy band diagram for an intrinsic semiconductor at 0K and at greater than 0K temperatures. The two energy bands are the conduction band and the valence band. Between these two bands there is a gap called forbidden energy gap.

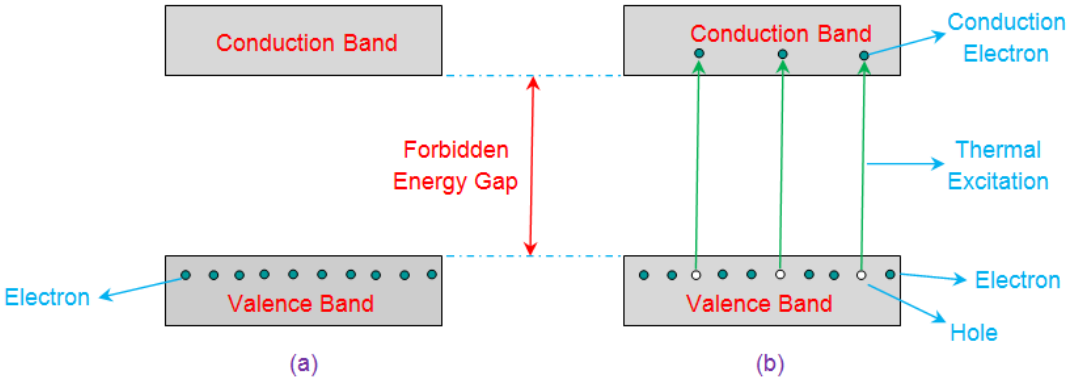

Figure 2.6: Intrinsic energy band diagram (a) 0K (b) Temperature > 0K [13].

At 0K there is no movement of the electron from one band to another because there is not sufficient energy to move the electron and it cannot break the bonding of energy level. If we look at the figure (b) we can see that few electrons move from valence to the conduction band; this happens due to the input temperature because the temperature make the electrons excite, break the energy bonding and move to the conduction band, thus generating free empty spaces.

This means that in the intrinsic semiconductor temperature has a great influence and the intrinsic carrier has great dependence on the temperature as well. The intrinsic carrier density temperature dependence is dominated by the exponential dependence on the band gap. The

temperature dependence of the effective densities of states and of energy band gap should be considered also. There is also a temperature dependence on the effective masses but it is not considered here as it is too small compared to the others.

The charge carrier densities in intrinsic semiconductors can be mathematically given by equations 2.2 and 2.3 where

N_c = the effective densities if states in the conduction band.

N_v = the effective densities of states in the valence band.

k = 1.38×10^{-23} JK^{-1} is the Boltzmann constant

T = the temperature

E_F = the Fermi energy.

Ev = the energy level of valence band.

Ec = the energy level of conduction band.

h = 6.624×10^{-34} Js is the Planck constant.

m_h = the effective mass of a hole.

$$n_i = N_c\left(\exp\left(\frac{E_F - E_c}{kT}\right)\right) \quad \text{where, } N_c = 2\left(\frac{2\pi m_e kT}{h^2}\right)^{\frac{3}{2}} \qquad (\mathbf{2.2})$$

$$p_i = N_v\left(\exp\left(\frac{E_v - E_F}{kT}\right)\right) \quad \text{where, } N_v = 2\left(\frac{2\pi m_h kT}{h^2}\right)^{\frac{3}{2}} \qquad (\mathbf{2.3})$$

In conclusion we can say that it is very difficult to make an intrinsic semiconductor. For constructing such a semiconductor we need highly pure materials.

(2) Extrinsic Semiconductor

An extrinsic semiconductor is created by doping of an intrinsic semiconductor. Doping is the introduction of impurity atoms that can add electrons or holes doping [12]. The properties of the extrinsic semiconductor are:

I. The number density of electrons is not equal to the number density of holes.
II. It is introduced with the process of doping.
III. In this type of semiconductor the electrical conductivity is high.
IV. The amount of impurity and the temperature of the semiconductor define the electrical conductivity.
V. At room temperature the conductivity is very low.

Extrinsic Semiconductor Temperature variation of Conductivity is shown in Figure 2.7:

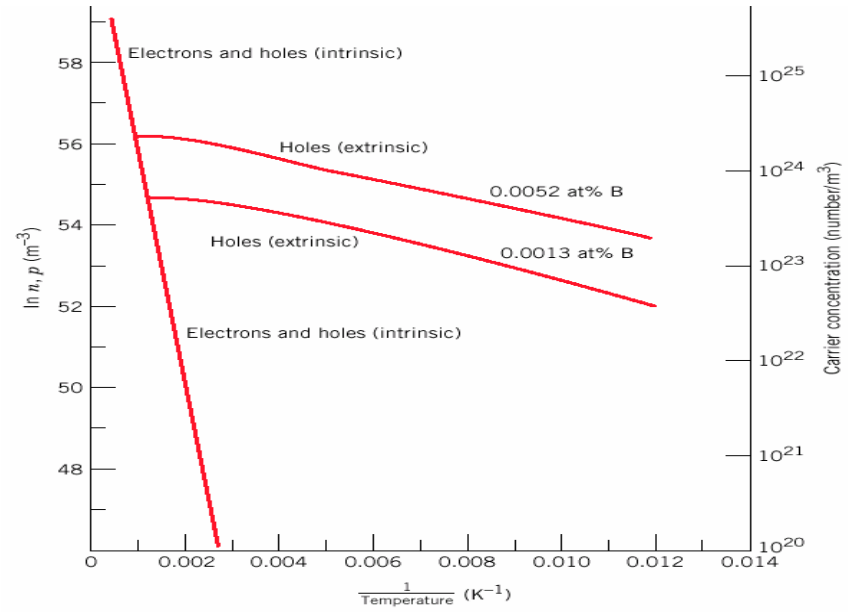

Figure 2.7: Extrinsic Semiconductor temperature conductivity with carrier concentration. [39]

Extrinsic semiconductors are divided in two kinds:

1. *n-type semiconductor*

This is the type of semiconductor that provides extra electrons to the host. An n-type dopant is called donor. Those are group V impurities such as Antimony, Phosphorous, Arsenic etc. An n-type dopant possesses five valence electrons and each atom tries to have a covalent bonding with five lattice atoms. This leaves an excess electron for every impurity atom in group IV matrix.

2. *P-type semiconductor*

A p-type semiconductor is produced by adding an acceptor impurity like gallium, boron, or indium to an intrinsic semiconductor. A p-type dopant is called acceptor. A p-type dopant possesses three valence electrons and each atom tries to have covalent bonding with three host atoms. The unmade bond that it leaves behind creates an excess hole for every impurity atom in group IV matrix. The main production of a p-type semiconductor occurs with doping an intrinsic semiconductor. P-type has holes dominate conduction process.

A classification of semiconductors is presented in figure 2.8:

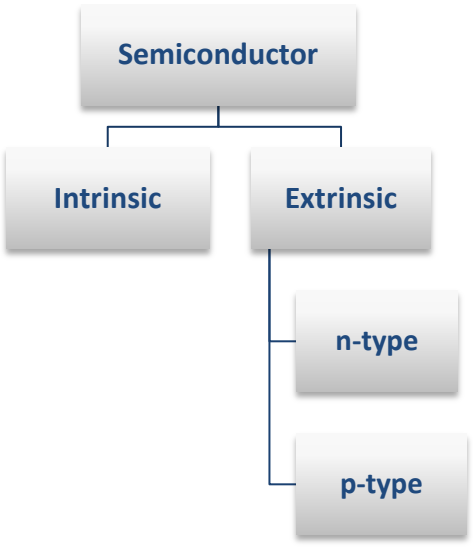

Figure 2.8: Classification of Semiconductors.

2.3 SEMICONDUCTOR DIODES

One of the simplest and most useful of all semiconductors is diode. For a wide range of applications many types of diodes are used. A semiconductor diode device has a fundamental two-terminal electronic element similar to a resistor in linear circuits. It conducts the current in only one direction. We know that the current-voltage (I-V) relationship of a resistor is linear according to the description of Ohm's law. The I-V characteristic of a diode is depended on operating region and it is nonlinear also. The semiconductor diode is sometimes called junction diode because the diode is produced by making a junction between p-type and n-type semiconductors.

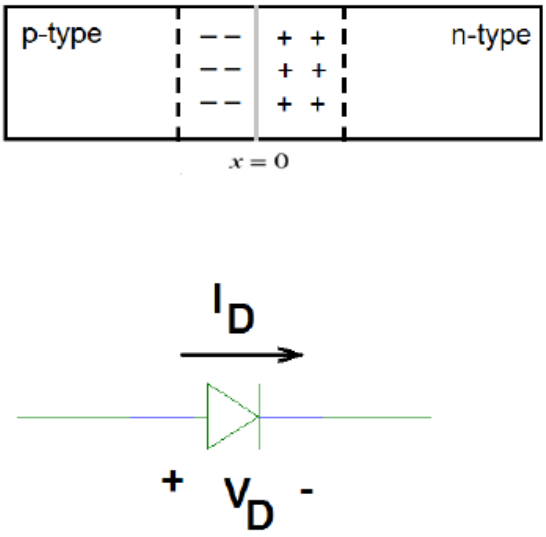

Figure 2.9: Symbol for diode.

Figure 2.9 presents a simple diode symbol. It states the diode sign and direction; it also reflects the positive type (p-type) and negative type (n-type) of the diode.

In order to have an extensive idea about diode it is useful to have an idea of diode ideal characteristics. The diode that has ideal characteristics is ideal diode. However, the physical diodes do not behave as ideal diodes; we cannot use the mathematical relationships except in simple circuits for circuit analysis purposes. The rectification is a process of converting the ac signals to dc signals and it is an important application of diodes.

There are various kinds of diode already. The different types of diodes emphasize different aspects of a diode often by geometric scaling, doping level, and the right electrodes. Next section describes shortly all the types of semiconductor diodes.

2.3.1 Types of Semiconductor Diodes

2.3.1.1 Normal Diode

These types of diodes are usually made of doped silicon or, more rarely, germanium. Previously cuprous oxide and later selenium were used before the development of modern silicon power rectifier diodes. They have less efficiency and much higher forward voltage drop, typically 1.4-1.7 V per cell [40].

2.3.1.2 Shockley Diode

The first semiconductor device was the Shockley diode; it is also known as PNPN diode. The gate terminal is disconnected and is equal to a thyristor without a gate. The diode can only conduct by providing forward voltage because there is no trigger input in it.

If we turned it 'ON' then it stays on; when turned 'OFF' then stays off. The two operating principles are conducting and non-conducting. The diode conducts with less voltage in the non-conducting state. A Shockley diode is represented in Figure 2.10:

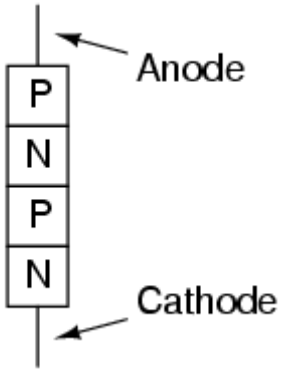

Figure 2.10: A Shockley diode.

The main applications of Shockley diode are trigger switches for SCR and it acts as relaxation oscillator.

The symbol of Shockley diode is presented in the figure 2.11.

Figure 2.11: Symbol of Shockley diode.

2.3.1.3 Photodiode

Normally all types of semiconductors are dependent on optical charge carrier generation. Most semiconductors are packaged in light blocking material due to its optical carrier generation and typically it is an undesired effect. Photo diodes are packaged in materials that allow light to pass as the diodes are intended to sense light. The use of photodiode is considered in solar cell, in photometry or in optical communications. With the linear array packaging or dimensional array packaging multiple photo diodes can be packaged in a single device [14].

2.3.2 Ideal Diode

A simplest nonlinear element is an ideal diode. It is the combination of a p-n junction in where the p-type to n-type material is considered to occur instantaneously. It is also known as abrupt junction. We ignore the effect of the depletion region and the built-in voltage when assuming a diode as an ideal diode. The terminal which has positive voltage is called anode and the terminal which has negative voltage is called cathode. The current is always considered to flow from anode to cathode and usually the passive sign convention is used in the circuit symbol. Figure 2.12 presents the diode circuit symbol:

We can see that the diode has two terminals are anode and cathode. The diode is forward biased if the positive polarity is at the anode and diode is conducting. The diode is reverse biased and is not conducting if the polarity is at the cathode and it is not conducting.

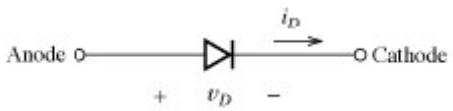

Figure 2.12: Circuit symbol of a diode.

2.3.2.1 Ideal Diode Characteristics

Normally an ideal acts like as switch, when it is forward biased then it acts like a closed switch and when it is reverse biased it act like a open switch. The current-voltage (I-V) characteristics are the most important relationship for the ideal diode.

- An ideal diode is the simplest two-terminal device
  - Anode: the positive terminal
  - Cathode: the negative terminal

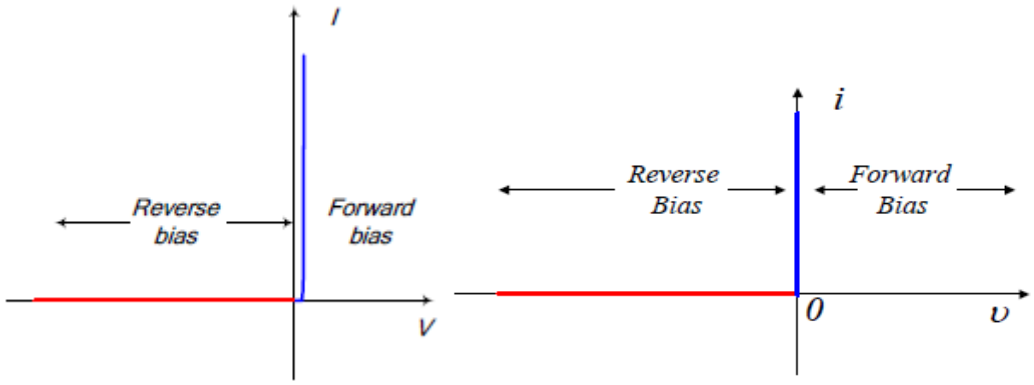

(a) (b)

Figure 2.13: Diode characteristics (a) Real diode (b) Ideal diode.

Figure 2.13 (a) shows the real diode characteristics and figure 2.13 (b) shows the ideal diode. They are very close to each other and a very good approximation to the actual diode can be represented by the ideal diode.

This simplified real diode given model is very useful in the case of fast approximate analysis and provides a very helpful introduction to diode circuit analysis

2.3.3 I-V Characteristics of Junction Diodes

The current-voltage (I-V) characteristics of a junction diode depend on the diode saturation current, ideality factor and its thermal voltage. And there is an exponential form in the diode I-V characteristics.

□ Diode Current: $i = I_s\left(\exp\left(\frac{v}{nV_t}\right) - 1\right)$ (**2.4**)

- I_s : It is diode saturation current and proportional to diode area.
- n : It is the diode ideality factor which varies between 1 and 2.
- V_t : It is the thermal voltage and it is equal to room temperature.

Figure 2.14 shows the i-v characteristics of a diode in both forward and reverse region.

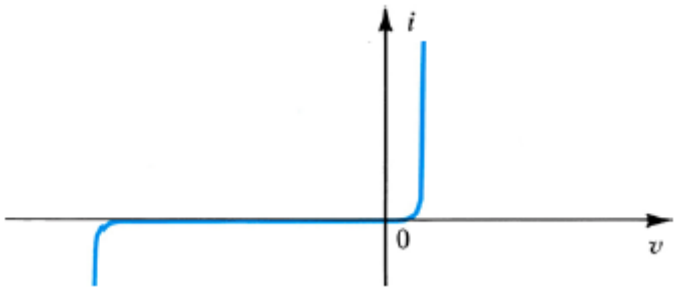

Figure 2.14: i-v characteristics of a diode [14].

□ Diode is in forward-biased region when v>0

- The associated resistance of the diode in the forward biased region is zero and there will be a replacement with a short by the diode. The ideal curve of forward-biased diode has infinite slope.

□ Diode is in reverse-biased region when v<0

- The associated resistance of the diode in the reverse biased region is infinity and there will be a replacement with an open by the diode. The ideal curve of reverse-biased diode has slope of zero.

□ Diode is in breakdown region when $v < -V_{ZK}$.

Figure 2.15 presents the i-v characteristics of a diode with all regions.

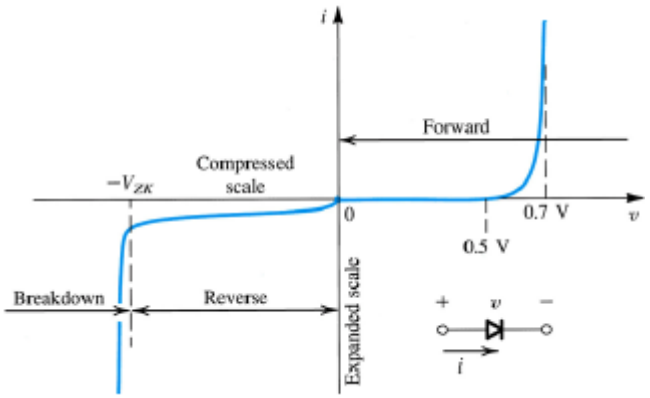

Figure 2.15: i-v characteristics of a diode with all regions [14].

2.3.3.1 Diode Forward-biased Region

The junction of a diode is said to be forward biased when we connect p-type region of a junction with positive terminal and n-type region of a junction with negative terminal of the voltage source. The characteristics of diode forward biased region are as follows:

- The I-V relationship of simplified forward-biased region:

  - For a given forward voltage:

$$i \approx I_s \exp^{\frac{v}{nV_T}} \quad (2.5)$$

  - For a given forward current:

$$v = n V_t \ln\left(\frac{I}{I_s}\right) \quad (2.6)$$

- The I-V relationship due exponential term

  - For cut-in voltage: $i = 0$ while $v < 0.5$ V.
  - For whole conduction: $0.6V < v < 0.8$ V.

2.3.3.2 Diode Reverse-biased Region

The junction of a diode is said to be reverse biased when we connect p-type region of a junction with negative terminal and n-type region of a junction with positive terminal of the voltage source. The characteristics of diode reverse biased region are as follows:

- Diode reverse current is denoted by i and it can be written by the following equation: $i \approx I_s$.
- Practically it is found that I_s is smaller than reverse current.
- It is also found that reverse current increases a little with the reverse bias.
- Reverse current is not dependent of reverse bias theoretically.
- There is temperature dependence of the reverse current. It is seen that for every 10ºC of temperature rises reverse current increases almost double.

2.3.4 The Effects of Photovoltaic System

Power generation cannot be risen itself with the collection of light-generated carriers. The main path of generating power is to generate voltage with generated current. The photovoltaic effect is responsible to generate voltage in a solar cell. The effect that is based on the conversion of sunlight to electricity is the photovoltaic (PV) effect. We can describe it as the close contact between two dissimilar materials that produces electricity or voltages while the sunlight strikes on it. Simply, it can be described as follows: when the pure energy light strikes a PV cell it transmits the amount of energy necessary for the negatively charged atomic particles, which are known as electrons, to be easily freed [41]. The voltage or photovoltage is created by acting a built-in-potential barrier in the cell. The direct conversion of sunlight into electricity can be an appropriate definition of the photovoltaic effect, which is responsible for all of its uses. The basic principles that posses the photovoltaic effects are:

- A junction in photovoltaic system can be obtained by generating charge carriers. The charge carrier generation happens by the photon absorption.
- In the junction, the following separation processes of the photo-generated charge carriers occur.
- At the terminals of the junction the collection of the photo-generated charge carriers is completed and that is the main important part.

In a photovoltaic system the sunlight strikes the crystal (for example silicon or germanium). In this type of crystals we know that the electrons are not usually free and, as a result, they cannot move from one atom to another within the crystal. With the striking of the light some of the electrons become free from the bonded situation by using the gained energy.

There are two types of junction in a system one is positively charge and another is negatively charged. The free electrons can easily jump to another junction more freely; then, on the other side, they can make bonding by positive and negative charge very easily.

The photovoltaic effect continues till the sunlight is provided to the cell. In a solar power system, the current is used to measure the incident light brightness level or as a power source in an electrical circuit. An image of the photovoltaic effect is given figure 2.16:

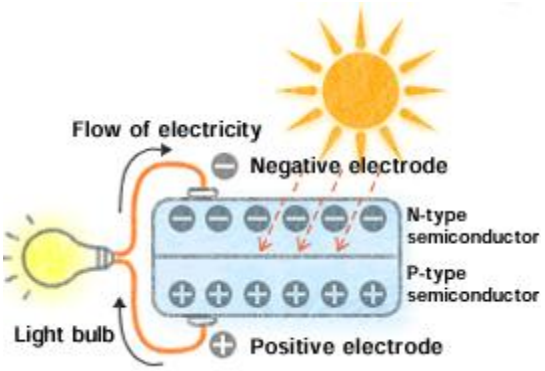

Figure 2.16: Photovoltaic effect principles. [42]

The effects of photovoltaic mainly work with a material to convert sunlight into electrical energy. In order to be able to produce electrical energy it is required to follow few conditions and work in accordance with it. Through the promotion of higher levels of energy the incident photons must be absorbed and it is the first criteria for the electricity generation. In order to have electrical current it should have an internal electrical field that is able to accelerate the promoted electrons in a particular direction.

2. 4 SOLAR CELL TECHNOLOGY

The main and only way of producing electricity by sunlight is through the photovoltaic effect and the device is used to produce electricity is usually called solar cells. The source of energy is the sunlight which is free and abundant. It is found that the intensity of the sunlight in the Earth is about one thousand watts per square meter. For this reason to produce sufficient electric energy the occupying area by the solar cells has to be large enough.

For the commercial purpose the costs must also be considered; the decision should be taken based on the costs per unit of electricity. The photovoltaic system also has installation and operating costs.

Figure 2.17: Industrial level silicon solar cell. [43]

Solar cells are found economically competitive among alternative energy sources as that are already being used in terrestrial applications. Among other renewable energy sources, the solar energy will be cheaper and easier to implement in future. There will be rapid expansion of solar energy market in renewable energy sector if the technological development occurs.

If we want more development and advancement in the sector, some tasks to be completed.

Mainly, we have to look for higher efficient solar cell because current cell are not so efficient. Another thing is that the production costs of cells and, modules, installation costs and other equipment are very expensive; we should look for the low cost instruments and installation costs for the solar energy production.

2.4.1 The Working Principles of a Solar Cell

Solar technology is the main and most important part of producing electricity using sunlight. Generally, the structure of a solar cell is based on an absorption layer. By creating electron-hole pairs after efficiently absorbing incident radiation, the solar cell produces electricity. There are semi-permeable membranes that are attached on the both sides of the solar cell absorber; the membrane is special in the way that it allows only specific types of charge carrier to pass through. This is used to separate the electrons and holes produced by photo-generation from one another.

The main and most required purpose of a PV cell is efficiency. It also depends mainly on the use of semi-permeable membrane also. If the charge carrier can pass through the membrane efficiently then the solar cell will be more efficient. In order to acquire this, the thicknesses of the absorber should be smaller than the diffusion lengths of the charge carriers.

The procedure of electricity production of a solar cell starts when the sun light strikes on it and the voltage potential difference established across the terminals of the cell is 0.5 volt normally. The produced voltage is nearly dependent on the intensity of the incident light. The current capacity is also nearly proportional to the intensity of incident light as well as to the area that exposed area of the light. The solar PV cell is structured with one positive and one negative terminal as in the same way as all other battery types. In the middle of the two contacts a semiconductor p-n junction is placed. With the striking of the sunlight, the photons of the light are absorbed by the solar cell; some of the absorbed photons gain higher energy than the energy gap between valence-band and conduction band in the semiconductor crystal.

The used membrane is a material with high electrons conduction capacity and low conduction rate for the holes. For example a material is p-type semiconductors which can conduct large amount of holes. And, the n-type semiconductor can conduct a large amount of electron rather than a large amount of holes. With the transport of holes that are minority carriers in that type of material the electron can easily flow through the n-type semiconductor.

The key requirement for the photovoltaic energy conversion is the n-type and p-type asymmetric in electronic structure. Figure 2.18 shows a schematic band diagram of an illuminated idealized solar cell structure with an absorber and the semi permeable membranes

at two conditions and E_{FC} is the quasi-Fermi level for electrons; and E_{FV} is the quasi-Fermi level for holes.

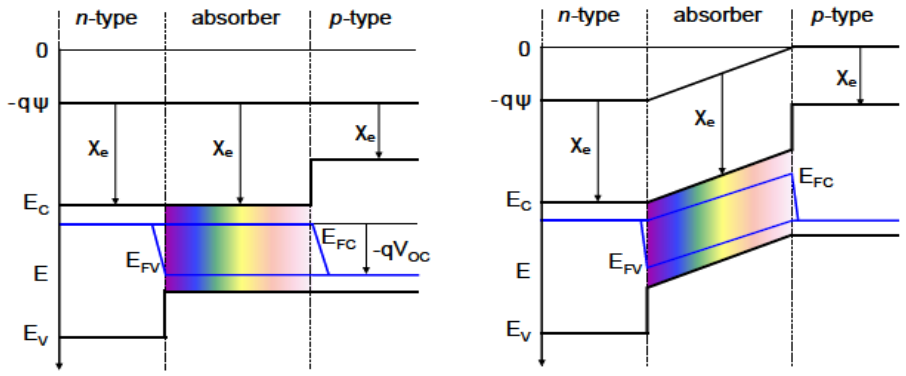

(a) (b)

Figure 2.18: Idealized solar cell structure Band diagram at the (a) open circuit conditions

(b) Short circuit conditions [38].

We already know that the solar cell works with the principles of photovoltaic effect. The photovoltaic effect is mainly based on the generated potential difference between two junctions of different materials in electromagnetic radiation response. According to Albert Einstein the light is the composition of quanta of energy, which is called photons. The photon energy is given by:

$$E = hv \tag{2.4}$$

where h is the Planck's constant and v is the light frequency. The equation states that the multiplied result of Planck's constant and light frequency is equal to the energy.

There are several steps of solar cell operations principles. Figure 2.19 shows the photovoltaic effect.

The photon absorption is illustrated in a semiconductor with bandgap E_G. Here E_V is the valence band and E_C is the conduction band both of them are separated by the bandgap. If the photon energy is greater than the bandgap energy then it is thermalised.

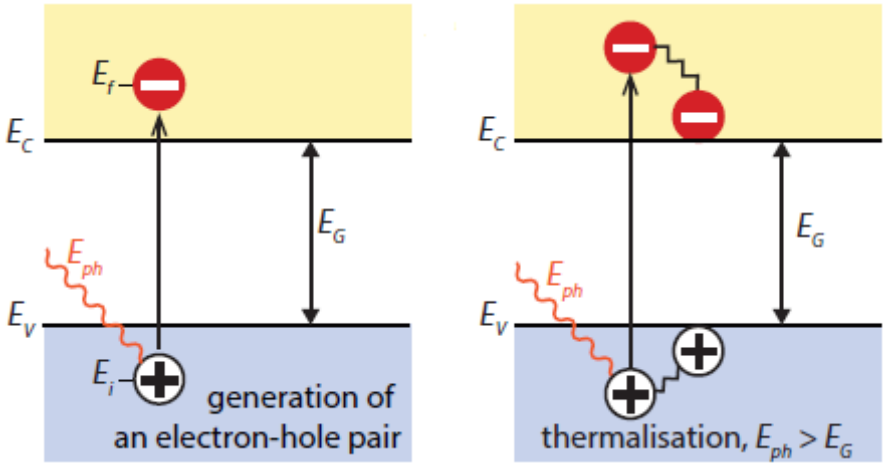

(a) (b)

Figure 2.19: (a) Photon Absorption (b) Thermalised part. [44]

2.5 PV CELL MODELS

A PV module consists of several PV cells. The physical model of a PV cell can be made equivalent to an electrical circuit in order to predict its behavior and estimate the parameters values. There are different equivalent circuits like the single diode PV cell model or the four-parameter model, the single diode detailed model or the single-exponential five-parameter model and the double diode PV cell model or double-exponential model [8].

The available electrical power can be estimated using different types of electrical equivalent cell models [9], because modeling of a PV device output is important to the analysis of PV system performance [7].

In order to increase the penetration in the electrical grid it is becoming very important to improve the precision in the prediction of PV plants power production. The production calculation can start by taking suitable equivalent electrical circuit. PV module is the combination of several PV cells, and several modules connected in series creates PV array.

2.5.1 Important Parameters of the Model

Before having a brief discussion about the different types of cell model it is important to discuss the significant parameters of a PV cell. It is also important to know how the parameters change with the operating conditions (like the operating environment which includes temperature and irradiation).

2.5.1.1 Photo Current (I_{ph})

The current generation in a solar cell is known as 'light-generated current' or solar photo current and it has two main processes. The photo current usually relies on the cell temperature (T) and solar irradiance (I_r). It is shown by the following equation:

$$I_{ph} = I_{ph,ref}\left(\frac{I_r}{I_{r,ref}}\right)\left[1+\alpha'_T\right] \quad (\mathbf{2.7})$$

where $I_{ph,ref}$ refers the photo current at standard reference condition. With respect to temperature the changing rate of short circuit current is the relative temperature coefficient of the short-circuit current. The relative temperature of the short circuit current is α'_T .

For a particular panel, the manufacturer´s absolute temperature coefficient of the short-circuit current and it is often used; the absolute temperature coefficient is α_T [15]. The relationship between those two can be defined by the equation:

$$\alpha_T I_{sc} = \alpha'_T I_{ph,ref} \quad (\mathbf{2.8})$$

2.5.1.2 Cell Temperature (T)

The efficiency of a solar cell depends on the cell temperature. Changes in insolation and in ambient temperature cause the variation in cell temperature. The cell temperature is defined in [16] as:

$$T = T_{amb} + \left(\frac{NOCT - 20^{o}C}{0.8}\right)G \quad (\mathbf{2.9})$$

where T_{amb} is the ambient temperature and, NOCT means the nominal operating cell temperature by manufacturer.

2.5.1.3 Ideality Factor (n)

We know that there are many moving carriers across the junction. Ideality factor of a diode is responsible for different operations of the moving carriers. The value of the diode ideality factor varies in accordance with its characteristics: if the movement technique is purely diffusion then the value of n is 1; if it has the primary recombination in the depletion region then the value for n is approximately 2.

In a PV system the ideality factor is considered one of the unknown parameters while in the extraction process, but it can be found if the other parameters value is known. The value of ideality factor does not depend on the operating conditions; it is equal to the value of the referred ideality factor at standard reference conditions.

2.5.1.4 Saturation Current of Diode (I_s)

The dependency of diode saturation current on cell temperature can be defined by the following equation [15].

$$I_s = I_{s,ref}\left[\frac{T}{T_{ref}}\right]\exp\left[\frac{E_{g,ref}}{kT_{ref}} - \frac{E_g}{kT}\right] \qquad (\mathbf{2.10})$$

where $I_{s,ref}$ is another unknown parameter which is the saturation current of diode in the referred cell temperature condition. E_g is the band gap energy of the diode.

2.5.1.5 Series Resistance (R_s) and Shunt Resistance (R_{sh})

There are another two parameters in the PV system: the series resistance and the shunt resistance. The shunt resistance is also known as parallel leakage resistance. The approximation of shunt resistance given by [15] is

$$R_p > \frac{10V_{oc}}{I_{sc}} \qquad (\mathbf{2.11})$$

where I_{sc} represents the short-circuit current and V_{oc} represents the open circuit voltage in the system.

The relationship between the irradiation and shunt resistance at standard operating conditions can be achieved by [17]:

$$\frac{R_p}{R_{p,ref}} = \frac{I_r}{I_{r,ref}} \quad (\mathbf{2.12})$$

Finally it is obtained [17] that:

$$R_s < \frac{0.1V_{oc}}{I_{sc}} \quad (\mathbf{2.13})$$

In [17] it is said that the series resistance has no dependency on irradiation and temperature in all conditions, so it can be defined as

$$R_s = R_{s,ref} \quad (\mathbf{2.14})$$

The above equation states that the series resistance in referred condition is equal to the series resistance in the circuit.

2.5.2 PV Cell Ideal Model

The ideal model of a PV cell equivalent circuit is presented in figure 2.20. It is characterized by three parameters: the circuit consists of a photo current source with a diode connected in parallel which represent the light-generated current and the electrical behavior of the PN junction respectively. A photo current, which is proportional to the solar radiation, is generated if the photon energy is greater than the band gap energy [18]. This is considered the most simplified form of a PV equivalent circuit as it does not take account of the effect of internal electrical series resistances and parallel resistance as well. The space-charge region can be neglected and the use of a second diode can be omitted based on Shockley's diode theory [45]. It is acknowledged that the PV cell is neither a constant voltage source nor a constant current source; the voltage can be related with the externally measured current and the connection between them (current and voltage) is investigated in [46] [47]. The ideal mathematical model for an individual PV cell can be expressed based on Queisser and Shockley diode equation [13] [48]as:

$$I = I_{ph} - I_D = I_{ph} - I_s\left(\exp\left(\frac{qV}{NKT}\right) - 1\right) \quad (\mathbf{2.15})$$

where I_{ph} is the photo current (A), assumed constant along the I-V curve and proportional to the irradiance; I_s is the diode reverse saturation current (A); $V_t = \frac{NKT}{q}$ is the diode thermal voltage; N is the diode ideality factor, K is Boltzmann's constant (1.381× 10^{-23} J/K); q is the absolute value of the charge of an electron (-1.602× 10^{-19} C) and T is the cell temperature (K), that's assumed equal to the temperature of the P-N junction. Without having internal resistance effects it is found that this model is not appropriate for the actual PV cell current and voltage characteristics [46].

The characterization of the solar cell is greatly influenced by short circuit current (I_{sc}), open circuit voltage (V_{oc}) with diode ideality factor (N) [18]. With the solar irradiance (I_r) of an equal p-n junction temperature (T), the cell has the highest value of current and it is named as short circuit current (I_{sc}). This current is given by [18]:

$$I_{sc} = I = I_{ph} \quad \text{when} \quad V = 0 \tag{2.16}$$

In addition, with the equal solar irradiance and the same p-n junction temperature the cell has the highest value of voltage in its terminals [49]. The open circuit voltage V_{oc} is given by [18]:

$$V = V_{oc} = \frac{nKT}{q} \ln\left(1 + \frac{I_{sc}}{I_s}\right) \qquad \text{when I=0} \tag{2.17}$$

and the output power is described in Eq. (2.16) [18].

$$P = V\left[I_{sc} - I_s\left(\exp\left(\frac{qV}{NKT}\right) - 1\right)\right] \tag{2.18}$$

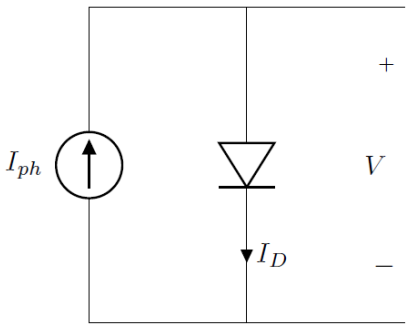

Figure 2.20: Ideal model of PV cell equivalent circuit.

2.5.3 The single diode simple model

A second PV cell equivalent electrical circuit can be illustrated by the figure 2.21. This equivalent circuit consists of a constant current source and a diode in parallel, which accounts for an ideality factor for the recombination in the space charge region [50]. This is called the single diode simple model or four-parameter model of a PV cell [8] [7] [19]. The accuracy can be increased by adding a resistance in series; the parallel resistance is considered infinite, its effect is not taken into account [7].

In a PV cell equivalent circuit the shunt resistance generally assumes very high values and the impact on I-V curve is very low [19]. That's why, a simpler equivalent circuit can be developed neglecting its contribution and it is the motivation of building the four-parameter model [51]. This model accounts the losses due to the contact and interconnections between cells and modules. It also considers the losses due to the module internal series resistance. The model can be considered as the most appropriate model for the diagnostics of PV modules as it has relatively good approximation precision. It shows good relation between approximation precision and simplicity [8].

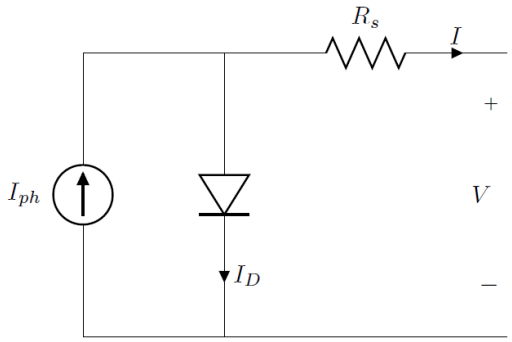

Figure 2.21: Four-parameter model of PV cell equivalent circuit.

The four-parameter mathematical model describes the I-V characteristics of a PV cell and the equation is defined as [8] [7] [19]

$$I = I_{ph} - I_D = I_{ph} - I_s\left(\exp\left(\frac{qV + qR_sI}{NKT}\right) - 1\right) \quad (\mathbf{2.19})$$

where, R_s (Ω) is module internal series resistance. With the consideration of same irradiance and p-n junction temperature conditions, the short circuit current I_{sc} can be obtained by

$$I_{sc} = I = I_{ph} - I_s\left(\exp\left(\frac{q(R_s I_{sc})}{NKT}\right) - 1\right) \qquad \text{when } V=0 \tag{2.20}$$

With the above-explained same conditions, the open circuit voltage V_{oc} is given by [18]

$$V = V_{oc} = \frac{NKT}{q}\ln\left(1 + \frac{I_{sc}}{I_s}\right) \qquad \text{when } I=0 \tag{2.21}$$

and the obtained output power is described as Eq. 2.20.

$$P = V\left[I_{sc} - I_s\left(\exp\left(\frac{q(V + R_s I)}{NKT}\right) - 1\right)\right] \tag{2.22}$$

Recent conducted research shows that the ignorance of the shunt resistance effects on four-parameter model is not adequate in experimental I-V and P-V data fitting in the current-source operation [52]. This work also demonstrates that it does not satisfactorily reflect the effect of high temperature on the current. In comparison with five-parameter model it is found that in the four-parameter model has less accuracy prediction of current [53] [54].

2.5.4 The Single Diode Full Model (Five-parameter model)

The single diode full model is known as single diode detailed model or single-exponential five-parameter model [55]. A parallel resistance is used in this model in order to improve the accuracy. It also takes account the losses due to the leakage current in the junction and within the cell due to crystal imperfections and impurities [8].The electrical equivalent circuit of PV cell single diode full model is shown in figure 2.22. This model is considered one of the most complex models.

The five-parameter model is based on I_{ph}, I_D, N and the two resistances R_s and R_{sh} [55]. The reason of making the equation implicit is the contribution of series resistance (R_s). Additionally, the series resistance values have significant effect on the I-V and P-V characteristics. The cell in circuit behaves like an ideal voltage source and the impact of series resistance is shown in high cell voltages. On the other hand, the shunt resistances impact occurs at low cell voltages where the cell behaves like an ideal current source [19].

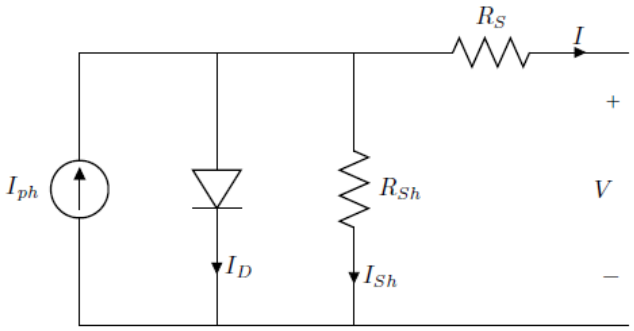

Figure 2.22: Five-parameter model of PV cell equivalent circuit.

In this model, $\mathrm{R_{sh}}$ is the shunt resistance of the PV cell equivalent circuit. The mathematical model of the five-parameter model can be defined as [56]:

$$\mathrm{I = I_{ph} - I_s\left(\exp\left(\frac{qV + qR_sI}{NKT}\right) - 1\right) - \frac{V + R_sI}{R_{sh}}} \qquad \textbf{(2.23)}$$

And the expression for the voltage is

$$\mathrm{V = I_{ph}R_{sh} - I\,R_{sh} + I_s\left(\exp\left(\frac{qV + qR_sI}{NKT}\right) - 1\right) - I\,R_s} \qquad \textbf{(2.24)}$$

The current-voltage (I-V) curve characteristics have the following behavior:

- *Short circuit current* $\left(\mathrm{I_{sc}}\right)$: The short circuit current is the maximum current produced by the PV cell under specific condition of irradiance and temperature. It corresponds to zero output voltage with zero power output also.
- *Open Circuit Voltage* $\left(\mathrm{V_{oc}}\right)$: The open circuit voltage is the maximum voltage potential produced by the PV cell under specific condition of irradiance and temperature. It corresponds to zero output current with the zero output power also.
- *Current at Maximum Power* $\left(\mathrm{I_{mp}}\right)$: The current is referred as the current at maximum power under given conditions of irradiance and temperature. That current is used as the rated current of a PV cell.
- *Voltage at Maximum Power* $\left(\mathrm{V_{mp}}\right)$: The voltage is referred as the voltage at maximum power under given conditions of irradiance and temperature. That voltage is used as the rated voltage of a PV cell.

2.5.5 The Double Diode Model

In the single diode full model it predicts that there is no effect of the recombination loss in the depletion region. But, this recombination loss must be taken into consideration in a practical solar cell. That's the reason introducing the double diode model [3].

With the single diode full model we can achieve acceptable accuracy [7], but, in reality, we know that due to the linear superposition of charge diffusion and recombination in the space layer, the saturation current of the PV cell occurs [57]. According to the previous explanation, the saturation can be modeled by two Shockley terms like, for example, the double diode model.

This model is characterized by its high accuracy though it is relatively complex and suffers from low computational speed. Specifically at the low irradiation level it has been shown that the double diode model has more accuracy in representing the behavior of a PV module when compared with the single diode model.

The schematic diagram of the equivalent electrical circuit of double diode model is given in figure 2.23.

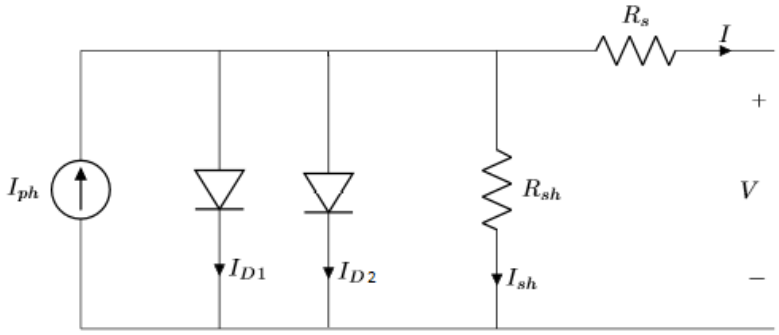

Figure 2.23: Double Diode model of PV cell equivalent circuit.

The double diode model is the known as double-exponential model as well. It is nothing but an addition of the diode to the single diode full model. The diode is considered here to account for the losses due to the carrier recombination in the space charge region of the junction and due to surface recombination. For the diffusion current component first diode is responsible. [58]

The basic equation of this model is given by the following equation (2.25)

$$I = I_{ph} - I_{D1} - I_{D2} \qquad (\mathbf{2.25})$$

Both diode reverse saturation current can be defined as follows:

$$I_{D1} = I_{s1}\left(\exp\left(\frac{qV + qR_sI}{N_1KT}\right) - 1\right) \quad (\mathbf{2.26})$$

and,

$$I_{D2} = I_{s2}\left(\exp\left(\frac{qV + qR_sI}{N_2KT}\right) - 1\right) \quad (\mathbf{2.27})$$

The mathematical model of the double diode electrical circuit can be defined as:

$$I = I_{ph} - I_{s1}\left(\exp\left(\frac{qV + qR_sI}{V_1KT}\right) - 1\right) - I_{s2}\left(\exp\left(\frac{qV + qR_sI}{V_2KT}\right) - 1\right) - \frac{V + R_sI}{R_{sh}} \quad (\mathbf{2.28})$$

where,

I_{s1} = the reverse saturation current for first diode.

I_{s2} = the reverse saturation current for second diode.

N_1 = the diode ideality factor for first diode.

N_2 = the diode ideality factor for second diode.

Particularly at low irradiance level and during partial shadowing conditions the two-diode model can achieve greater accuracy when compared to single diode full model. The two-diode model has better perfection for parameter characterization though the addition of another diode increases the number of computed parameters. Few researchers consider the diode ideality factor of double diode model as a variable; and it is considered as fitting parameters also because it has higher fitting capacity with 6 or 7 parameters though it increases the complexity of parameter calculation. This model is considered the most accurate model between all other physical models.

To improve the accuracy and to overcome the disadvantages of the single diode model the double diode model is introduced. The main challenge of the double diode model is to estimate the values for all the model parameters within a reasonable simulation time.

Chapter 3. MEASUREMENT AND CHARACTERIZATION OF A PV PANEL

3.1 MODELING THE PV SYSTEM

In this chapter about the modelling of the PV system for PV cell particular conditions is discussed. The most used PV equivalent circuit is discussed and characterized here. The main purpose is to observe the behaviour of the PV cell/module for all the parameters variation including internal and external parameters. It is also considered the power output, maximum power point tracking, and variation of the I-V and P-V curve under different conditions. In order to explain and characterize it is significant to analyse the equivalent circuit, its modelling, output behaviour and the mathematical and physical model. In the previous chapter a discussion of several types of PV cell model was made.

As I already mentioned that there are different types of equivalent circuit model. All of the model can be used to analyse the PV system in different situation. This chapter considered the single diode full model or Five-parameter model; this model is obtained by adding a parallel resistance to the four-parameter model. The reason and purpose of using the model was already discussed in chapter 2.

3.1.1 Characterization of a PV Cell

In order to increase the penetration in the electrical grid and to progress in the PV cell prediction behaviours it is important to characterize the PV cell and module. To initiate the process firstly a suitable model of an electrical equivalent circuit should be considered. For a whole PV array it is sufficient to characterize a single PV cell rather considering the set of cells.

In order to characterize a PV cell in various conditions it is important to choose the right equivalent circuit model. For this work the considered equivalent circuit is presented on figure 3.1.

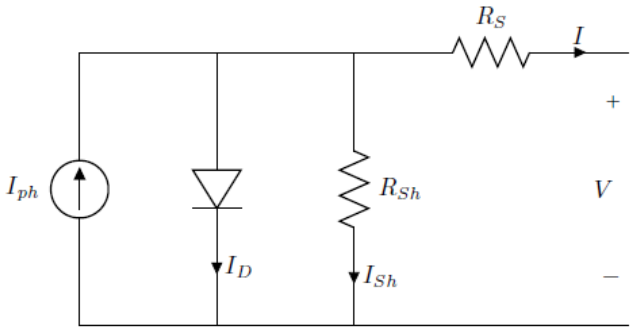

Figure 3.1: Single diode cell equivalent circuit.

The single diode model equivalent circuit is the simplest way to represent the solar cell. This type of circuit consists of a photo current source, a diode, a series resistance and a shunt resistant. The considered five parameters are photo current (I_{ph}), diode current (I_D), diode ideality factor (N), series resistance (R_s), shunt resistance (R_{sh}) [59].

In this part it is important to analyse the mathematical model. Applying Kirchhoff's current law in the figure 3.1 we obtain:

According to KCL, for a meeting point:

Incoming current + outgoing current = 0

$$I_{ph} = I + I_D + I_{sh} \quad (\mathbf{3.1})$$

where, I is the load current of the circuit.

Using Shockley diode equation the current across the diode is given by:

$$I_D = I_s\left(\exp\left(\frac{qV + qR_sI}{NKT}\right) - 1\right) \quad (\mathbf{3.2})$$

where,

I_s = the diode reverse saturation current.

q = the electrons charge.

V = the voltage across the diode.

K = the Boltzmann's constant.

N = the diode ideality factor.

T = the ambient temperature.

And the current across the shunt resistor can be calculated as:

$$I_{sh} = \left(\frac{V + R_s I}{R_{sh}} \right) \quad \textbf{(3.3)}$$

By putting the values from equation (3.2) and (3.3) at equation (3.1) we get:

$$I = I_{ph} - I_s \left(\exp\left(\frac{qV + qR_s I}{NKT} \right) - 1 \right) - \left(\frac{V + R_s I}{R_{sh}} \right) \quad \textbf{(3.4)}$$

This is the load current equation of a PV cell calculated using its equivalent circuit.

Next, we are going to see if it is possible to solve the equation analytically and, if not what changes are needed for the analytical solution.

We can re-write the equation (3.4) as:

$$I = I_{ph} - I_s \left(\exp\left(\frac{qV + qR_s I}{NKT} \right) - 1 \right) - \frac{V}{R_{sh}} - \frac{R_s I}{R_{sh}} \quad \textbf{(3.5)}$$

$$\Rightarrow I + \frac{R_s I}{R_{sh}} + I_s \left(\exp\left(\frac{qV + qR_s I}{NKT} \right) \right) = I_s - \frac{V}{R_{sh}} + I_{ph} \quad \textbf{(3.6)}$$

Dividing by I_s in the both side we have:

$$\left(\frac{R_s + R_{sh}}{R_{sh} I_s} \right) I + \left(\exp\left(\frac{qV + qR_s I}{NKT} \right) \right) = 1 - \frac{V}{R_s I_s} + \frac{I_{ph}}{I_s} \quad \textbf{(3.7)}$$

$$\Rightarrow \left(\frac{R_s + R_{sh}}{R_{sh} I_s} \right) I + \left(\exp\left(\frac{qV}{NKT} \right) \times \exp\left(\frac{R_s I}{NKT} \right) \right) = 1 - \frac{V}{R_{sh} I_s} + \frac{I_{ph}}{I_s}$$

(3.8)

From equation (3.8) we can see that it is not possible to solve the load current equation analytically. The two terms $\left(\frac{R_s + R_{sh}}{R_{sh} I_s} \right)$ and $\left(\exp\left(\frac{qV}{NKT} \right) \times \exp\left(\frac{R_s I}{NKT} \right) \right)$ contain the load current (I). So, it is almost impossible to solve it analytically as it is impossible to extract load current from it. We can try an alternative solution by ignoring some parameters. For example, it

is found that if we make the series resistance $R_s = 0$ then the term $\left(\frac{R_s I}{NKT}\right) = 0$ .Then, we get the equation as

$$\Rightarrow \left(\frac{R_{sh}+0}{R_{sh}I_s}\right)I + \left(\exp\left(\frac{qV}{NKT}\right) \times \exp(0)\right) = 1 - \frac{V}{R_{sh}I_s} + \frac{I_{ph}}{I_s} \quad (\mathbf{3.9})$$

$$\Rightarrow \left(\frac{R_{sh}}{R_{sh}I_s}\right)I + \left(\exp\left(\frac{qV}{NKT}\right) \times 1\right) = 1 - \frac{V}{R_{sh}I_s} + \frac{I_{ph}}{I_s} \quad (\mathbf{3.10})$$

$$\Rightarrow \left(\frac{R_{sh}}{R_{sh}I_s}\right)I = 1 - \frac{V}{R_{sh}I_s} - \left(\exp\left(\frac{qV}{NKT}\right)\right) + \frac{I_{ph}}{I_s} \quad (\mathbf{3.11})$$

$$\Rightarrow I = \frac{1}{\left(\frac{R_{sh}}{R_{sh}I_s}\right)} - \left(1 - \frac{V}{R_{sh}I_s}\right) - \left(\exp\left(\frac{qV}{NKT}\right)\right) + \frac{I_{ph}}{I_s} \quad (\mathbf{3.12})$$

So, equation 3.12 can be considered the analytical solution of the load current equation under the condition of series resistance, $R_s = 0$.

As already mentioned, it is impossible to find the analytical solution of the load current equation [60] [31], so, we have to look for a numerical one in order to characterize of the PV cell/module. For the numerical solution we have to consider the data sheet value provided by the industry. There are several types of numerical method is available and we analyzed several some.

It is impossible to find direct analytical solution of the load current equation of a PV cell. So, we should consider numerical solution in order to solve the equation. Primarily, the bisection numerical method is used to analyse the different parameters variations behaviour on a PV panel.

3.1.2 Parameters Extraction of a PV Cell

In order to characterize the PV systems, the parameters extraction of a PV cell is discussed here. For this, the diode characteristics, the irradiance and temperature effects are considered using the datasheets parameters as input data [23]. The voltage and current at all points are based on datasheets parameters, the effects of irradiance and temperature as well.

By using the above information and the values from the industry or product datasheets the sets of equations can be built as follows [23]:

$$V_{oc} = 0 = I_{ph} - I_s\left(\exp\left(\frac{V_{oc}}{V_t}\right)\right) - \frac{V_{oc}}{R_{sh}} \quad (\mathbf{3.13})$$

$$I_{mp} = I_{ph} - I_s\left(\exp\left(\frac{V_{mp} + I_{mp}R_s}{V_t}\right)\right) - \frac{V_{mp} + I_{mp}R_s}{R_{sh}} \quad (\mathbf{3.14})$$

$$I_{sc} = I_{ph} - I_s\left(\exp\left(\frac{I_{sc}R_s}{V_t}\right)\right) - \frac{I_{sc}R_s}{R_{sh}} \quad (\mathbf{3.15})$$

$$\left.\frac{dP}{dV}\right|_{\substack{P = P_{mp} \\ V = P_{mp}}} = 0 \quad (\mathbf{3.16})$$

$$\left.\frac{dI}{dV}\right|_{\substack{I = I_{sc} \\ V = 0}} = -\frac{1}{R_{sh}} \quad (\mathbf{3.17})$$

All the details and the solution of the equations with explanations are given in [23]. Due to transcendental nature of the equation system the analytical formulas cannot be found. In that circumstance the numerical method is used to solve the equations though there is the drawback of larger computation and initial conditions dependency.

It is found in [23] that the consideration of shunt resistance in the five parameter model has a huge impact on the calculation of parameters; the values are determined using an iterative method. It is also found that the five parameter single diode model does not carry the significant physical values.

3.2 PARAMETERS VARITION EFFECTS ANALYSIS

The typical used parameters are shown in table 3.1.

Table 3.1: Typical Parameters.

Name	Symbol	Unit
Open Circuit Voltage	V_{oc}	[V]
Short Circuit Current	I_{sc}	[A]
The MPP Voltage	V_{mp}	[V]
The MPP Current	I_{mp}	[A]
The MPP Power	P_{mp}	[W]
V_{oc} Temp. Coefficient	k_v	[V/ºC]
I_{sc} Temp. Coefficient	k_i	[A/ºC]
Total Number of Cell	n_s	n/a

As already mentioned, MATLAB is used for simulation purpose to characterize and analyse the process; the mathematical model analysis and curve producing is also done using MATLAB environment.

3.2.1 Simulation Parameters

The single diode PV cell with five parameters is used to study the model. Based on the load requirement it is possible to add sufficient number of cells in series or parallel in this model.

The parameters shown in the table 3.2 are used in the simulation and are given by the industry datasheets. Nonetheless, the values might vary in accordance with the types of PV cell and its efficiency. We considered the mono-crystalline silicon solar cell for the characterization; for this cell some values are constant.

Table 3.2: Parameters Specifications.

Name	Symbol	Unit	Value
Ideality Factor	N	n/a	1.2
Electron Charge	q	[C]	1.6×10^{-19}
Series Resistance	R_s	[Ω]	0.00001
Shunt Resistance	R_{sh}	[Ω]	10000
Solar Radiation	I_r	[Wm^{-2}]	1000
Boltzmann's Constant	K	[$m^2kgs^{-2}K^{-1}$]	1.3806488×10^{-23}
Saturation Current	I_s	[A]	1×10^{-10}
Junction Temperature	T	[K]	293.15
Temperature Coefficient	k_i	[A/ºC]	0.0017
Short Circuit Current	I_{sc}	[A]	3.885
Open Circuit Voltage	V_{oc}	[V]	0.74

In the next sub-sections the most important and significant parameters are studied. The main purpose is to analyse and characterise the whole PV system by analysing a single PV cell.

3.2.1.1 I-V Curve (Current-Voltage) curve of a PV Cell

In figure 3.2 a typical current-voltage (I-V) curve of the solar cell is presented. This curve was obtained through simulation using specific values for solar radiation, ambient temperature and other parameters given by the data sheet.

The curve shows the behaviour of the current with respect to its voltage. Looking at the curve we can conclude that a PV cell has a constant current source at low voltages; this means that it behaves like a constant current source which is almost close to its short circuit current.
In the I-V curve of a PV cell there is a short circuit current (I_{sc}) where current value is maximum and open circuit voltage (V_{oc}) where voltage value is maximum. The obtained primary value for short circuit current is 3.885 ampere and open circuit voltage is 0.74 volt.

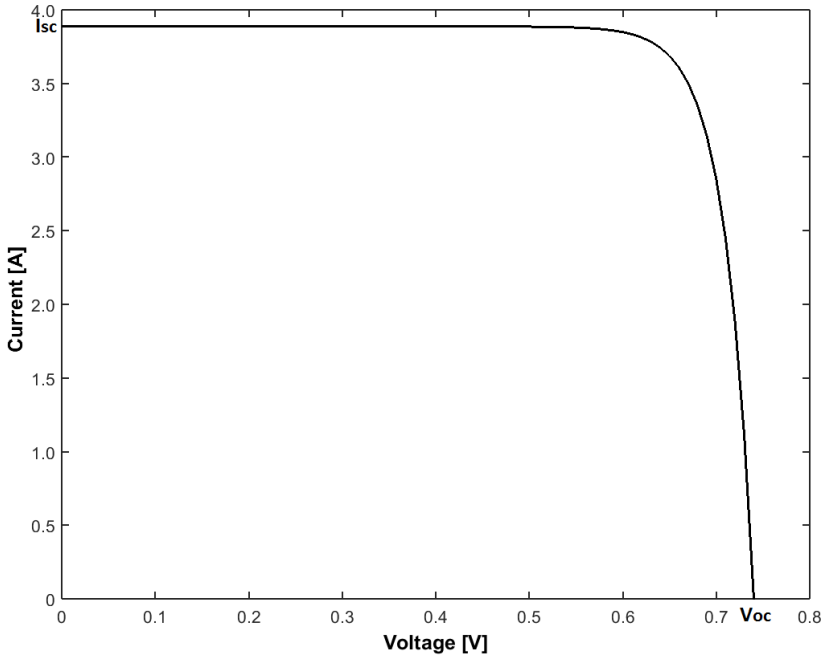

Figure 3.2: I-V curve of a solar photovoltaic cell.

3.2.1.2 P-V Curve (Power-Voltage) curve of a PV Cell

Figure 3.3 presents the typical power-voltage (P-V) characteristics curve of a photovoltaic solar cell. The curve was generated in MATLAB. In order to generate power-voltage (P-V) curve, values of solar radiation, ambient temperature and others specified by the industry are used.

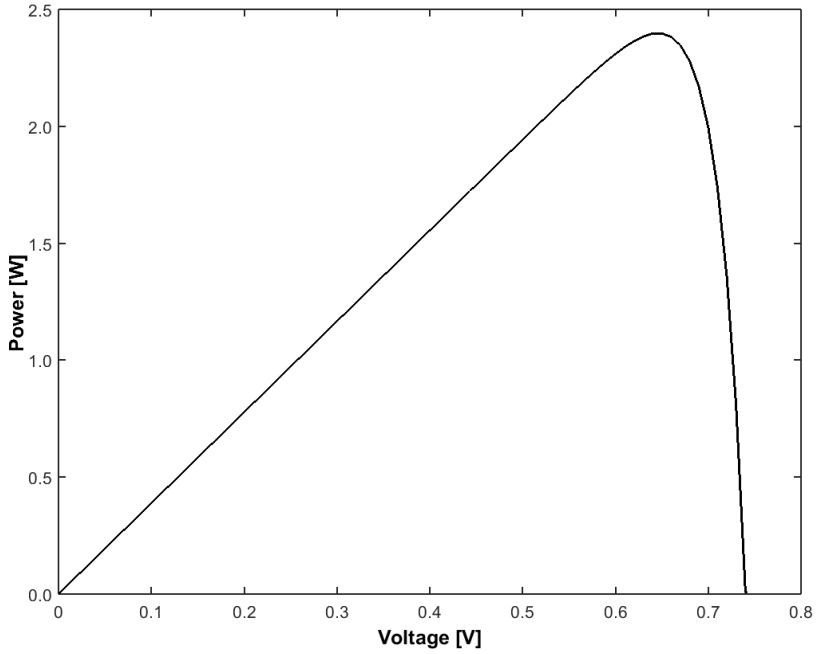

Figure 3.3: P-V curve of a solar photovoltaic cell.

Power is obtained by the multiplication of both current and voltage. The main purpose of the P-V curve is to show the characteristics of the curve and its output behaviour. The electrical characteristics of solar cells can be represented by I-V and P-V curves.

3.2.2 Solar Radiation Variation Effects

The main reason for sustaining life on Earth and determining climate behaviour is the radiation from the sun, which is named solar radiation. The radiant energy particularly the electromagnetic one emitted by the Sun can be presented as solar radiation. It is the combination of infrared, visible and ultraviolet light. Normally the radiation range of sun is in all regions from radio waves to gamma ray [24].

In the wavelengths ranging from 400-700 nm our eyes are responsive. About 45% of radiated energy is emitted by the Sun in the visible range. The solar radiation is not uniform and it varies with the day time [24]. The procedure for measuring the solar radiation is done either by pyranometer (for global radiation measurement) and/or by pyrheliometer (for direct radiation measurement). The PV cell photo-current depends on the solar radiation and temperature. The photo-current equation according to [21] is

$$I_{ph} = \left[I_{sc} + k_i \left(T - 298 \right) \right] \frac{I_r}{1000} \qquad (\mathbf{3.18})$$

The above equation defines the dependecy of the photo-current on temperature and solar radiation mainly; it also depends on the short circuit current and its temperature coefficient [21].

Next, we are going to discuss the results and analyse for different solar radiation behaviour on a PV cell. As the solar radiation is not uniform in all the places of the Earth, the behaviours of a PV cell varies with the place its placed on.

In figure 3.4 the produced I-V curves for the different solar radiations variations are shown. The considered values for the solar radiation are 500 Wm^{-2}, 750 Wm^{-2} and 950 Wm^{-2}. Because, it is most important to know the solar radiation level during simulation and real calculation in order to characterize the solar PV cell [25]. The generated I-V curve by simulation is presented.

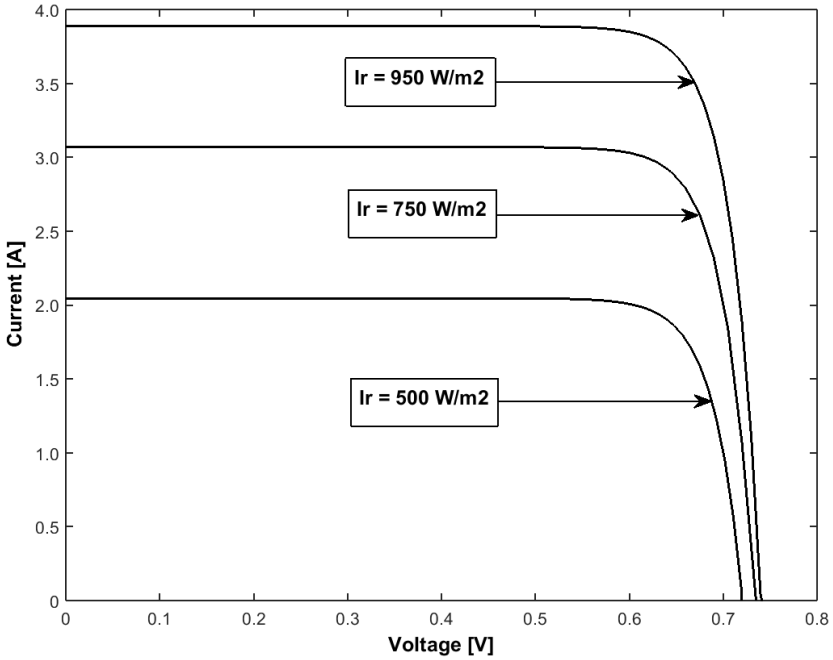

Figure 3.4: I-V curve for different solar radiation.

From the figure 3.4 we can clearly see that with the increase of irradiance the cell short circuit current (I_{sc}) and cell open circuit voltage (V_{oc}) both increases [22] [20] [26] [27] [28] [29] [61] [62], but, the increment in short circuit is much higher in comparison to the open circuit voltage. Open circuit voltage increases slightly [63].

On the contrary, the cell temperature increases with the decrease of solar radiation [22]. This justifies that the solar cell characteristics and output behaviour is highly dependent on the solar radiation.

This behaviour can be explained as follows: with more sunlight on solar cell the electrons gain higher energy and thus get excited. Thereby, due to the increase of electron mobility the current-voltage (I-V) curve characteristics changes giving an increase in the curve. The simulation considered solar radiation as the only variable with constant values for the other parameters values.

From the simulation we find that, the value of short circuit current at solar radiation of 500 Wm^{-2} is 2.05 A and the value of open circuit voltage is 720 mV. The value of short circuit current at solar radiation of 750 Wm^{-2} is 3.07 A and the value of open circuit voltage is 735 mV. If we compare the values between 500 Wm^{-2} and 750 Wm^{-2} we find that the short circuit current

increases 1.02 A and the open circuit voltage increase 15 mV while increasing the solar radiation level from 500 Wm^{-2} to 750 Wm^{-2}.

With the increase of the solar radiation level from 750 Wm^{-2} to 950 Wm^{-2} we find that the value of short circuit current increases 0.81 A and open circuit voltage increases 5 mV.

These values are shown in the table 3.4. We can see that with the increase of solar radiation in a PV cell there is a rapid increase the photo current and short circuit current. Also, with the increase of solar radiation there is a change in open circuit voltage. Though it is a minor change but it has effect on the cell characteristics.

On the other hand, if the solar radiation drops then open circuit voltage and short circuit current also reduces. But, in open circuit voltage the reduction is relatively less due to the logarithmic relationship.

Table 3.3: Result Analysis of different Solar Radiation variation (I-V Curve).

Solar Radiation [Wm^{-2}]	(I_{sc}) [A]	(V_{oc}) [mV]	(I_{sc}) Difference [A]	V_{oc} Difference [mV]
500	2.05	720	n/a	n/a
750	3.07	735	1.02	15
950	3.88	740	0.81	5

Next we are going to discuss about the power-voltage (P-V) curve characteristics. For that the considered solar radiations are: 500 Wm^{-2}, 750 Wm^{-2}, and 950 Wm^{-2}.

The power-voltage (P-V) characteristics for the different solar radiations variations are presented in the figure 3.5. The considered samples for the solar radiation are 500 Wm^{-2}, 750 Wm^{-2} and 950 Wm^{-2}.

In the previous part, we have seen that with the increase of solar radiation open circuit voltage (V_{oc}) and short circuit current (I_{sc}) increases simultaneously. By the same way, in the P-V curve of a PV cell, while we increase the solar radiation there is also an increase in the P-V curve. The main purpose of simulating the curve is to show the power output differences and changes due to the changes in solar radiation.

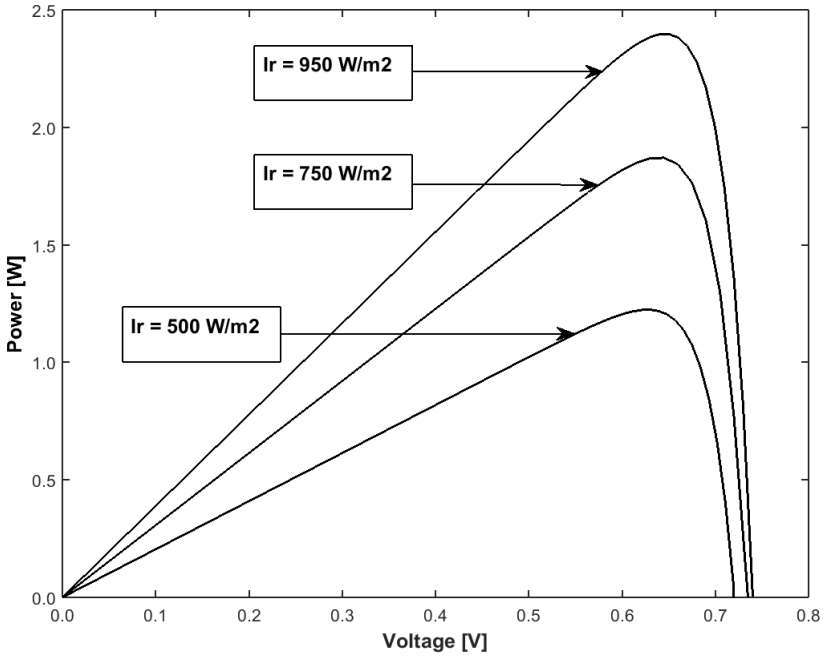

Figure 3.5: P-V curve for different solar radiation.

As power output increases there is increase in Maximum Power Point (MPP) also. The values and the MPP differences are shown in table 3.4.

Table 3.4: Result Analysis of different Solar Radiation variation (P-V Curve).

Solar Radiation [Wm^{-2}]	I_{mp} [A]	V_{mp} [mV]	MPP [W]	MPP Difference [mW]
500	1.943	630	1.224	n/a
750	4.833	387	1.871	647
950	3.688	650	2.397	527

From the table we can find that, as we increase the radiation the power increases with the increase in maximum power point also. The MPP at a solar radiation of 500 Wm^{-2} is 1.224 watt. And, at a solar radiation of 750 Wm^{-2} is 1.871 watt, so an increase of 200 Wm^{-2} in solar radiation results in an increase in the maximum power point (MPP) of 647 milli watt. For a solar radiation of 950 Wm^{-2} the MPP is 2.397 watt, so, with the increase of 150 Wm^{-2} in solar radiation results in an increase of 527 mW in the maximum power point. This means that there is a direct and continuous impact on the power-voltage curve (P-V) of a cell with the change of solar radiation. If we increase the solar radiation we will increase in output power of a PV cell.

After observing all the simulation and characteristics of I-V and P-V cell with the solar radiation variation we can state that an increase in sunlight means an increase in photo current that in turn produces an increase in power output.

3.2.3 Temperature Variation Effects

Temperature is one of the most important factors in solar photovoltaic system. The temperature has an effect on the efficiency of a solar cell as the voltage is highly dependent on the cell and ambient temperature. There is also a relation between diode reverse saturation current and temperature that it can be expressed as the cubic function of the temperature [21] [20] [22]. The equation is as follows:

$$I_s(T) = I_s\left(\frac{T}{T_{nom}}\right)^3 \exp\left[\left(\frac{T}{T_{nom}} - 1\right)\frac{E_g}{N.V_t}\right] \quad (\mathbf{3.19})$$

For the simulation we used temperature of 20, 40 and 60 ºC. Table 3.5 presents the values of the remaining parameters.

Table 3.5: Parameters Specifications.

Name	Symbol	Unit	Value
Ideality Factor	N	n/a	1.3
Electron Charge	q	[C]	1.6×10^{-19}
Series Resistance	R_s	[mΩ]	0.001
Shunt Resistance	R_{sh}	[Ω]	100
Solar Radiation	I_r	[Wm^{-2}]	1000
Boltzmann's Constant	K	[$m^2kgs^{-2}K^{-1}$]	1.3806488×10^{-23}
Saturation Current	I_s	[A]	1×10^{-16}
Junction Temperature	T	[K]	Variable
Temperature Coefficient	k_i	[A/ºC]	0.0017
Short Circuit Current	I_{sc}	[A]	0.270
Band Gap Energy	E_g	[eV]	1.11
Series Connected Cells	N_s	n/a	11

Figure 3.6 presents simulation curve showing the temperature variation effect on the I-V curve of a PV cell. Because, it is most important to know the temperature level during simulation and real calculation in order to characterize the solar PV cell [25].

From the figure 3.6 we can see that an increase in temperature decreases the cell short circuit current (I_{sc}) and decrease in cell open circuit voltage (V_{oc}). In this regard, the output power also decreases [20] [22] [63]. On the other hand, if we decrease the cell temperature then the cell short circuit current (I_{sc}) increases and the open circuit voltage (V_{oc}) increases too [28] [29] [22]. It is considered the solar cell gives better output at cold condition but there are limitations also.

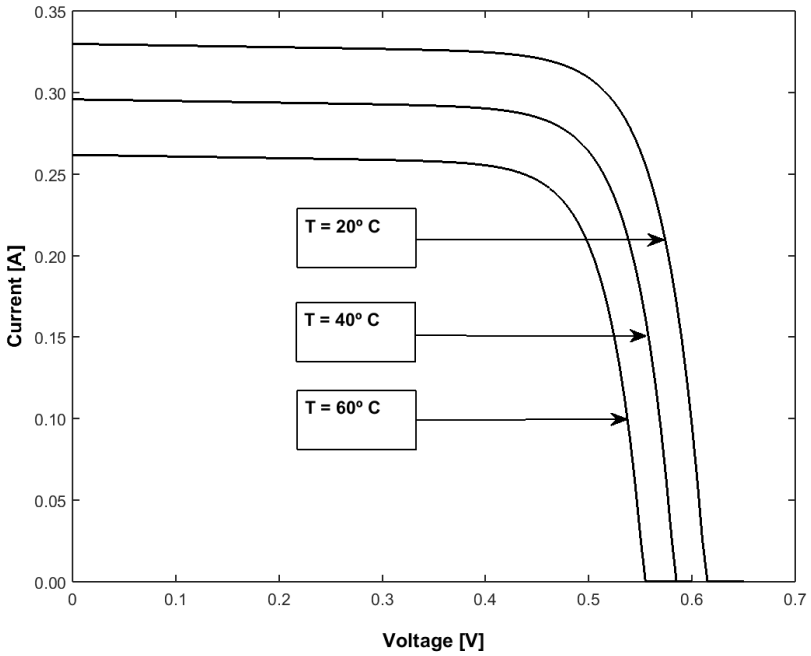

Figure 3.6: I-V curve for different cell temperature.

At a temperature of 20°C, we obtain a value for short circuit current of 329 mA and a value of open circuit voltage of 615 mV. At 40°C, the value of short circuit current is 295 mA and the value of open circuit voltage is 585 mV.

If we compare the results at 20°C and 40°C we find that the short circuit current decreases 34 mA and that the value of open circuit voltages decreases 30 mV.

At 60°C the value of short circuit current is 262 mA and the value of open circuit voltage is 555 mV.

If we compare the results obtained for 40°C and 60°C, we can see that the open circuit voltage and short circuit current decreases. The decreased value of short circuit current is 33 mA and the decrease of open circuit voltage is 30 mV. These results are shown in the table 3.6.

Table 3.6: Result Analysis of different temperature variation (I-V Curve).

Temperature [°C]	I_{sc} [mA]	V_{oc} [mV]	I_{sc} Decrease [mA]	V_{oc} Decrease [mV]
20	329	615	n/a	n/a
40	295	585	1.02	15
60	262	555	0.81	5

In the case of cell temperature, we can state that with the increase of temperature, the cell efficiency decreases. The efficiency decreases because the output of the PV cell decreases with the increase in cell temperature. The module temperature can be achieved with the following equation [27]:

$$T_{module}(^{o}C) = 0.943\, T_{ambient} + 0.028\, \text{Irradiance} - 1.528\, \text{Windspeed} + 4.3 \quad (\textbf{3.20})$$

where, $T_{ambient}$ is given in [°C], irradiance in [W/m^2] and wind speed in m/s.

Next we are going to describe the effect of temperature in the P-V curve. We are going to see the characteristics and its behaviour while changing the temperature of a PV cell.

In the figure 3.7 we can observe different P-V curves for different temperature values. We made simulations for temperatures of 20°C, 40°C and 60°C because, it is most important to know the temperature level during simulation and real calculation in order to characterize the solar PV cell [25].

From the figure 3.7 we can see that in the P-V curve changes with different temperatures variation. If we increase the cell temperatures then cell open circuit voltage decreases and short circuit current decreases slightly too [20] [22] [63] [21].

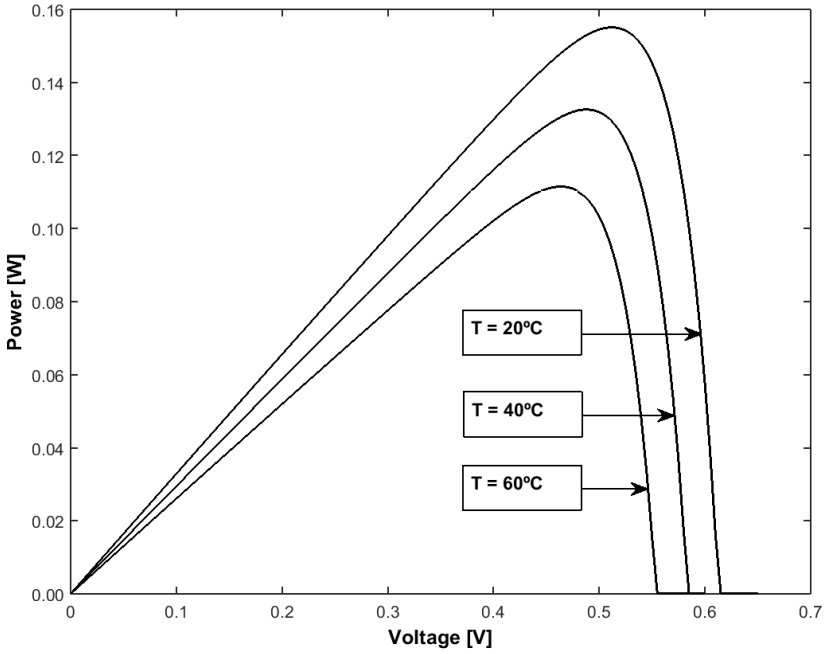

Figure 3.7: P-V curve for different cell temperature.

When we increase the temperature from 20°C to 40°C ,the short circuit current increases 1 mA and open circuit voltage decreases 30 mV and when we increase the value of temperature from 40°C to 60°C, the short circuit current increases 1 mA and open circuit voltage decreases 30 mV.

On the other side, if we decrease the cell temperature then the open circuit voltage increases and short circuit current increases slightly [18] [22]. From 20°C to 40°C, the open circuit voltage decreases 30 mV and power decreases 22.5 mW; from 40°C to 60°C the open circuit voltage decreases 30 mV and power decreases 21.1 mW. Concluding, a temperature increase in a PV cell reduces the cell efficiency.

In the next section we are going to discuss the series resistance variation effect on a PV cell. We use several values in order to compare the outputs.

3.2.4 Series Resistance Variation Effects

The series resistance is an important parameter as like as irradiances and cell temperatures of a PV cell [27]. In [27] it is found that the output of the PV cell varies 5% to 8% annually if the 'accurate' series resistance is not used. There are several methods to define and develop PV cell series resistance. Among all those method one of the most used is town-send method.

The series connection defines the only path between two components. In a PV cell a series resistor is a contact resistance between the metal contact and silicon. The main reason for using a resistance is to reduce or control the available voltage or current of a circuit. The considered series resistance in a PV cell is very low and it is negligible in some cases [21]. The main purpose of varying the series resistance for a PV cell is to predict the effect of its variation and the behaviour of output characteristics.

In figure 3.8 the produced I-V curves for different series resistances are shown. It can be seen that there is an inward bending at the corners of the I-V curve with the increase of series resistance. There is no change in short circuit current and open circuit voltage of the PV curve due to the change in series resistances. There is decrease in current-voltage curve (I-V) also with the increase of series resistance and there is increase in current-voltage (I-V) curve with the decrease of series resistance.

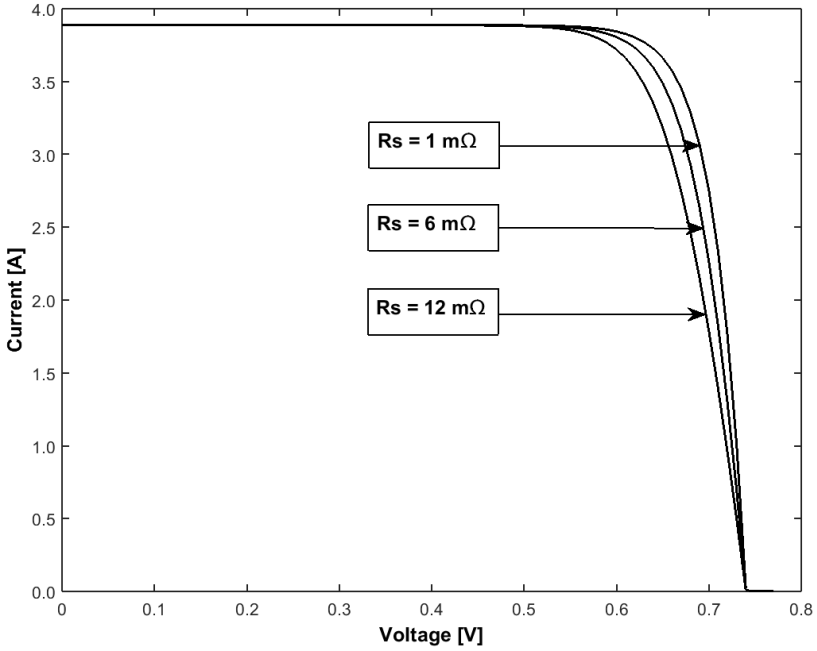

Figure 3.8: I-V curve for different Series Resistance.

When we increase series resistance from 1 mΩ to 6 mΩ then the curve has inside bending tendency. And, also the curve is more bended as we increase the series resistance value from 6 mΩ to 12 mΩ. If we decrease the values then there is outward bending tendency.

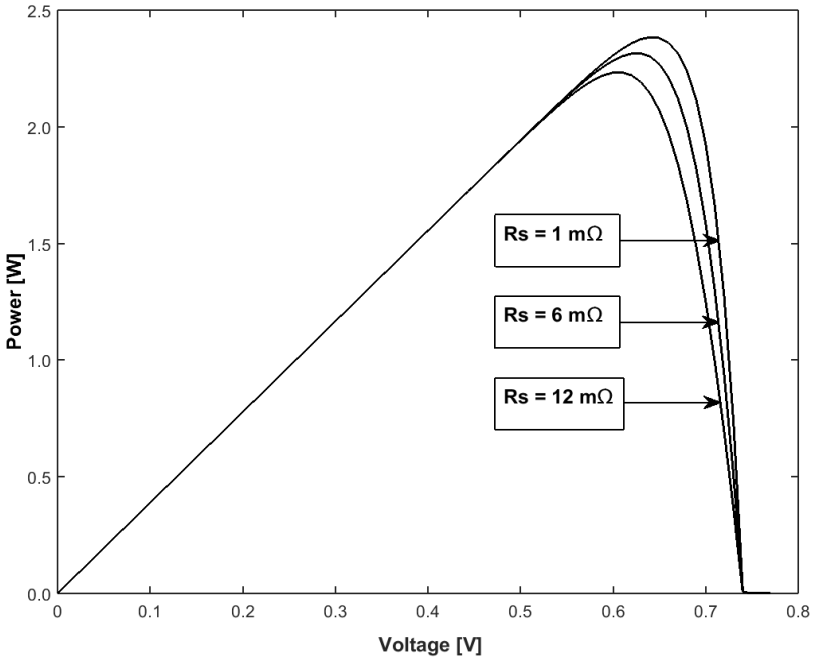

Figure 3.9: P-V curve for different Series Resistance.

From the figure 3.9 it can be seen that with the increase in series resistance there is an inward bending at the corners of the power-voltage (P-V) curve but with the increase of series resistance there is no change in cell short circuit current and open circuit voltage. Though, there is bending in the inside of the both I-V and P-V curve. This change can be seen in the generated figure. With the increase in series resistance the area under the P-V curve also decreases. With that decrease area it decreases the power output of the cell as well.

For simulation purpose we used the values for resistances 1 mΩ, 6 mΩ, and 12 mΩ. There is decrease in the slope of the power curve with the increase of the series resistance. If we increase the value of the series resistance from 1 mΩ to 6 mΩ the the P-V curve bends in its inside part that means that the area has decreased in that P-V curve. So, with the increase of series resistance in a PV cell there is decrease in the total output power. And, with the decrease in series resistance there is an increase in I-V and P-V curve which results an increase in maximum power point also [22] [27] [18].

The fill factor (FF) is the area of the largest rectangle which will fit in the IV curve. It is a measure of the 'square-ness' of the solar cell. There is a relation between the fill factor (FF) and the series resistance of the diode. It is found that with the increase of series resistance the fill factor (FF) decreases [21]. It can be defined as the ratio of the maximum power from the solar cell to the product of open circuit voltage (V_{oc}) and short circuit current (I_{sc}). The equation is shown as

$$FF = \frac{V_{mp} \times I_{mp}}{V_{oc} \times I_{sc}} \quad (\mathbf{3.21})$$

3.2.5 Shunt Resistance Variation Effects

Shunt resistor is also a vital parameter for a solar PV cell. It is a precision device which is used in an electrical circuit to measure the current. The meaning of shunt is the process of turning aside or moving an alternative course actually. The main purpose of using it is to measure high current. In a PV cell equivalent circuit, it is used with the load, diode and photo current parallelly.

In order to have better output the shunt resistance of a PV cell must have to be good and high enough. After simplifying the load current equation we can obtain the simplified equation of the shunt resistance. it is represented by the equation 3.22.

$$R_{sh} = \frac{\left(V + R_s I\right)}{\left(I_{ph} - I_s\left(\exp\left(\frac{qV + qR_s I}{NKT}\right) - 1\right) - I\right)} \quad (\mathbf{3.22})$$

So, it is the simplified equation of the shunt resistance that is dependent on the other parameters of a PV cell.

The shunt resistor plays an important role in the PV performance. With the variation of shunt resistances there are considerable changes in the output power. Next part the shunt resistance variation in a PV cell is discussed. The considered values for the shunt resistances are 1, 3 and 20 Ω. The generated current-voltage (I-V) for various shunt resistance is shown [22] [59] [18].

Figure 3.10 shows the current-voltage (I-V) curve for the different series resistances. From the figure it can be seen that there is an outward bending at the MPP point of the curve. So, if we increase the shunt resistance of a PV cell then there is an increase in its voltage also.

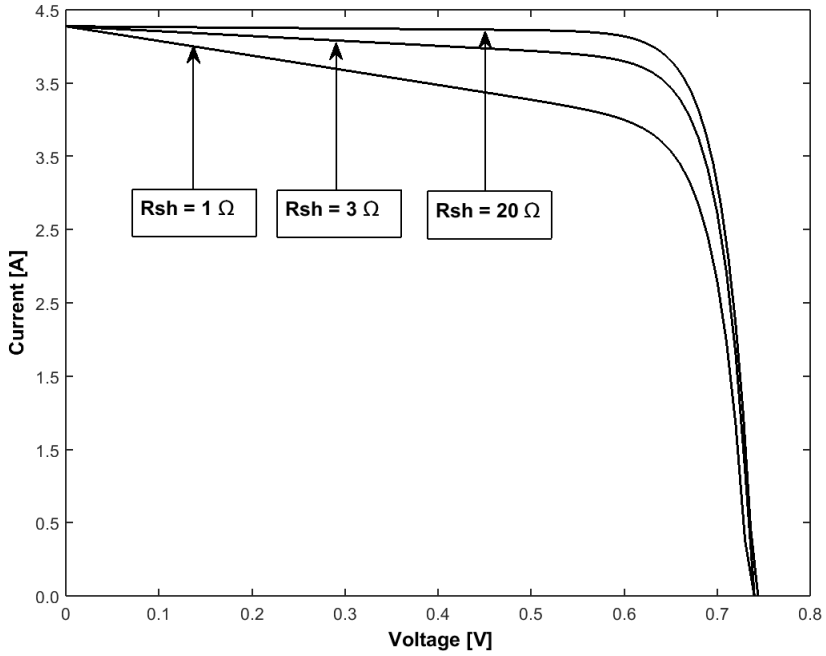

Figure 3.10: I-V curve for different shunt resistance.

As we look at the figure 3.10 we can see that with the change of shunt resistances value from 1 Ω to 3 Ω the I-V curve has an outward bending that results an increase in the voltage. The voltage increases from 737 mV to 738 mV and the current increases from 3.882 A to 3.886 A. It shows the same result as we change the value from 3 Ω to 20 Ω. The voltage increases from 738 mV to 741 mV and the current increases from 3.886 A to 3.887 A.

Table 3.7: Result Analysis of different Shunt resistance variation (I-V Curve).

Shunt Resistance [Ω]	I_{sc} [A]	V_{oc} [mV]	I_{sc} Increase [mA]	V_{oc} Decrease [mV]
1	3.882	737	n/a	n/a
3	3.886	738	4	1
20	3.887	741	1	2.5

Concluding we can say that there is increase in I-V and P-V curve with the increase of shunt resistance value and decrease in curves with the decrease in shunt resistance.

Next we discuss the power-voltage (P-V) curve of the PV cell for different shunt resistances. The figure 3.11 describes the power-voltage (P-V) curve for the different values of shunt resistance.

In previous figure 3.10 we have seen that with the increase of shunt resistance there is increase in I-V curve [18] [20] [22] [21].

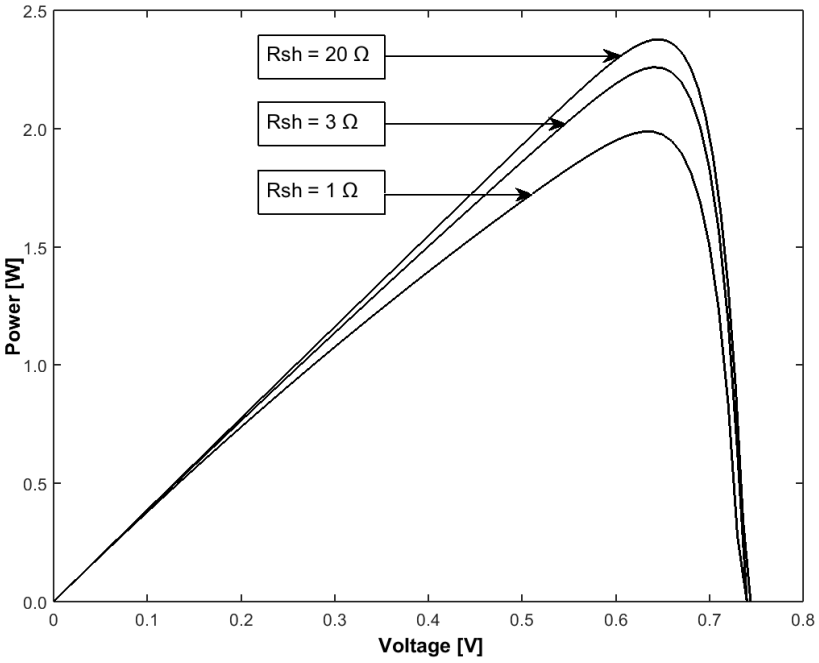

Figure 3.11: P-V curve for different shunt resistance.

There is increase in power-voltage (P-V) curve with the increase of shunt resistance. As we can see in the figure 3.11 that with the increase of shunt resistance the maximum power point (at P-V curve) has outward bending that results an increase in MPPT as well.

Table 3.8: Result Analysis of different Shunt resistance variation (P-V Curve).

Shunt Resistance [Ω]	I_{mp} [A]	V_{mp} [mV]	MPP [W]	MPP Difference [mW]
1	3.679	640	2.36	n/a
3	3.675	650	2.39	30
20	3.700	648	2.40	10

From the above table we find that with the increase of shunt resistance there is increase of maximum power point by outward bending of the P-V curve. The values at shunt resistance of 1 Ω are: current at maximum point 3.679 A, voltage at maximum point 640 mV and the maximum power point value is 2.36 W. If we change the value of shunt resistance from 1 Ω to 3 Ω the power increases with the increase of shunt resistance. The MPP at this point is 2.39 W and the increased value of MPP is 30 mW.

The MPP at shunt resistance of 20 Ω is 2.40 W. So, it is also increased from the previous value. The MPP difference between the previous and present is 10 mW. In conclusion we can say that in every case there is an increase of maximum power point with the increase of shunt resistance.

3.2.6 Saturation Current Variation Effects

The reverse saturation current of a diode is another parameter that affects the cell behaviour. The influence of diode reverse saturation current on PV cell characteristics cannot be ignored. It is also known as dark saturation current of diode. It is an extremely important parameter which value varies different diode to diode. It is the measure of the recombination of a device.

The diode which has larger recombination will have more saturation current. An excellent discussion of the variation of the diode reverse saturation current and its effect is described in the next part. The used values for the saturation current (I_s) of simulation purpose are 1 nA, 20 nA and 100 nA. The simulated I-V curve is shown in figure 3.12.

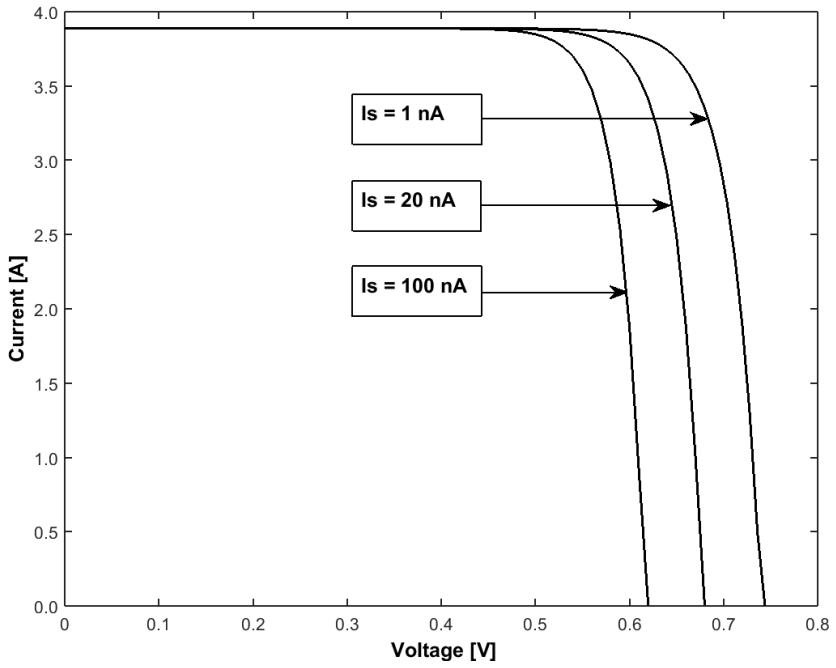

Figure 3.12: I-V curve for different saturation current.

Figure 3.12 shows the current-voltage (I-V) curves for the different diode reverse saturation current variation. It can be clearly seen from the figure 3.12 that with the increase of saturation

current there is changes in I-V curves. The most interesting matter is that the short circuit current does not change that much, it remains almost same.

From the result we see that value of short circuit current (I_{sc}) is 3.89 A and that is same for every saturation current. At saturation current of 1 nA, the value of open circuit voltage (V_{oc}) is 670 mV and short circuit current (I_{sc}) is 3.89 A. As we increase the saturation current value from 1 nA to 20 nA we can see the variation of I-V curves in the presented figure. There is an inward bending of the I-V curve and there is a decrease in open circuit voltage. At 20 nA, the open circuit voltage is 584 mV. So, with the increase of 19 nA of saturation current there is decrease of open circuit voltage with 584 mV.

And, if we change the value from 20 nA to 100 nA then we can see that it decreases the open circuit voltage but the short circuit current remains same. The open circuit voltage at 100 nA is 0.532 V. With the comparison between the open circuit value at 20 nA and 100 nA it shows that it decreases 0.052 V.

Table 3.9: Result Analysis of different saturation current variation (I-V Curve).

Saturation Current [nA]	(I_{sc}) [A]	(V_{oc}) [mV]	I_{sc} Increase [A]	V_{oc} Decrease [mV]
1	3.89	670	n/a	n/a
20	3.89	584	n/a	86
100	3.89	532	n/a	52

The above table shows the result analysis of different diode reverse saturation current variation for current-voltage curve of a PV cell. It shows the decrease in open circuit voltage and I-V curve with the increase of reverse saturation current. In the next part we discuss the power-voltage curve for the variation of the saturation current of a PV cell.

The figure below shows the power-voltage curve for different saturation current. As we can look at the figure we see that there is inside bending of P-V curve with the increase of saturation current. The open circuit voltage also decreases with the decrease in maximum power point [18] [20] [22].

The figure 3.15 shows the power-voltage curve for different values of saturation current. The figure is presented in here.

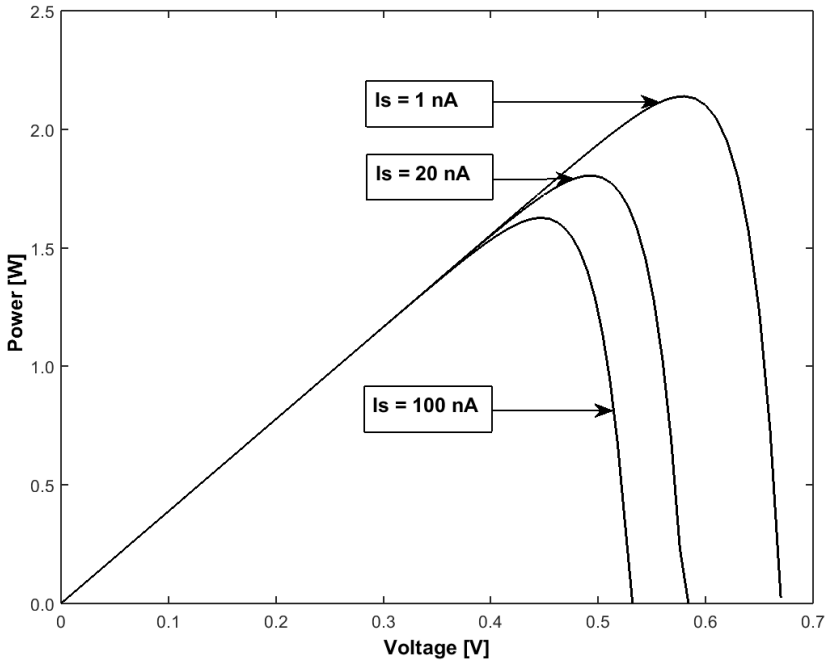

Figure 3.13: P-V curve for different saturation current.

From the simulation result we can see that there is decrease in maximum power point (MPP) with the increase in diode reverse saturation current. The value of MPP at 1 nA is 2.14 W. Then, while we increase the saturation current from 1 nA to 20 nA the MPP decreases as there is decrease in P-V curve. The value of MPP at 20 nA is 1.80 W. Also, in the next level if we increase the value of saturation current from 20 nA to 100 nA then there is also decrease in MPP of the curve. The MPP value at 100 nA is 1.63 W.

The result analysis of the P-V curve for different saturation current is shown in table below:

Table 3.10: Result Analysis of different saturation current (P-V Curve).

Saturation Current [nA]	I_{mp} [A]	V_{mp} [mV]	MPP [W]	MPP Decreases [mW]
1	3.69	580	2.14	n/a
20	3.64	496	1.80	340
100	3.63	448	1.63	170

From the result described in table 3.17 we can see that with the increase of saturation current there is decrease in maximum power point (MPP) of a PV cell [29] [20] [22] [21] [18]. With the increase in saturation current the current at maximum power point (I_{mp}) and voltage at maximum power point (V_{mp}) also decreases which results in the decrease in maximum power point (MPP).

3.2.7 Ideality Factor Variation Effects

The measure of closeness with the ideal diode equation of a diode is the diode ideality factor. The characteristics of PV cell have dependency on the variation of the diode ideality factor. It has influence on the I-V and P-V curve of the solar cell. In this section the variation effects of the PV cell on diode ideality factor is discussed.

The used values of the diode ideality factor (N) for the simulation are 1, 1.1 and 1.2. The obtained current-voltage (I-V) curve for various diode ideality factors is presented in figure 3.14.

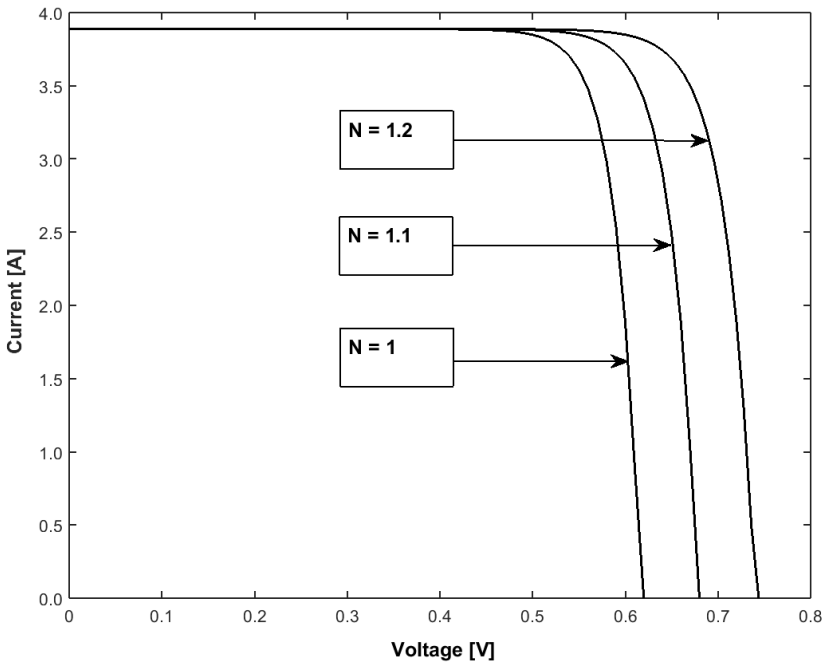

Figure 3.14: I-V curve for different diode ideality factor.

Figure 3.14 shows the current-voltage (I-V) curve variation for different diode ideality factor (n). It shows that with the increase there are changes by increase in I-V curve [18] [29] [20] [59] [21].

From the result analysis we can see that the diode ideality factor has an increasing tendency in the I-V curve. As we increase the ideality factor there is increase in that curve. The value of short circuit current remains same with the variation of ideality factor (n).

The value of open circuit voltage (V_{oc}) at ideality factor of 1 (one) is 620 mV and the short circuit current (I_{sc}) is 3.89 A. With the change of the ideality factor to 1.1 from 1 then the value of short circuit current (I_{sc}) remains same and the open circuit voltage (V_{oc}) increases that is 680 mV. Then if we increase the ideality factor value to 1.2 from 1.1 then the short circuit current value remains same but open circuit voltage increases that is 744 mV.

With the variation of ideality factor from 1 to 1.1 and 1.2 the open circuit voltage increases 60 mV and 64 mV consecutively.

Table 3.11 shows the result analysis. After the analysis, it is achieved that with the increase in diode ideality factor there is increase in open circuit voltage. So, with the increasing variation of ideality factor there is increasing tendency of I-V curve of a PV cell [18] [20] [22] [21].

Table 3.11: Result Analysis of different saturation current variation (I-V Curve).

Ideality Factor	I_{sc} [A]	V_{oc} [mV]	I_{sc} Increase [mA]	V_{oc} Increase [mV]
1	3.89	620	n/a	n/a
1.1	3.89	680	n/a	60
1.2	3.89	744	n/a	64

In the next we are going to discuss the power-voltage (P-V) curve of the PV cell for various values of diode ideality factor. The obtained power-voltage (P-V) curve for various diode ideality factors is presented in figure 3.15.

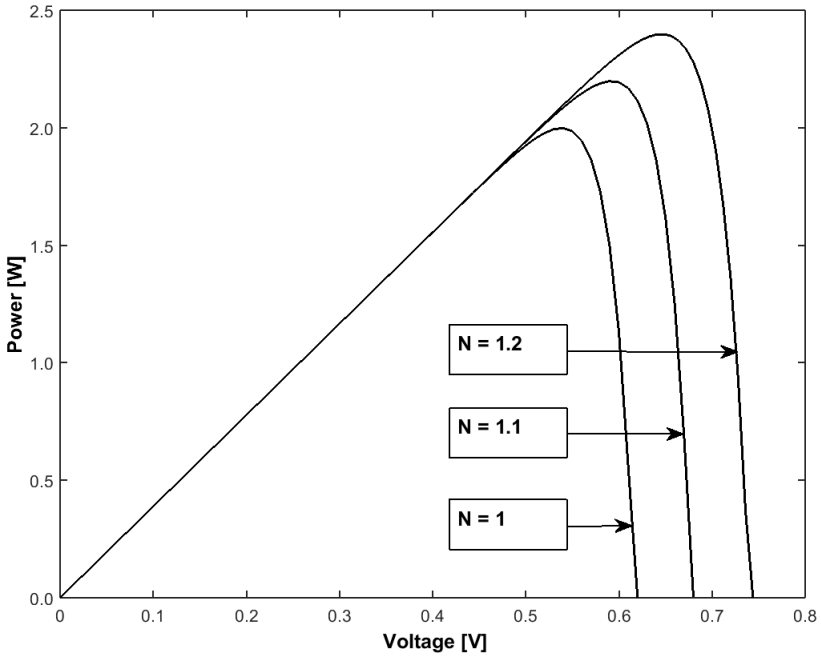

Figure 3.15: P-V curve for different diode ideality factor.

Figure 3.15 represents the power-voltage (P-V) curve for various diode ideality factors. From the figure we find that with the variation of ideality factor there are changes in P-V curve definitely. As we increase the value of ideality factor there is increase in the power curve too. It results with the increase in maximum power point (MPP) [59] [18].

Table 3.12: Result Analysis of different ideality factor (P-V Curve).

Ideality Factor	I_{mp} [A]	V_{mp} [mV]	MPP [W]	MPP Increases [mW]
1	3.70	540	2.00	n/a
1.1	3.72	590	2.20	200
1.2	3.70	648	2.40	200

The above table 3.12 describes the results obtained by simulation from the PV cell. It shows the variation of the ideality factors and its influences on the PV characteristics. If we analyse the result we see that the value of maximum power point at ideality factor of one (1) is 2.00 W. And, current at maximum point is 3.70 A and voltage at maximum point is 540 mV. With the increase of the value of ideality factor from 1 to 1.1 then the value of MPP increases that is2.20 W and the difference of MPP between 1 and 1.1 is 200 mW.

The value of current at maximum point at this stage is 3.72 A and value of voltage at maximum point is 590 mV. So, there is increase in MPP after increasing ideality factor. The results are same with the change from 1.1 to 1.2. At this point we find the MPP is 2.40 W which is 200 mW higher than the MPP value at ideality factor of 1.1. The current value at maximum power point is 3.70 V and voltage value at maximum power point is 648 mV. In here, we see that there is also increase with the increase in diode ideality factor.

In the previous discussion we have analysed the parameters variation of PV cell by bisection algorithm method for numerical analysis. In this part, we analyse the simulated figures obtained by Newton-Raphson algorithm method. The result and discussion for parameters variation on a PV cell is described in the next part.

3.2.8 Simulation Parameters

The single diode PV cell with five parameters is used to study the model. Based on the load requirement it can add another sufficient number of cells in series or parallel in this model. The PV cell's parameters specifications are presented in the table 3.13.

Table 3.13: Parameters Specifications.

Name	Symbol	Unit	Value
Ideality Factor	N	n/a	1.2
Electron Charge	q	C	1.6×10^{-19}
Series Resistance	R_s	mΩ	0. 01
Shunt Resistance	R_{sh}	Ω	10000
Solar Radiation	I_r	Wm^{-2}	1000
Boltzmann's Constant	K	$m^2kgs^{-2}K^{-1}$	1.3806488×10^{-23}
Saturation Current	I_s	A	1×10^{-10}
Junction Temperature	T	K	293.15
Temperature Coefficient	k_i	A/ºC	0.0017
Short Circuit Current	I_{sc}	A	3.885
Open Circuit Voltage	I_{oc}	V	0.74

These are the parameters used in the simulation that is given by the industry datasheets. But, the values might vary in accordance with the types of PV cell and its efficiency. We considered the mono-crystalline silicon solar cell for the characterization purpose.

There are some parameters values are constant; in that case the values are used their as usual values. In the next section parameters characterization by varying its important and most significant parameters is presented. The main purpose is to analyse and characterise the whole PV system by analysing a single diode PV cell.

3.2.9 I-V Curve (Current-Voltage) curve of a PV Cell

In the figure 3.16 a typical current-voltage (I-V) characteristic of the solar cell is given. In the I-V curve generation process, specific value of solar radiation, ambient temperature and other values given by the data sheet are used. The obtained I-V curve after simulation is presented in the figure 3.16.

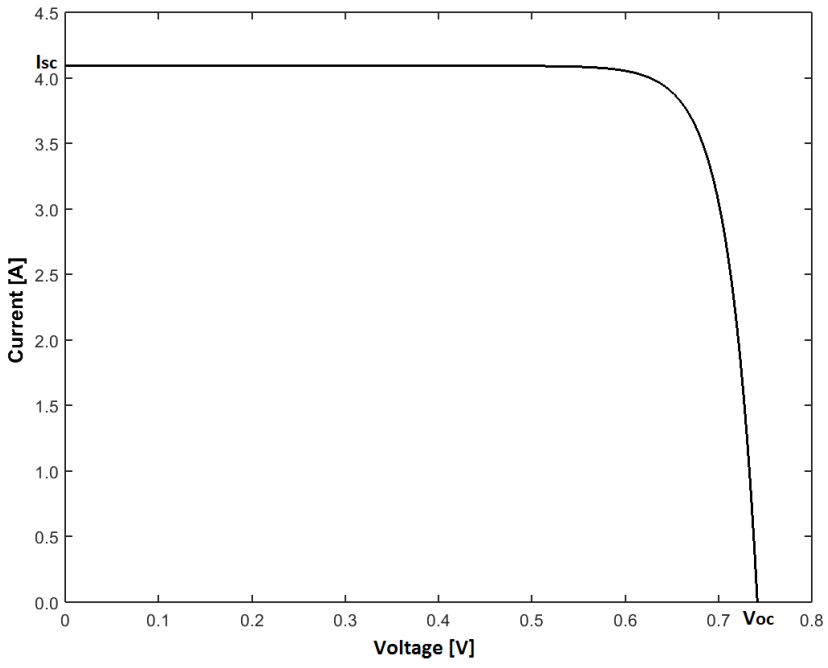

Figure 3.16: I-V curve of a solar photovoltaic cell.

The current-voltage (I-V) curve is generated by the simulation in Matlab. From the I-V curve, it is seen that a PV cell is a constant current source at low voltages. It means that it behaves like a constant current source that is almost close to its short circuit current. The curve shows the behaviour of the current with respect to its voltage. There is a short circuit current (I_{sc}) in the

curve where current value is maximum and open circuit voltage (V_{oc}) where voltage value is maximum. The obtained primary value for short circuit current is 4.1 ampere and open circuit voltage is 743.2 mV.

3.2.10 P-V Curve (Power-Voltage) curve of a PV Cell

In the following figure 3.17 the typical power-voltage (P-V) characteristics curve of a photovoltaic solar cell is presented. In order to generate power-voltage (P-V) curve, certain value of solar radiation, ambient temperature and other values specified by industry are used. The obtained P-V curve after simulation is shown in the figure 3.17.

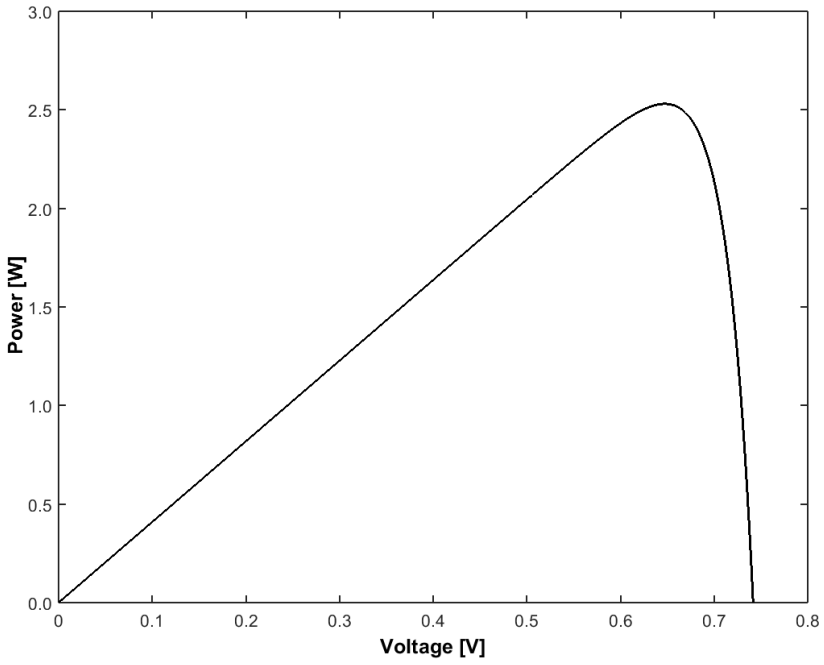

Figure 3.17: P-V curve of a solar photovoltaic cell.

The above generated figure 3.17 is obtained by simulation in MATLAB. It is the typical power-voltage (P-V) curve of a PV cell with standard values. Power is obtained by the multiplication of both current and voltage. The main purpose of the P-V curve is to show the characteristics of the curve with its output behaviour. We can represent the electrical characteristics of solar cells by I-V and P-V curve.

3.2.11 Solar Radiation Variation Effects

The used values for the various solar radiations are 500, 750 and 1000 Wm^{-2}. The obtained current-voltage (I-V) curve for different solar radiation values is presented in figure 3.18.

From the figure 3.18 we can see that with the increase of solar radiation there is increase of current-voltage (I-V) curve of a PV cell.

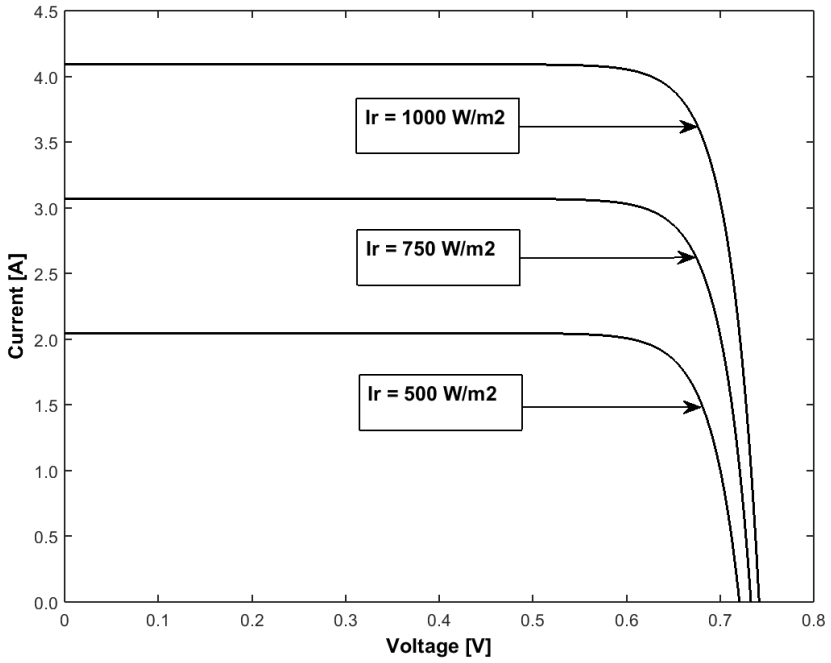

Figure 3.18: I-V curve for different solar radiation.

The obtained power-voltage (P-V) curve for different solar radiation values is presented in the figure 3.19. From the power-voltage (P-V) curve we can see that there are changes with the variation of solar radiation. If we increase the solar radiation there is increase in the P-V curve. As there is increase in the curve it also increases the maximum power point (MPP) too. So, we can conclude that if we increase the solar radiation then there is increase in the power also.

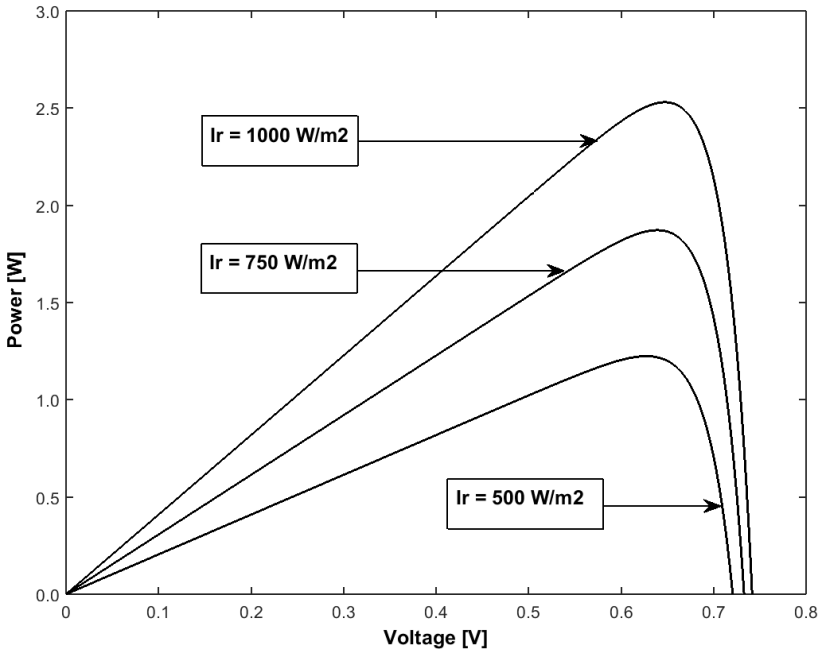

Figure 3.19: P-V curve for different solar radiation.

3.2.12 Temperature Variation Effects

Temperature is one of the most important factors in solar photovoltaic system. The temperature has an effect on the efficiency of a solar cell and its characteristics. The voltage is highly dependent on the cell ambient temperature. There is a relation between diode reverse saturation current and temperature also. It (reverse saturation current) can be expresses as the cubic function of the temperature [21] [20] [22].

The equation is as follows:

$$I_s(T) = I_s\left(\frac{T}{T_{nom}}\right)^3 \exp\left[\left(\frac{T}{T_{nom}} - 1\right)\frac{E_g}{N.V_t}\right] \tag{3.22}$$

In the figure 3.20, the different temperature variation effect on the I-V curve of a PV cell is presented. The considered values for the temperature are 20°C, 40°C and 60°C. It is mostly important to know the temperature level during simulation and real calculation in order to characterize the solar PV cell [25]. The generated I-V curve is presented in the figure 3.20.

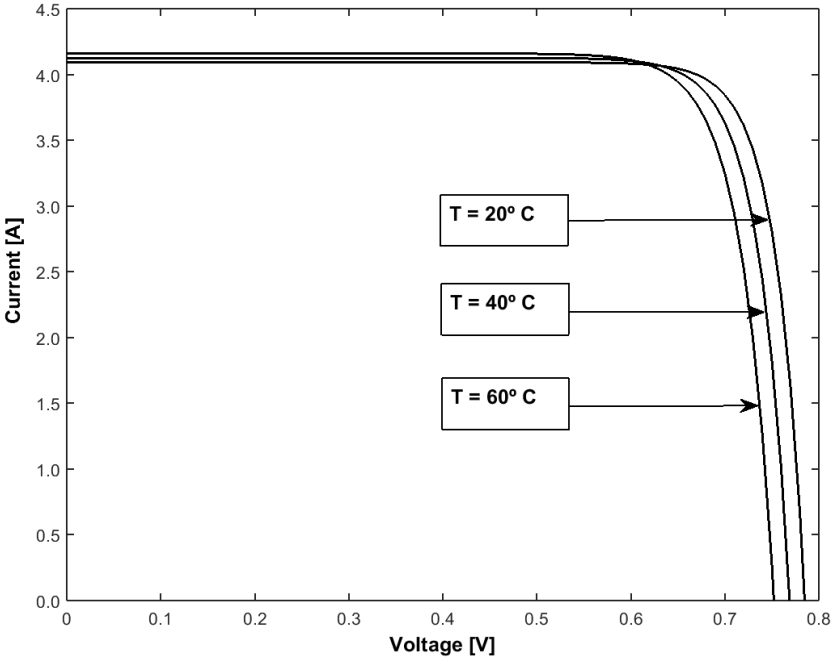

Figure 3.20: I-V curve for different cell temperature.

Here, we can see that if we increase the cell temperature there is decrease in open circuit voltage; but slight increase in cell short circuit current. Next part, we present the P-V curve characteristics with the changes of temperatures. The generated power-voltage curve is presented in the figure 3.21.

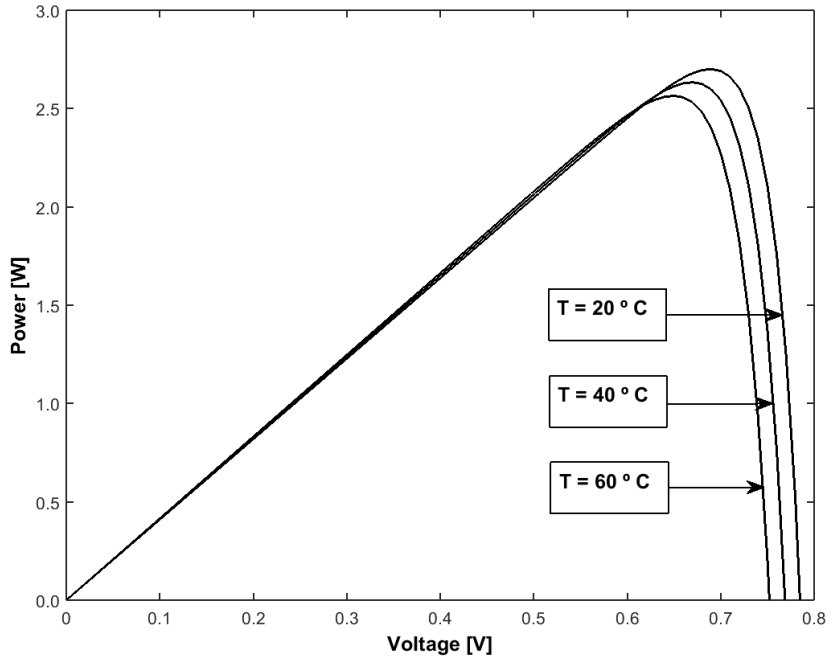

Figure 3.21: P-V curve for different cell temperature.

From the figure 3.21 we can see that with the increase of temperature from 20ºC to 40ºC and 40ºC to 60ºC there is decrease in open circuit voltage of the cell. With the increase in temperature decrease in output that results decrease in Maximum Power Point (MPP) of the cell also.

In the previous description, we explained the variation of parameters and its effects on the characteristics of PV cell/panel. In here, only irradiance and temperature is considered to show the parameters variation. Newton-Raphson algorithm is used here as the numerical analysis. In all of the parameters variation analysis we have used two different numerical algorithms that were implemented in the PV cell characterization. From the above explanation, we found that both methods have its own way of characterization. The characteristics of the two methods are explained here [30].

In the bisection method, the convergence is guaranteed, the root solution is expected to have all the time but speed of convergence is slow. In the Newton-Raphson method, it does not guarantee that we will have our solution because derivative is very sensitive. We have to guess one initial value. This initial value must be approximated to the root we want to find.

3.3 SIMULINK MODEL

3.3.1 Simulink Output

The main objective of this section is to generate and analyse the characteristics of current-voltage (I-V) and power-voltage (P-V) curve of PV cell/module by using MATLAB/Simulink. The main interface of the drawn simulink PV system is presented in the figure 3.22.

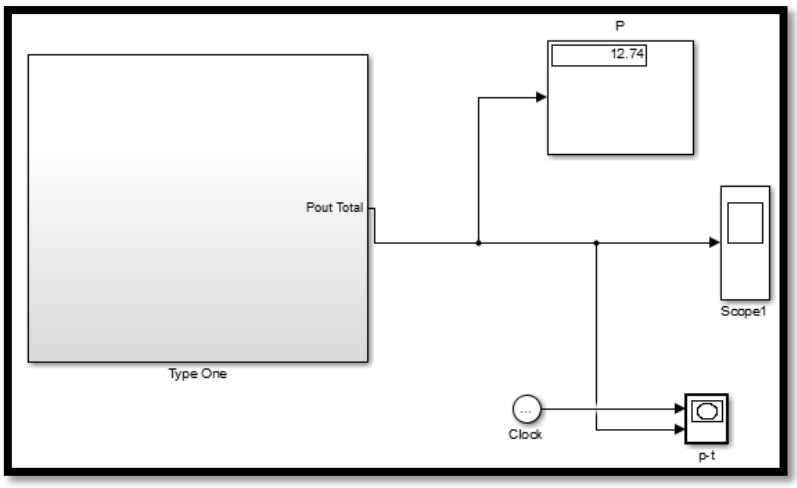

Figure 3.22: The main interface of the simulink PV system.

Figure 3.22 contains the PV system including power output and internal mechanism or management system in the type one part. The total considered power in here is 12.74 W.

In this part we consider the stand alone solar photovoltaic system and it deals with Direct Current (DC) only. The internal part of the management system contains voltage output system, a charge controller, a management system, battery for storage, control monitoring platform and loads platform. The internal part of the PV system is shown in the figure 3.23.

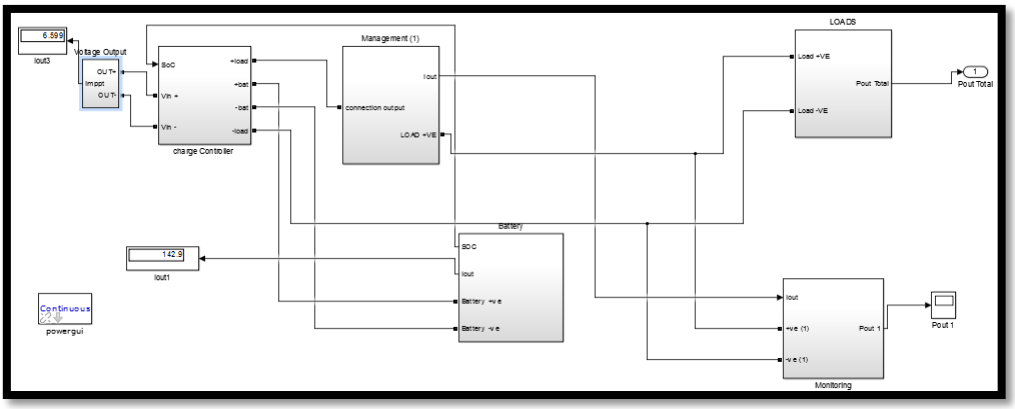

Figure 3.23: Overall view of the PV system.

A PV module is combined with many cells together and it is the primary component of a photovoltaic system. It represents the basic power conversion unit. They are made from semiconductor and converts sunlight into electricity. The block models a solar cell as a parallel combination of a current source, two exponential diodes and a parallel resistor (Rp), that are connected in series with a resistance (Rs).

The simulink diagram of a PV module consists of a set of cells connected together. There are 60 cells connected in series is considered in the PV module in here. The cells are used to obtain the DC current from the irradiance in order to use to in the stand alone solar system load. In here, we find the value of maximum voltage, maximum power output which gives I-V and P-V curve in result. The maximum power with maximum voltage and current is also calculated here. The generated simulink diagram of the PV module is presented in the figure 3.24.

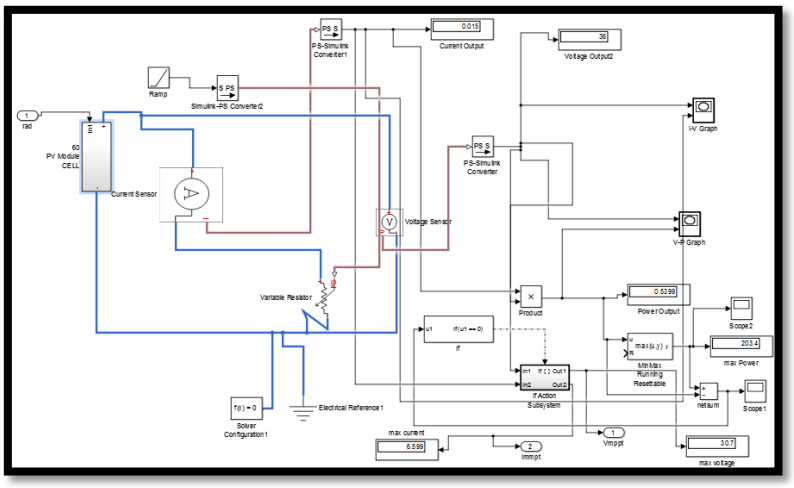

Figure 3.24: The simulink diagram of the PV module.

Table 3.14: Properties of used solar cell.

Name	Symbol	Value	Unit
Saturation Current	Is	1e-6	[A]
Photo Current	Iph	7.34	[A]
Irradiance	Ir	1000	Wm^{-2}
Ideality Factor	N	1.5	n/a
Series Resistance	Rs	0	[Ω]
Parallel Resistance	Rp	Infinity	[Ω]

We considered 60 solar cells that have a voltage of each 0.6 V. So, theoretically in here total voltage is 36 Volt.

A solar charge controller is known as voltage regulator as we use it to regulate the output voltage of a PV module and to send the regulated voltage to the load management. A solar regulator is a small box consisting of solid state circuitry that is placed between a solar panel

and a battery. Its function is to regulate the amount of charge coming from the panel that flows into the deep cycle battery bank in order to avoid the batteries being overcharged. A regulator can also provide a direct connection to appliances, while continuing to recharge the battery. The simulink model of solar charge controller is shown in the figure 3.25.

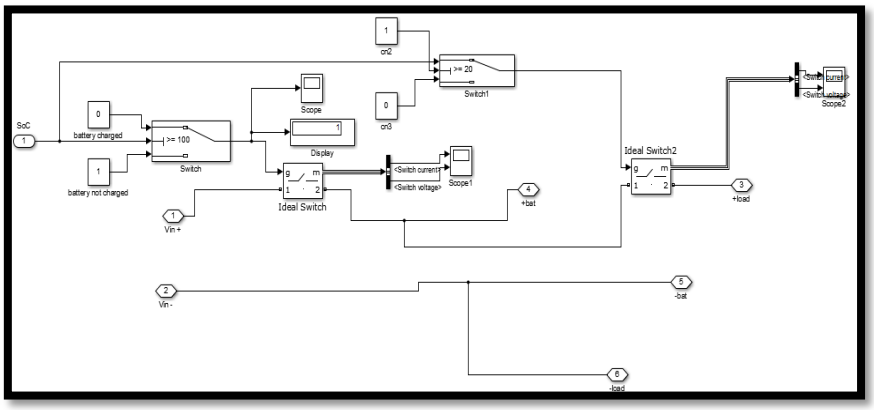

Figure 3.25: The simulink diagram of solar charge controller.

In the solar charge controller few switches are used in order to control the state of charge of the battery. If the battery is 100% charged then it will be disconnected in order to stop from over charging the battery. And, if the battery is discharged up to 20% then it will not be connected with the load means it will be disconnected.

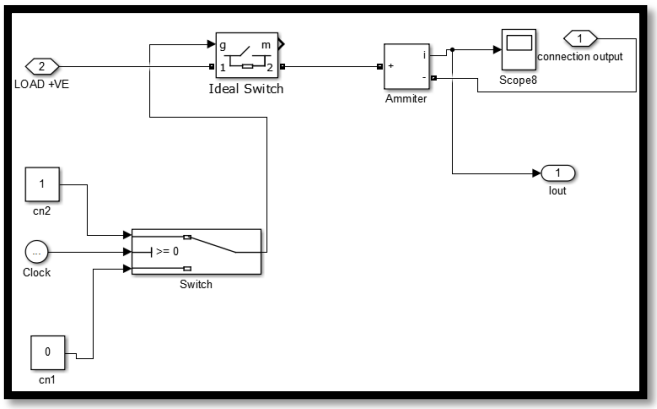

Figure 3.26: The simulink diagram of management system.

The management system is the important part of the program. That part lies between the charge controller and the load profiles. We used the switches to control the loads and it varies according to the load profiles. In next part we are going to describe about the battery what is

used as the storage of the solar system. The most used common type of battery is used in stand-alone solar systems comprises rechargeable lead-acid batteries. In my cases it is not different too.

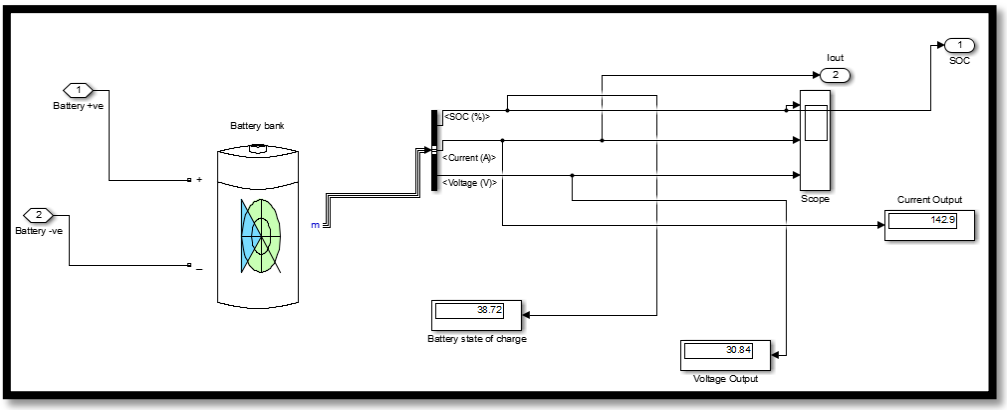

Figure 3.27: The simulink diagram of the used battery.

The properties of the Lead-Acid battery are presented in the table 3.15.

Table 3.15: Properties of used battery.

Parameter	Value	Unit
Nominal Voltage	36	[V]
Rated Capacity	100	Ampere-Hour
Initial State-Of-Charge (%)	20	n/a
Maximum Capacity	104.1667	Ampere-Hour
Fully charged Voltage (V)	39.1974	[V]
Nominal Discharge Current	20	[A]
Internal Resistance	0.0036	[Ω]
Nominal Voltage Capacity	31.0278	Ampere-Hour
Exponential Zone	[36.6513, 0.3333333]	[Voltage, Ampere-Hour]

The management system for different load profiles is presented in the figure 3.28.

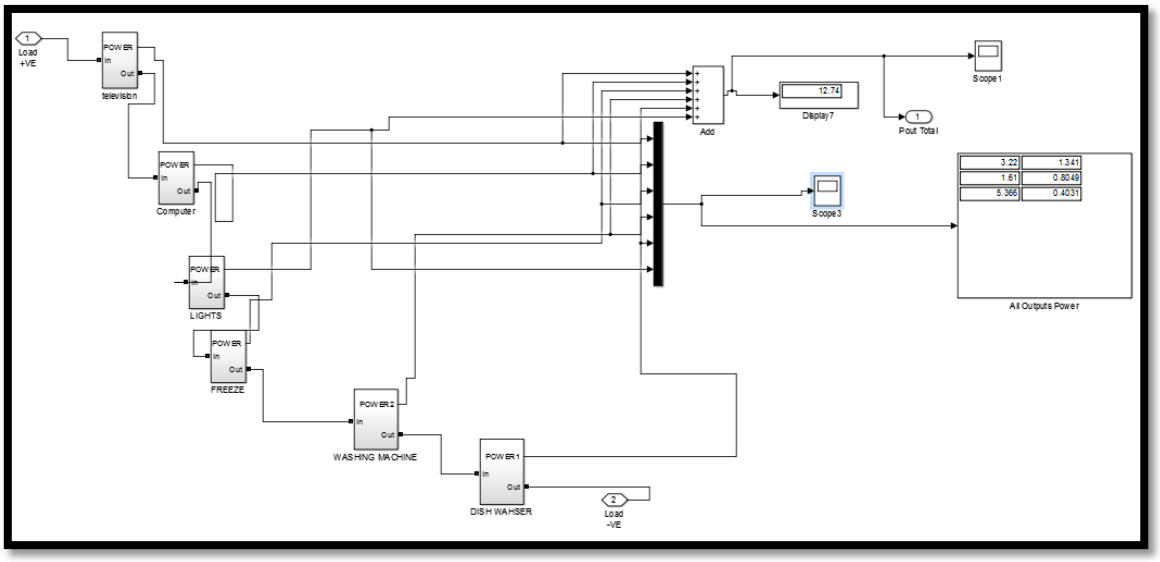

Figure 3.28: The simulink diagram of the loads with output power.

Figure 3.28 is used to accumulate the output power of the solar stand alone PV system. It shows all the related output of the used load profiles.

The used monitoring system for the load profiles is shown below:

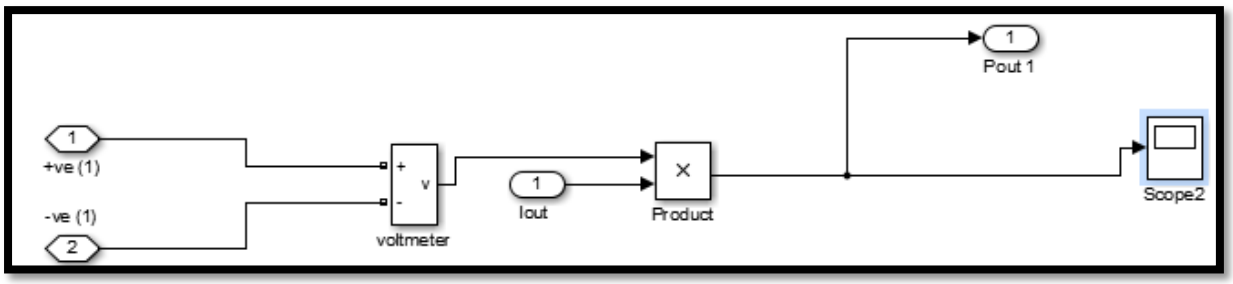

Figure 3.29: The simulink diagram of the loads monitoring system.

Figure 3.29 is used to monitor the all values of the PV system. Basically it is used as a voltmeter and also to see the output power of the system.

In my work DC load is used and all the loads are in series. The daily appliances and power consumptions theoretical value is shown below:

Table 3.16: Properties of used appliances.

No.	Appliances	Power [W]	No. of Hour [h]	Energy Consumption [WH]
1.	Television	50	3	150
2.	Computer	120	4	480
3.	Lights (4)	400	4	1600
4.	Refrigerator	100	8	800
5.	Washing Machine	200	3	600
6.	Dish Washer	30	2	60
	Total			3690 [WH]

3.3.2 Simulation Output

The generated simulation output will be shown in this part. The obtained current-voltage is presented in the figure 3.30.

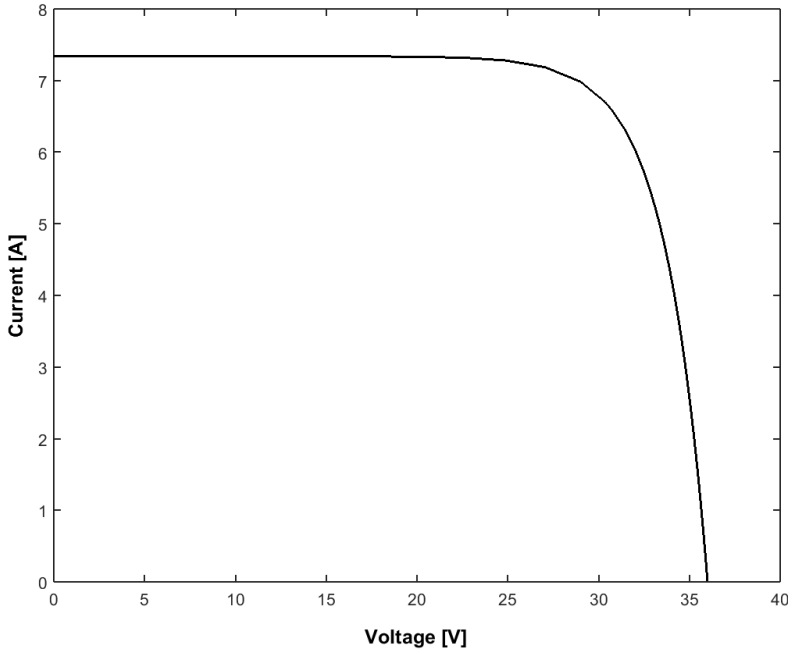

Figure 3.30: I-V curve from the simulink result.

Figure 3.30 it has the voltage values in x-axis and current values in y-axis. The obtained power-voltage curve is presented in the figure 3.31.

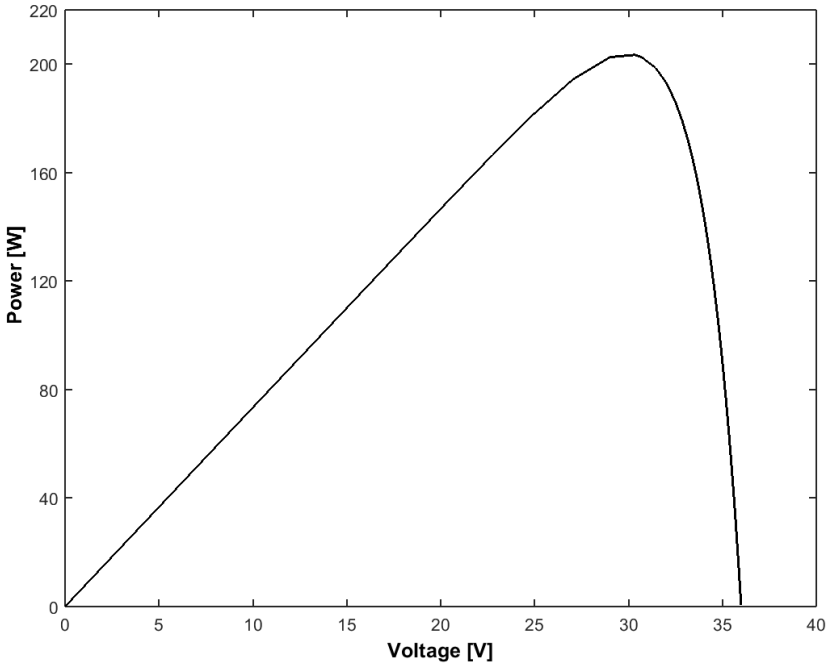

Figure 3.31: P-V curve from the simulink result.

Figure 3.31 corresponds the voltage in x-axis and power in y-axis. In the above figure there is a saturation point where current and voltage is maximum called Maximum Power Point (MPP). We have shown the solar photovoltaic cell/module characteristics for both MATLAB and Simulink simulation. The output and other characteristics are shown and described by the both process.

Till now we did the simulation of PV cell/module by MATLAB and in Simulink environment. Then we focused more on the practical and real time analysis in the laboratory environment. To do the experimental work we introduce the data analysis work by using different components.

3.4 MEASUREMENTS WITH DATA ACQUISITION SYSTEM

First, we started the discussion about the using of data acquisition for a PV panel. Before working about this topic have a glance about the introduction of “Data Acquisition”.

“Data acquisition (DAQ) is the process of measuring an electrical or physical phenomenon such as voltage, current, temperature, pressure, or sound with a computer. A DAQ system consists of sensors, DAQ measurement hardware, and a computer with programmable software. Compared to traditional measurement systems, PC-based DAQ systems exploit the processing power, productivity, display, and connectivity capabilities of industry-standard computers providing a more powerful, flexible, and cost-effective measurement solution.” [64]

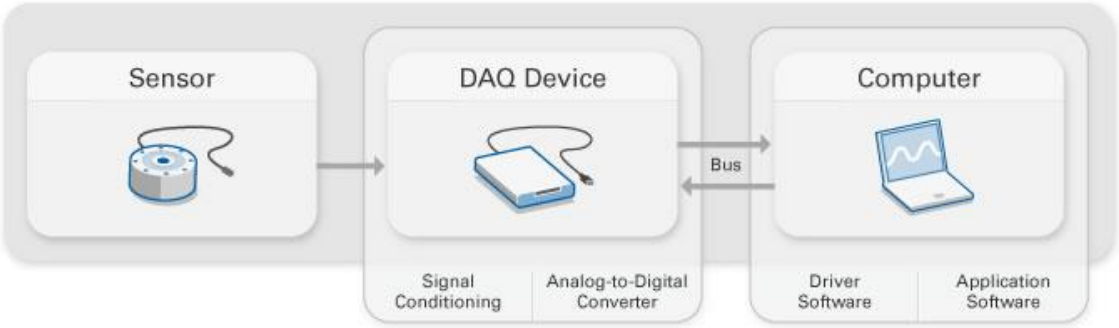

Figure 3.32: Parts of a DAQ System.

The used circuit diagram of the model is shown below:

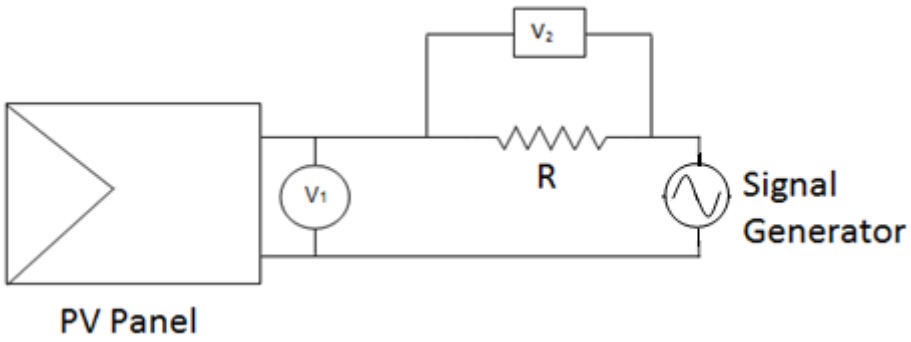

Figure 3.33: Data Acquisition Model.

In the figure 3.33, we can see that there is a PV panel, a load (resistor) approximately about 1 kΩ, a signal generator. Firstly, we calculate the voltage across the panel which will be denoted by V_1. And then we will measure the voltage across the load which is denoted by V_2. In the signal generator we will fix the values of frequency, DC offset and amplitude.

$$V_1\text{: DAQ (DC)} \rightarrow \text{CH1}$$

$$V_2\text{: DAQ (DC)} \rightarrow \text{CH2}$$

For starting the practical session we need to install software called data acquisition to the PC. For that purpose we should use a device is called NI USB 6009.

The image of NI USB 6009 is shown with details in the figure 3.34 and 3.35.

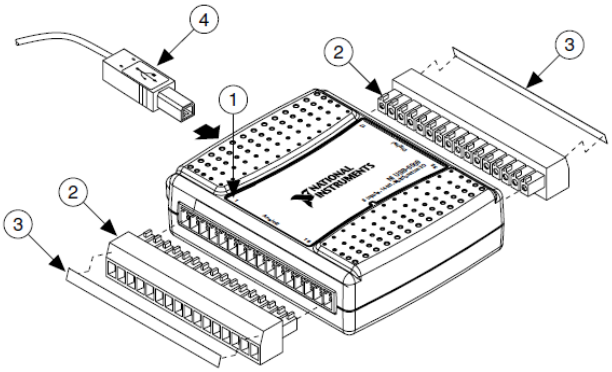

Figure 3.34: Signal Label Application Diagram.

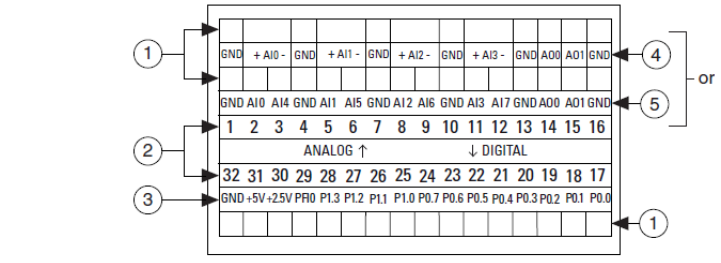

1. User-Defined Custom Label
2. Terminal Number Label
3. Digital I/O Label
4. Analog Input Differential Signal Name Label
5. Analog Input Single-Ended Signal Name Label

Figure 3.35: NI USB-6009 Signal Labels. (NI USB-6009 Manual)

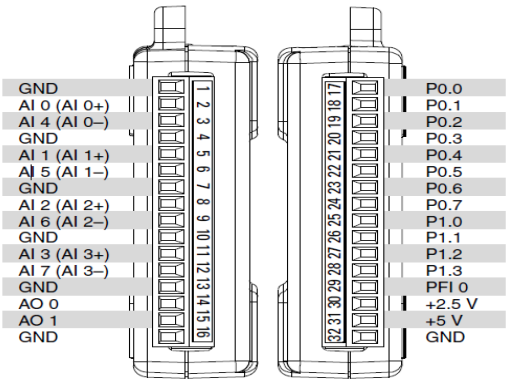

Figure 3.36: NI USB-6008/6009 Signal Descriptions.

Source: NI USB-6008/6009 Manual.

Figure 3.37: Used Function generator.

The function generator is also named as signal generator. There are four types of waveforms in the generator. The waveforms are sine, triangular, square, and DC. These types of generator are suitable for high distortion and instable signals. In our experiment we used the triangular signal.

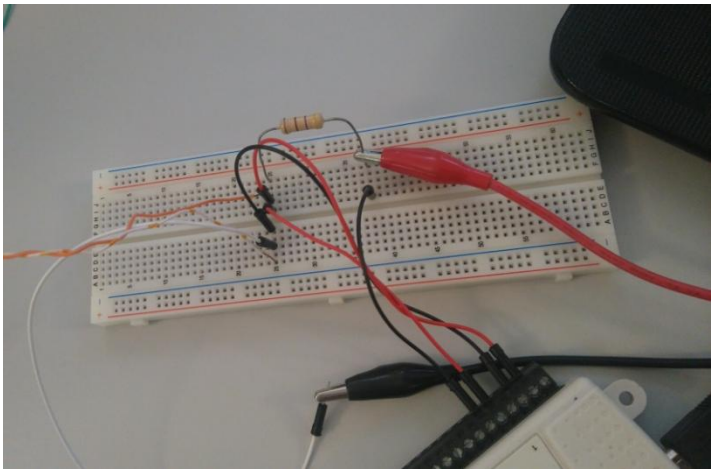

Figure 3.38: Circuit making.

To make a full circuit we required a small PV panel, a load resistance (500 Ω/1000 Ω), a data acquisition board (NI USB-6009) and the cables. In the cables red are for positive, black are negative and other colours are grounded. We have to keep in mind that channel 1 is for V_1 and channel 2 is for V_2. We connect panel with positive side, load (resistor) with positive side, channel one and channel two positive all together. And load (resistor) negative, signal generator positive and channel two negative together. On the ground we have to add negative of PV panel, negative of signal generator and negative of channel two.

After that we are ready to start our program. Before that we have to have a MATLAB program in our computer. We should calculate the open circuit voltage and at that time the grounded line should be removed from connection.

Then we run the program and we observe the outputs. We found that the curve goes to negative side. We regulate the value of amplitude, frequency and DC offset in order to achieve a better output.

The output figure by using data acquisition system is presented in figure 3.39 and 3.40.

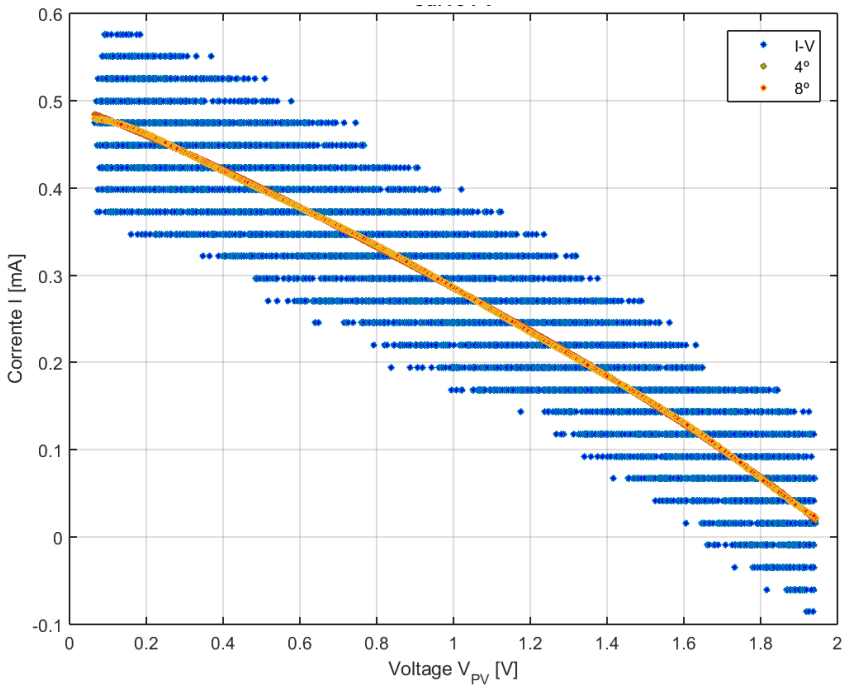

Figure 3.39: Output figure I-V curve from the data acquisition system (Without Light).

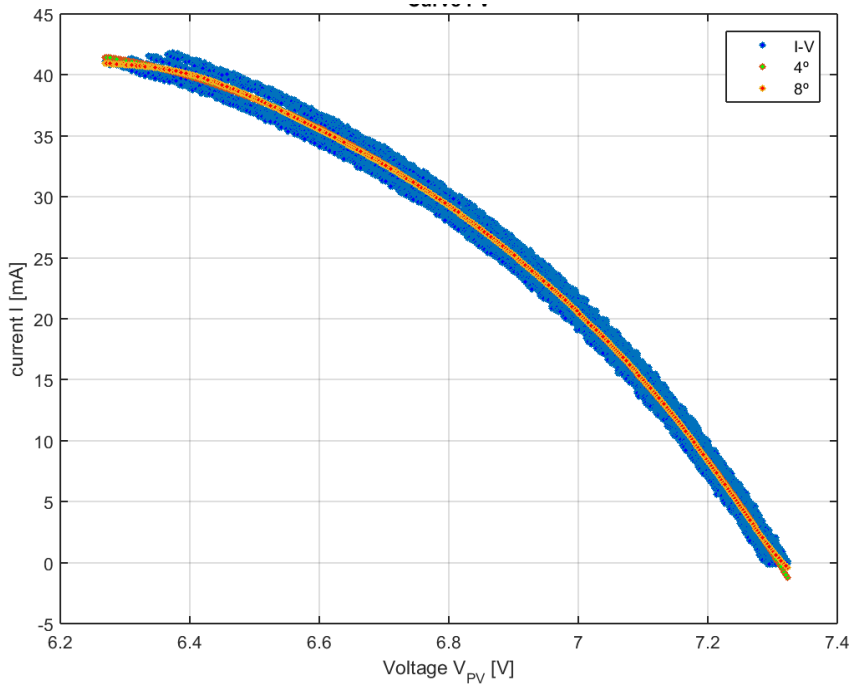

Figure 3.40: Output figure I-V curve from the data acquisition system (With Light).

Then we thought about the signal generator, the value of the amplitude, frequency and offset. Firstly we changed the signal generator and brought a good signal generator. Then we changed all its related values.

Figure 3.41: Signal generator.

In this type of signal generator we should enter the values manually. We have to fix all the values according to the output we want. But, we can control this situation by programming in MATLAB with the help of using a device. The device can be used is known as General Purpose Interface Bus (GPIB) according to IEEE-488.

Figure 3.42: GPIB Interface (NI).

3.5 EXPERIMENTAL RESULT ANALYSIS

The used lamp for the source of solar radiation is presented in the figure 3.43.

Figure 3.43: The used lamp as the source.

The lamp is used as a source in the laboratory environment. The power of the lamp is found 278 W. We considered it as enough for our experiment.

For our experiment we used mono-crystalline silicon solar PV module. Though it is very small but it is well enough for our experiment and using as characterization purpose. The image of the PV module is given below:

Figure 3.44: The used PV module for experiment.

Figure 3.44 shows the PV module of mono-crystalline silicon solar cell. For our experiment, we considered this type PV module as suitable. We focused our lamp directly on it by using certain area. After that, we took the readings by using MATLAB simulation. Then we started our experiment and the experimental results are shown below.

The first output figure of I-V curve from the experiment data is presented in the figure 3.45.

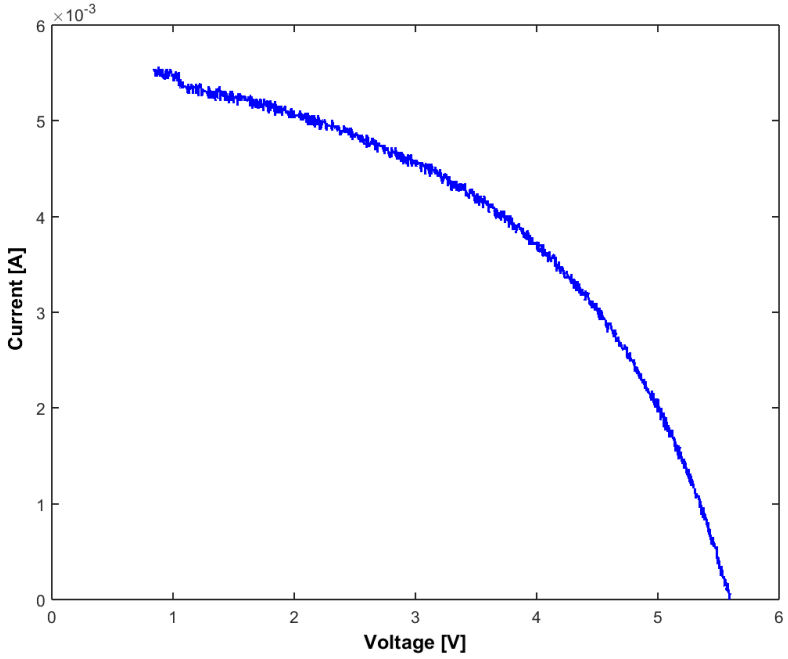

Figure 3.45: First output I-V curve from the PV system.

The above figure 3.45 obtained by experiment in the laboratory environment. This is the obtained current-voltage (I-V) curve of the PV module. It shows the I-V characteristics what we obtained in the first step of simulation. And, we took two measurements in order to grab the accurate and compare with each other result.

From the above experiment we have found that the module short circuit current (Isc) is 5.56 mA and the obtained module open circuit voltage (Voc) is 5595 mV. In the next part we discuss the power-voltage (P-V) curve of the PV module by experimentation in the lab environment. By obtaining the P-V curve we can realise the maximum power point of the module and its related characteristics as well.

Figure 3.46 shows the power-voltage (P-V) curve obtained by the experimental data sets. We obtain the maximum power point (MPP) from that curve also. From the obtained data, we find the value of MPP is 15.18 mW after calculation. The obtained power-voltage (P-V) curve by experimental value is presented in the figure 3.46.

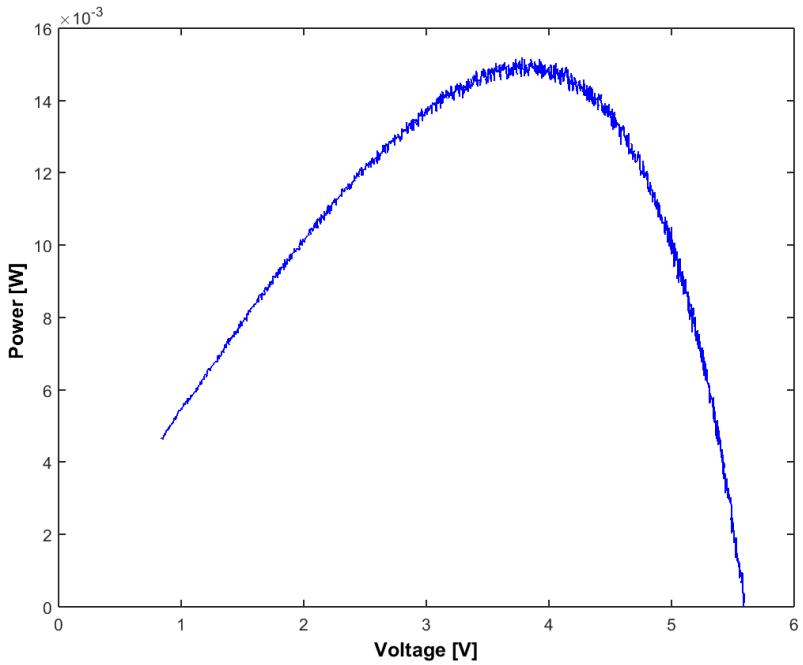

Figure 3.46: First output P-V curve from the PV system.

There are two experimental studies is conducted for the characterization purpose. And we considered ten thousand samples for obtaining the curves. In the previous part, we studied and analysed the I-V curve, P-V curve for the first experimental studies. The obtained current-voltage curve from second experimental data is shown below:

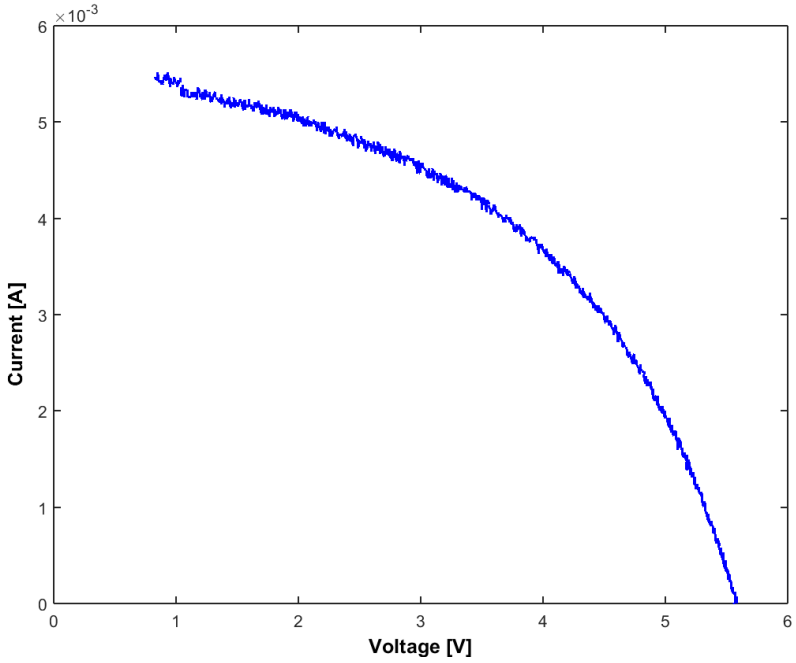

Figure 3.47: Second output I-V curve from the PV system.

Figure 3.47 shows the current-voltage (I-V) curve of a PV module obtained by the experiment in the laboratory environment. The figure contains a saturation point that is located in the middle of the curve. The main objective of experiencing the experiment is to compare with the simulated curve and to understand what happens in real time experiment.

For our case, we find the simulated curve and the experimental curve is almost similar in structure. The figure 3.47 is constructed by data set of current (I) and voltage (V) data. There is a point where the value of current is maximum that is known as short circuit current (Isc). The value of short circuit current found here is 5.51 mA. And there is a point where the value of voltage is maximum that is known as open circuit voltage (Voc). The value of open circuit voltage for this curve is 5595 mV. The obtained power-voltage curve by experimental value is presented in figure 3.48.

Figure 3.48 shows the power-voltage (P-V) curve obtained by the second experimental data sets. We can find the maximum power point (MPP) from that curve also. From the obtained data after calculation we find that the value of MPP is 14.99 mW. In the previous parts, we did the two experiments; obtained the I-V and P-V figures for both cases. The obtained values from both sides were almost close to each other. It was not that difference to be counted between the values.

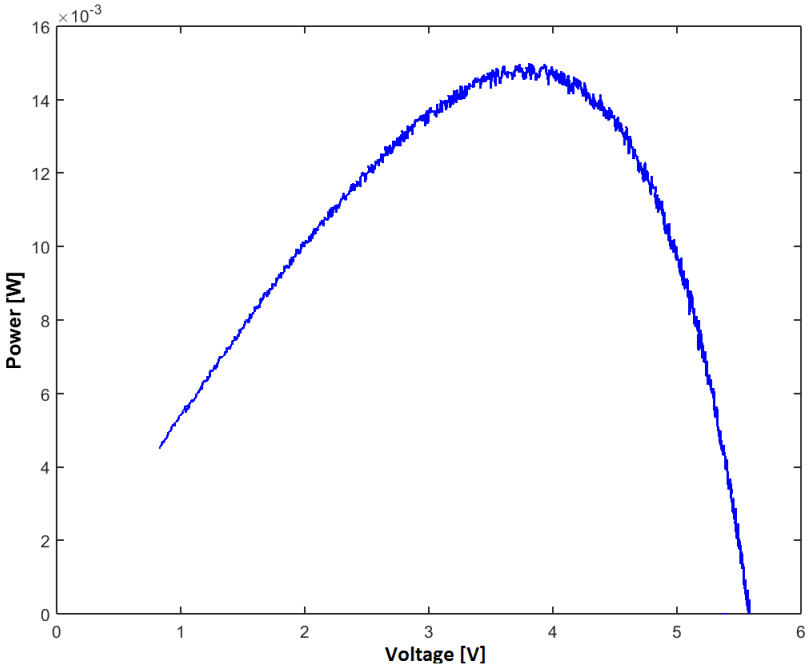

Figure 3.48: Second output P-V curve from the PV system.

In the next, part we compare the both experimental values. We also compare the I-V curves and P-V curves for both cases. The main objective is to see how close or far the curves from each other in the obtained experimental values. The obtained I-V figure by comparing both experimental values is presented in figure 3.49.

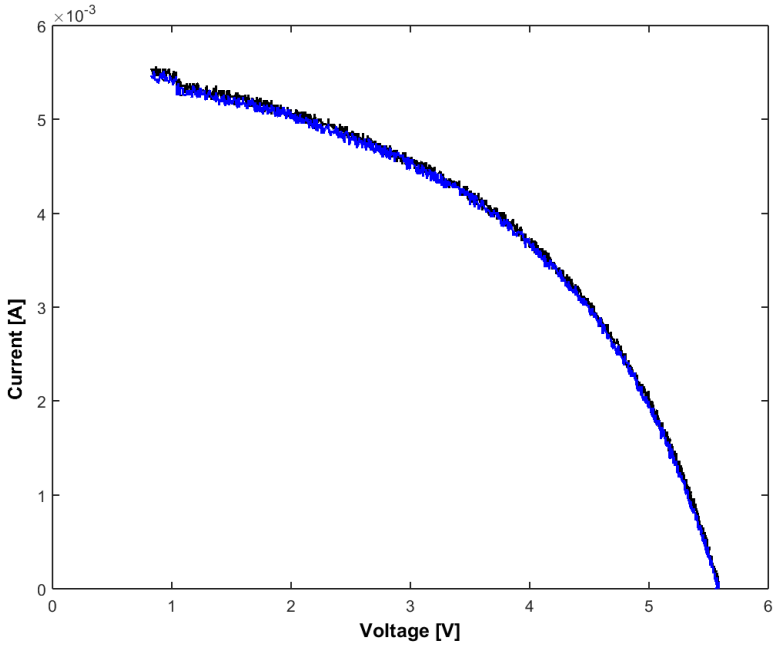

Figure 3.49: Comparison between two I-V curves.

We can see in the figure 3.49 that, I-V curve one and I-V curve two both are overlapping each other. There may be some differences between some points. But, we can consider the values are almost similar. The obtained P-V figure by comparing both experimental values is presented in figure 3.50.

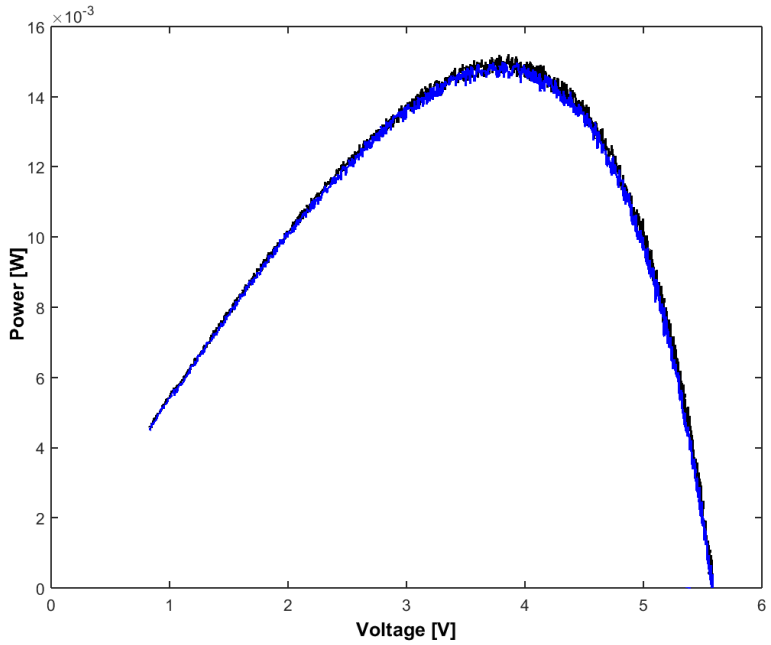

Figure 3.50: Comparison between two P-V curves.

From the figure 3.50 we can see that the two obtained power curve is almost same but the first power curve has higher MPP value than the obtained first power curve. Otherwise all the points are almost overlapping in each other.

Chapter 4. NOISE ANALYSIS, CURVE FITTING AND NON-ITERATIVE MPPT ALGORITHM

4.1 NOISE ANALYSIS

The unexpected modifications that may occur in a signal during its transmission, processing, conversion, storage or capturing in signal processing is known as noise. It is an unwanted form of signal. In this part we will discuss and analyse the white noise affect in the PV cell output characteristics. The noise what provides a random signal having equal intensity at different frequencies are known as white noise.

As we already discussed that we have used the single diode or five parameter solar cell model in here. We used this model in order to characterize the parameters and its output behaviour for variation of parameters. The ideal equation of the load current is [18] [31] [20] [22] [63]

$$I = I_{ph} - I_s\left(\exp\left(\frac{qV + qR_sI}{NKT}\right) - 1\right) - \frac{V + R_sI}{R_{sh}} \qquad (\mathbf{4.1})$$

The typical current-voltage (I-V) curve of a PV cell is obtained by simulation is [31] [31] [20] [22]

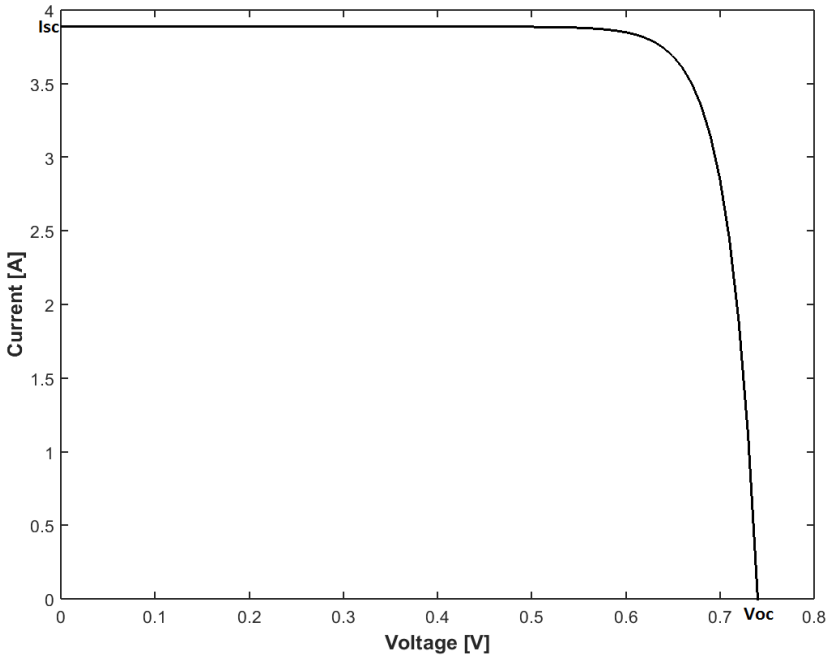

Figure 4.1: I-V curve of a solar photovoltaic cell.

Figure 4.1 represents the current-voltage (I-V) curve characteristics of a solar PV cell. There is a point where the current is maximum is called short circuit current and the point where there is maximum voltage called open circuit voltage.

The typical power-voltage (P-V) curve of a PV cell is obtained by simulation is presented in the figure 4.2. [31] [22] [59] [65]

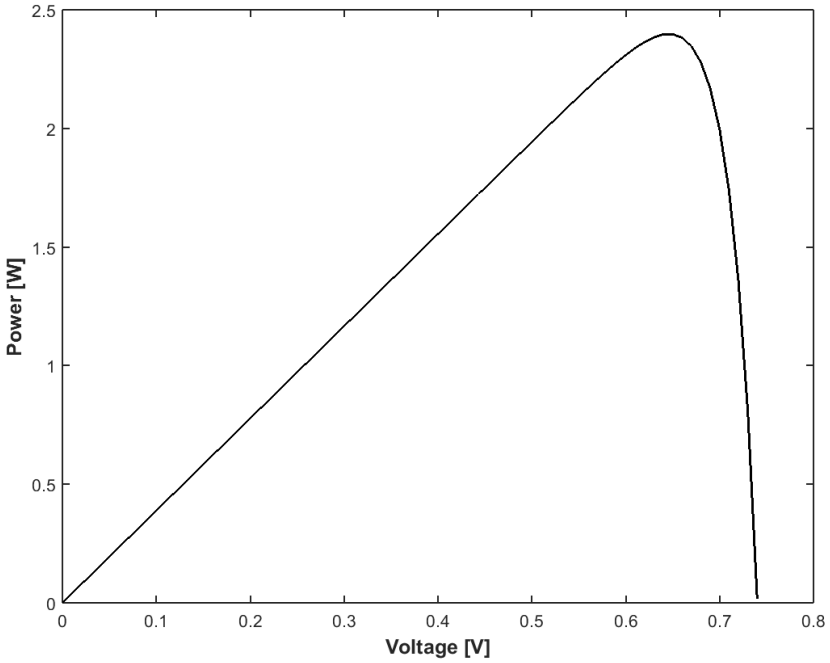

Figure4.2: P-V curve of a solar photovoltaic cell.

The generate power-voltage (P-V) curve is obtained by simulation in MATLAB. It is the typical power-voltage (P-v) curve of a PV cell with standard values. There is a point where PV power is maximum is known as maximum power point (MPP). The algorithm at which we achieve the MPP is called the maximum power point tracking. Next part, we are going to show the generated I-V and P-V curve from experimental data. The description about the experiment and used method is already described in the chapter 3.

Figure 4.3 and 4.4 describe the I-V curve and P-V obtained from the measured data. From the current-voltage (I-V) curve we find that the measured short circuit current (Isc) is 5.56 mA and open circuit voltage (Voc) is 5.60 V. And from the P-V curve the obtained maximum power point (MPP) is 15.18 mW. In the next part, we are going to discuss about the noise in the solar photovoltaic system [31]. We will discuss also how it effects in the current-voltage (I-V) and power-voltage (PV) curve of a PV cell.

The obtained I-V curve by experiment is presented in the figure 4.3.

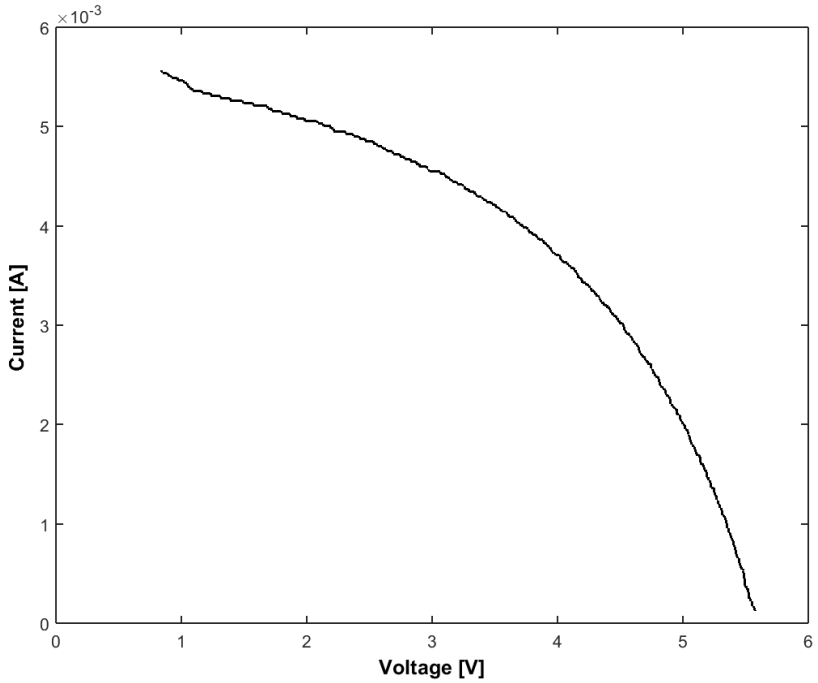

Figure 4.3: Obtained I-V curve from experimental data.

The obtained P-V curve by experiment is presented in the figure 4.4.

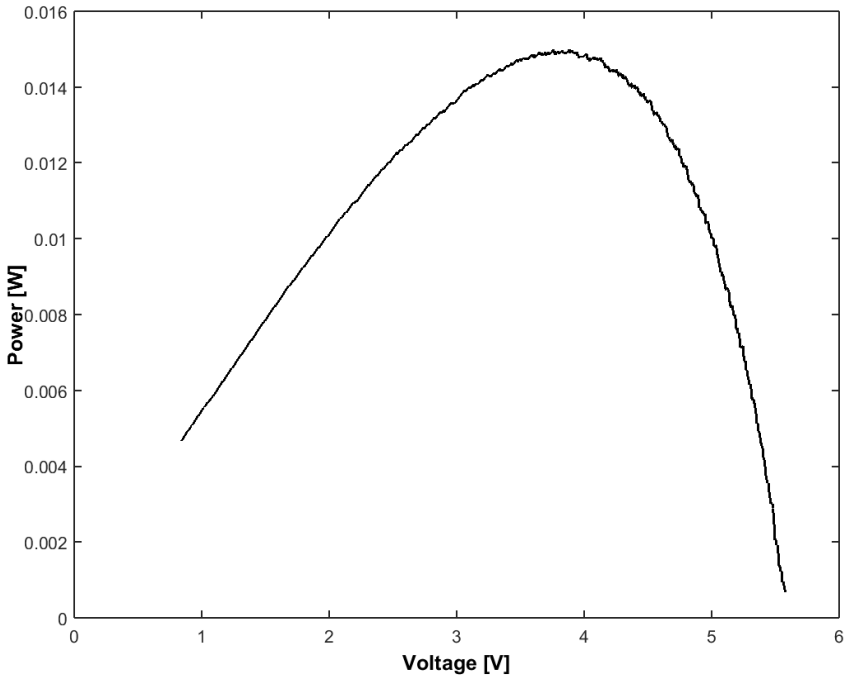

Figure 4.4: Obtained P-V curve from experimental data.

The work is conducted by MATLAB simulation. In this work we used specific values of the parameters given by datasheet. The single diode PV cell with five parameters model is used here.

The PV cell's parameters specifications are as follows:

Table 4.1: Parameters Specifications.

Name	Symbol	Unit	Value
Ideality Factor	N	n/a	1.2
Electron Charge	q	[C]	1.6×10^{-19}
Series Resistance	R_s	[Ω]	0.00001
Shunt Resistance	R_{sh}	[Ω]	10000
Solar Radiation	I_r	$[Wm^{-2}]$	10000
Boltzmann's Constant	K	$[m^2kgs^{-2}K^{-1}]$	1.3806488×10^{-23}
Saturation Current	I_s	[A]	1×10^{-10}
Junction Temperature	T	[K]	293.15
Temperature Coefficient	k_i	[A/ºC]	0.0017
Short Circuit Current	I_{sc}	[A]	3.885
Open Circuit Voltage	V_{oc}	[V]	0.74

In the above table it shows the values of used parameter in order to analyse the noise effects in the PV cell. There are some parameters which are constant and some of the parameters may vary in accordance with the characterization of PV cell.

The figure 4.5 shown below describes the current-voltage curve with noised data. The standard deviation considered here is two percent of the maximum current value.

By adding white noise we can be able to see the difference between the simulated data and real data. Because of adding noise in the curve we can see that there is deviation in the I-V curve. But, the curve without noise is very smooth and there is no deviation except in MPPT point.

The obtained I-V curve with noised is presented in the figure 4.5. [31]

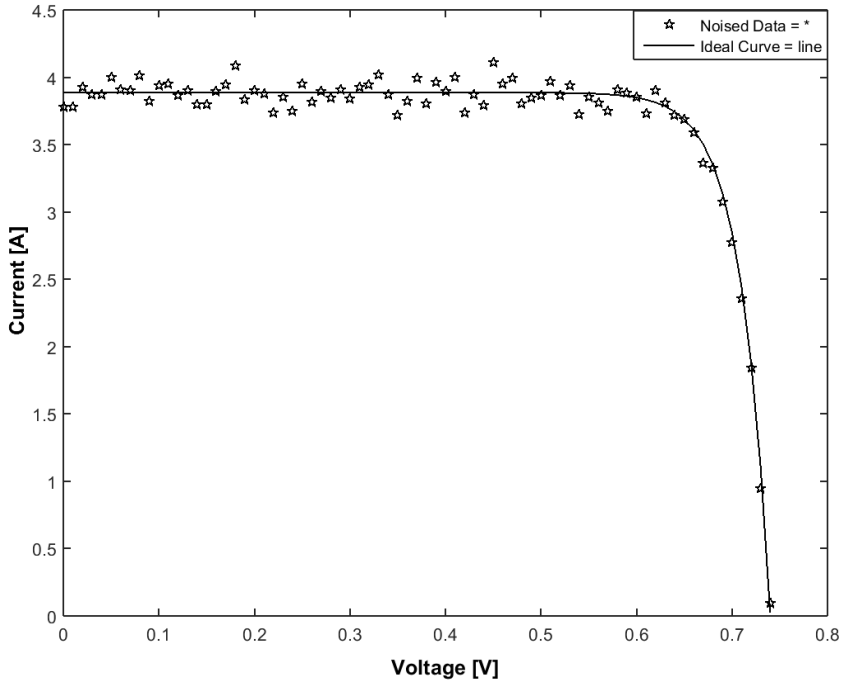

Figure 4.5: I-V curve with noised data.

In the above, we discussed the simulation part with white noise and its I-V characteristics. Now, we will see the characteristics of I-V curve with noise by using measured data. The obtained I-V curve by measured data with noised is shown below:

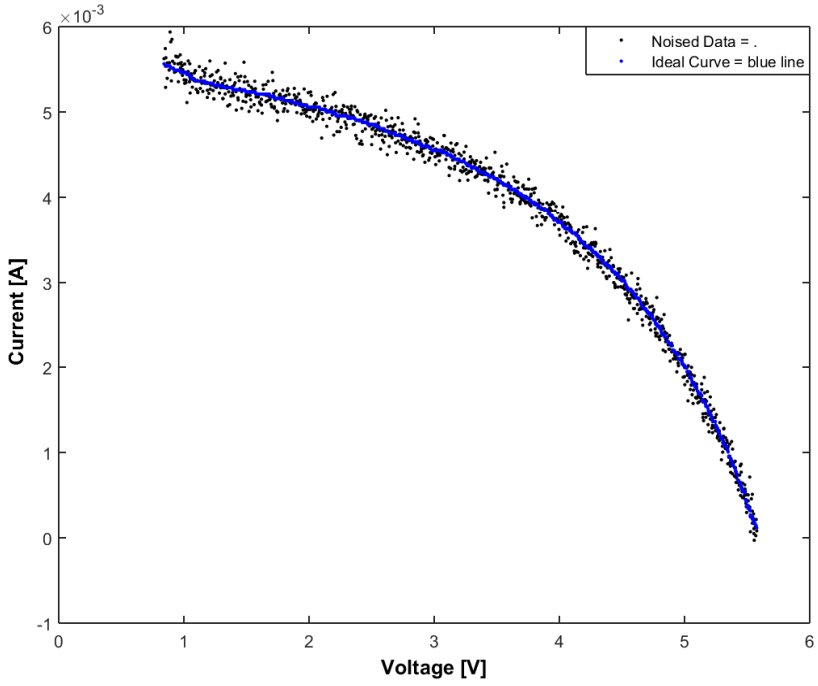

Figure 4.6: I-V curve with noised measured data.

Figure 4.6 shows the obtained current-voltage (I-V) curve with white noise. The curve is produced by the set of measured data. The blue curve in the figure is the ideal curve obtained by the measured data. And, the curve obtained by the scattered values is the curve with white noised data.

For the white noise we have used two percent of maximum of current. The main objective of adding noise is to see how the ideal curve deviates from its ideal position. Though we know that there is noise in real data already, but we used other certain value of white noise in it. The purpose is to show the I-V curve characteristics and behaviour after adding white noise.

Now, we are going to discuss about power-voltage (P-V) with white noise curve in the next section. In here, it is same the percentage of the white noise and standard deviation value. By obtaining the P-V curve with noise we get the idea about the MPPT deviation with noise also.

The obtained P-V curve with noised is presented in the figure 4.7. [31]

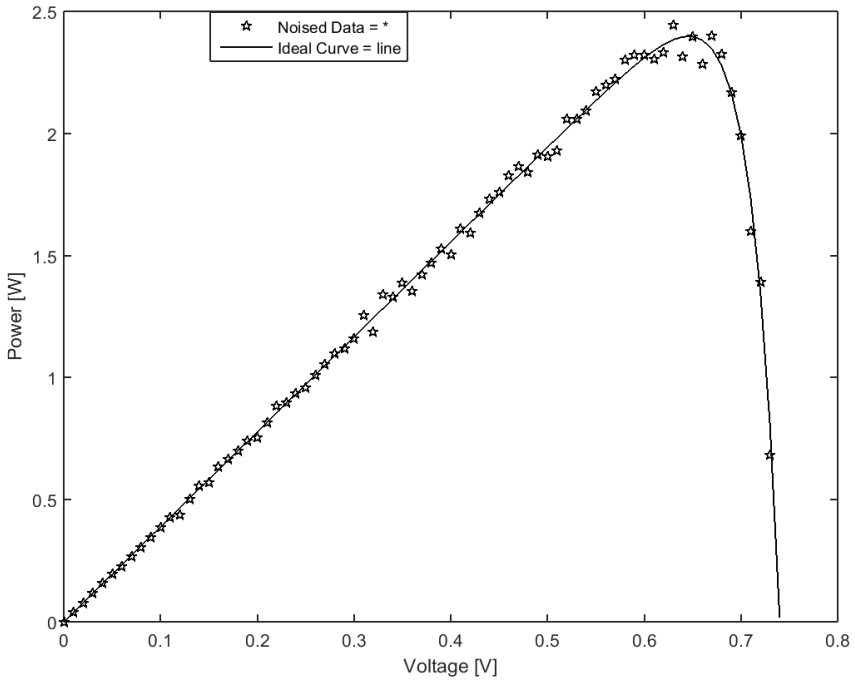

Figure 4.7: P-V curve of noised data.

Figure 4.7 shows the power-voltage (P-V) curve with noised data of the PV cell. In the figure there are two curves. One is the P-V curve with ideal data and that very smooth. And another is P-V curve with noised data and that has many fluctuations on the curve. In order to observe the variations in noise curve than ideal curve the noise is used. By adding white noise to the curve we can make the difference between simulated data and practical data. Because in reality there

must have some obstacles so it cannot be as smooth as ideal curve. The value of standard deviation is also 2% of maximum of current value.

The above figures are produced and obtained by simulation in MATLAB which deals with simulated data only. Now, we are going to show the power-voltage curve obtained from real data. And, the curve will be introduced by adding white noise data. Thus how we can see how it differs from the ideal curve generated by real measured data and measured noise data.

The obtained P-V curve by measured data with noised is presented in the figure 4.8.

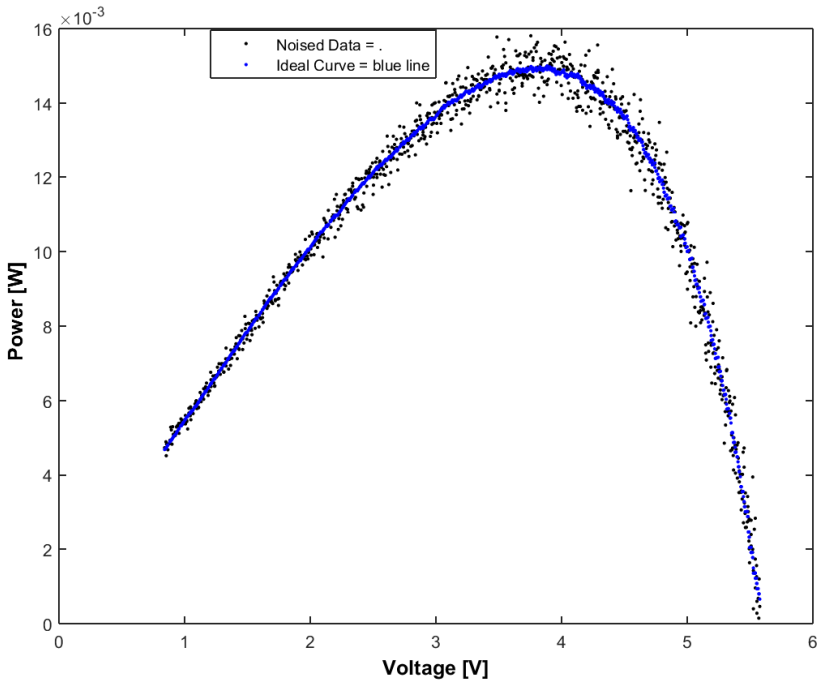

Figure 4.8: P-V curve with noised measured data.

Figure 4.8 shows the power-voltage curve (P-V) with noised measured data. The curve in blue is the ideal curve obtained by the measured data. And the curve obtained by scattered data sets is obtained by adding white noise in measured data. The amount of added white noise in here is two percent of maximum of current value.

From the figure we can see that the ideal curve is smoother than the noised curve. The purpose of using noise is to observe the curve in real situation means the deviation with the ideal curve.

We used the standard deviation of two percent of maximum of current value in the previous simulation. Now, we will use standard deviation of five percent of maximum of current value in order to see how it affects in both I-V and P-V curve.

The obtained I-V curve with noised is presented in the figure 4.9.

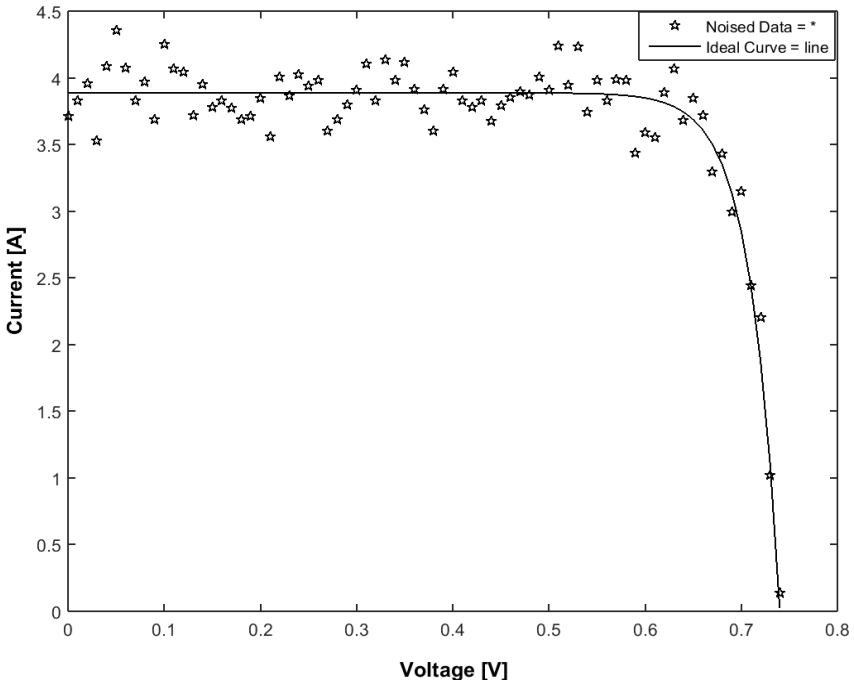

Figure 4.9: I-V curve of noised data.

Figure 4.9 shows the current-voltage (I-V) curve of PV cell with white noise. In the previous part we considered the value of standard deviation of two percent of maximum current value, but in here we considered standard deviation of five percent of maximum of current value. As we can see in the figure that by adding white noise there are deviations in the curve due to the noise. But, another curve with standard values does not have deviation in the curve.

The main objective of using the white noise in the PV cell is to see how the curve behaves in compare to simulated data and practical data. In the figure we can find that the points are far and dispersed from the ideal curve than the previous I-V curve. Because the standard deviation value of white noise is more than in the previous figure we used.

Figure 4.10 shows the obtained current-voltage (I-V) curve with white noise. The produced curve is obtained by the set of measured data. The ideal obtained from measured data is the blue curve in here. And, the other curve with scattered values is the curve with white noised data. In order to consider the white noised data we used the two percent of maximum of current value. In the previous part we used two percent of maximum of current as white noise but in here we used five percent. We find that the points are more scattered in here. The objective is to see how it differs from the ideal value. And, also to observe the current-voltage

curve characteristics after using the certain amount of white noise. The obtained I-V curve by measured data with noised is presented in the figure 4.10.

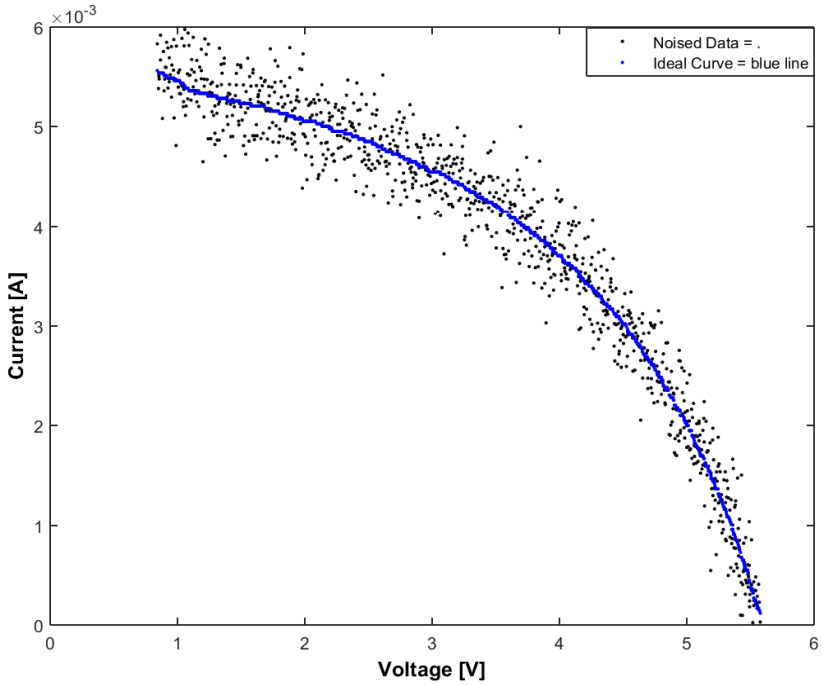

Figure 4.10: I-V curve with noised measured data.

Now, we will analyse the power-voltage (P-V) curve characteristics with the white noise. And we will see how it affects in the maximum power point (MPP) of PV cell also.

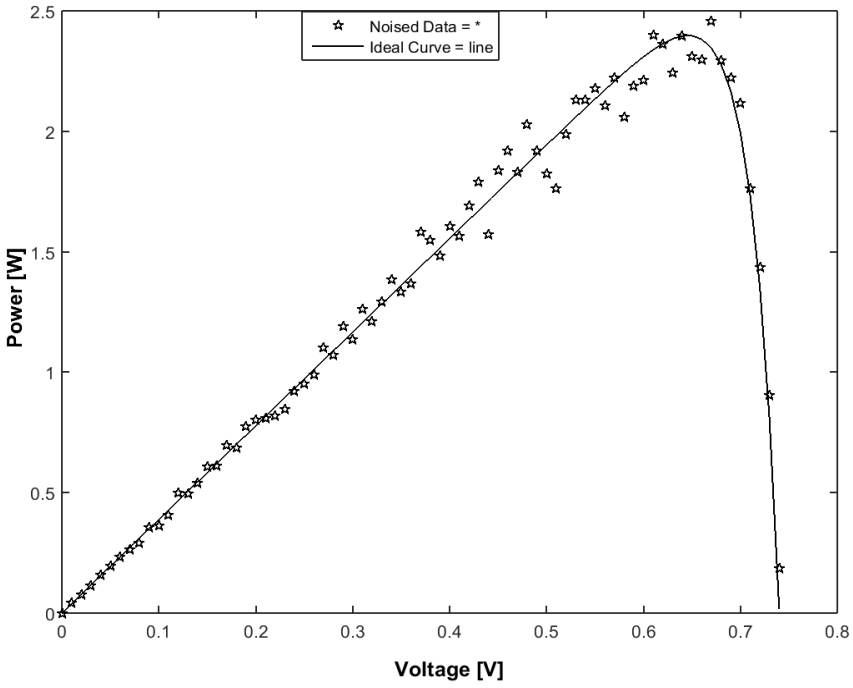

Figure 4.11: P-V curve of noised data.

The figure 4.11 describes the power-voltage (P-V) curve of the PV cell with white noise and ideal data. The curve which is smooth represents the PV curve with ideal data and the curve which has dispersion in the data is the PV curve with white noise.

In here we considered standard deviation of five percent of maximum current values. The PV curve with ideal values maximum power point can be identified very easily. But, in the PV curve with white noise it is difficult to locate the maximum power point (MPP) due to the scattered value. Basically, the noise is unwanted or unexpected signals which are occurring here. We always try to eliminate as much as noise possible. But, in real time production system there always have some noise in the system.

The above figure is generated and obtained by simulation in MATLAB which deals with simulated data only. Now, we are going to discuss about the power-voltage curve obtained from the real data. And, the curve will be introduced by adding white noise data. The obtained P-V curve by measured data with noise is presented in the figure 4.12.

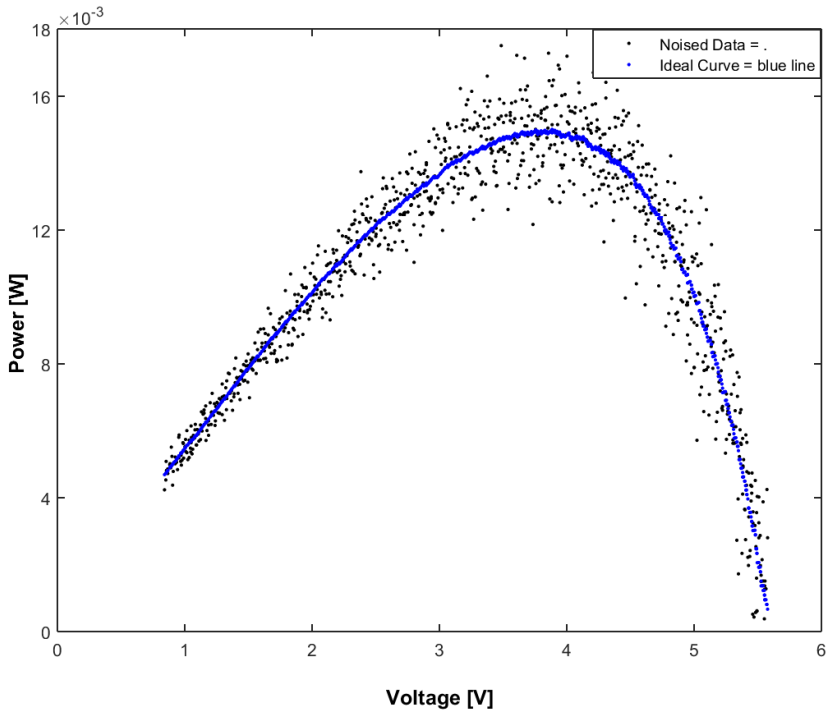

Figure 4.12: P-V curve with noised measured data.

The above figure 4.12 shows the power-voltage curve with white noise measured data. The blue curve we can see in the figure stands for the ideal curve obtained by the measured data. The curve with many scattered points is obtained by adding white noise in measured data. The amount of added white noise is five percent of maximum of current value.

From the figure we can also see that the ideal curve is smothering than the noised curve. By using noise for a certain amount in the ideal curve we can see the difference between the ideal situation and noised situation.

We have discussed the white noise in the I-V and P-V curve of the cell so far in this section. We also discussed the affects of noise in the PV characteristics and its related output behaviour. In the next part we are going to analyze the curve fitting approximation by using different polynomial method.

4.2 CURVE FITTING APPROXIMATION

The action of establishing a mathematical function or a curve by the best fit to a series of data points by giving the constraints is the curve fitting method. In here we are going to use the curve fitting approximation for both the ideal I-V and P-V curve and I-V and P-V curve with white noise data.

The obtained I-V curve by using polynomial presented in the figure 4.13. [31]

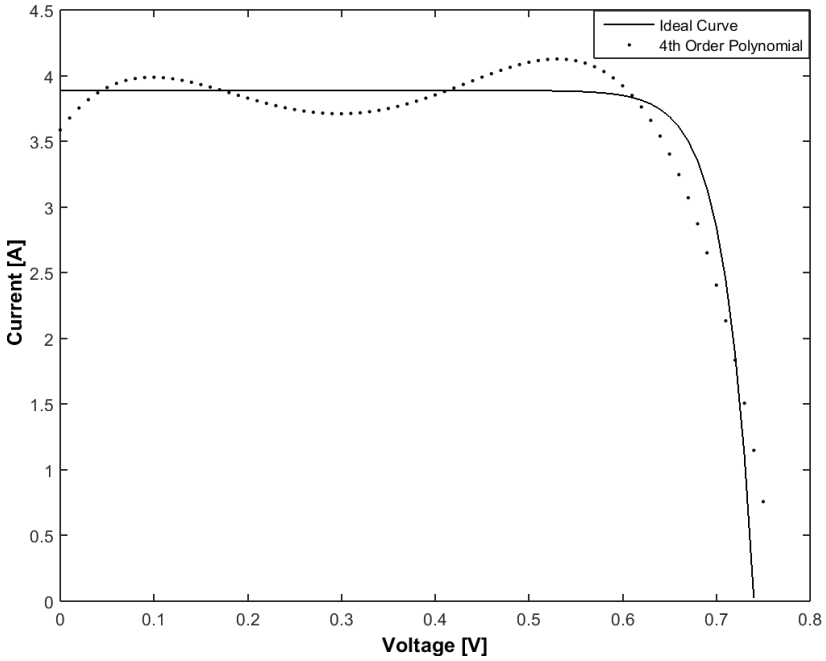

Figure 4.13: I-V curve with 4th order polynomial fitting.

Figure 4.13 shows the fitted curve from standard values of I-V curve by using fourth order polynomial curve fitting method. The main objective is to observe the fitted curve and make comparison between ideal and fitted curve.

If we look at the figure we can see that there are differences between the two curves. The curve obtained by ideal value looks smoother than the curve obtained by polynomial fitting. The curve obtained by polynomial fitting it has some deviations in there.

The obtained I-V curve from measured data by using 4th order polynomial is presented in the figure 4.14. It describes the current-voltage (I-V) obtained from measured data. The fourth order polynomial method is used to fit the curve. The blue curve show the ideal curve obtained from measured data and the other shows the fitted curve after using polynomial method.

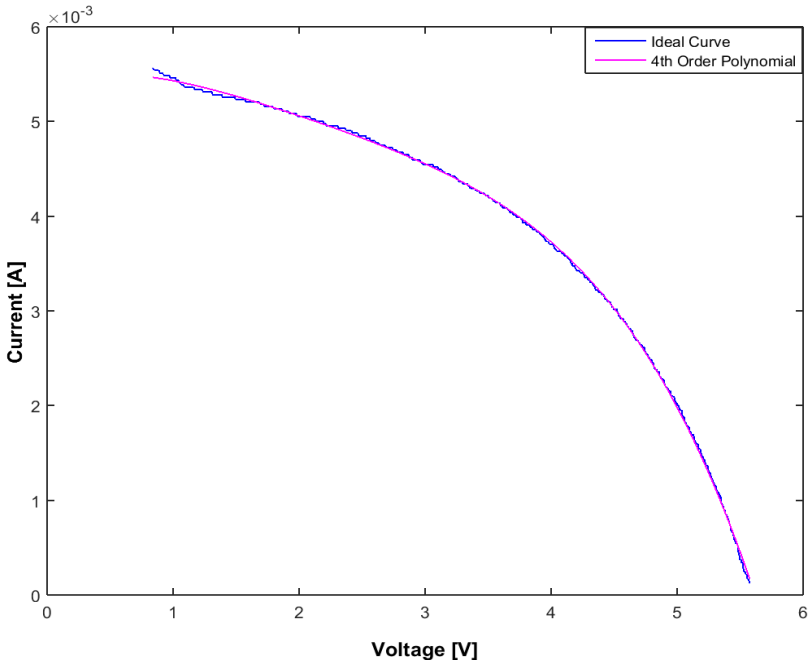

Figure 4.14: I-V curve with 4th order polynomial fitting.

The obtained P-V curve by using polynomial fitting is presented in the figure 4.15. [31]

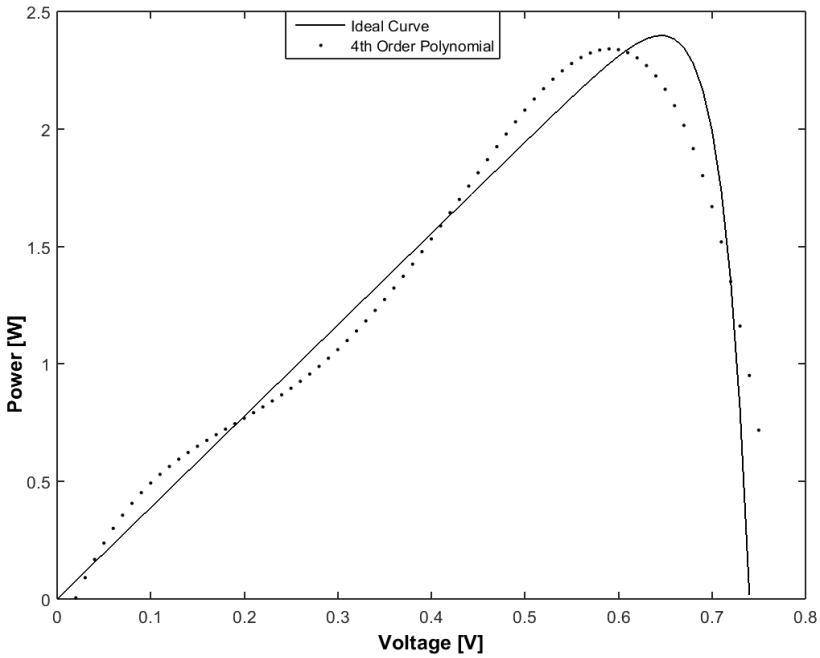

Figure 4.15: P-V curve with 4th order polynomial fitting.

The above figure 4.15 shows the power-voltage (P-V) curve for fourth order polynomial fitting. There are two figures we can see here one is the smoother which is P-V curve with ideal data and another is P-V curve with fitted data. The fourth order polynomial fitting method is

considered here in order to fit the curve. The obtained P-V curve from measured data by using 4^{th} order polynomial is presented in the figure 4.16.

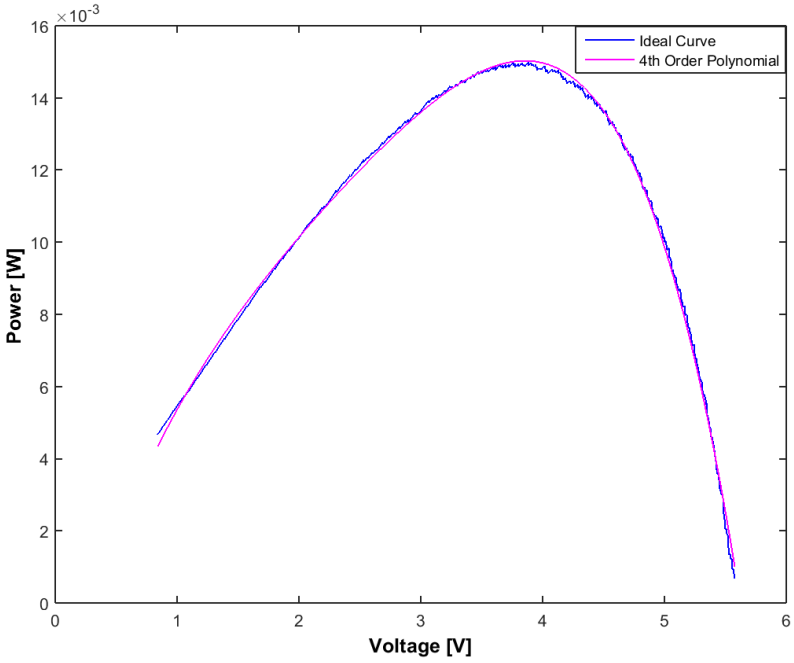

Figure 4.16: P-V curve with 4^{th} order polynomial fitting.

In the next part we are going to discuss the different fitting order method. There, we are going to discuss about the I-V and P-V curve fitting by using eighth order polynomial method. The obtained I-V curve by using 8^{th} order polynomial is presented in the figure 4.17.

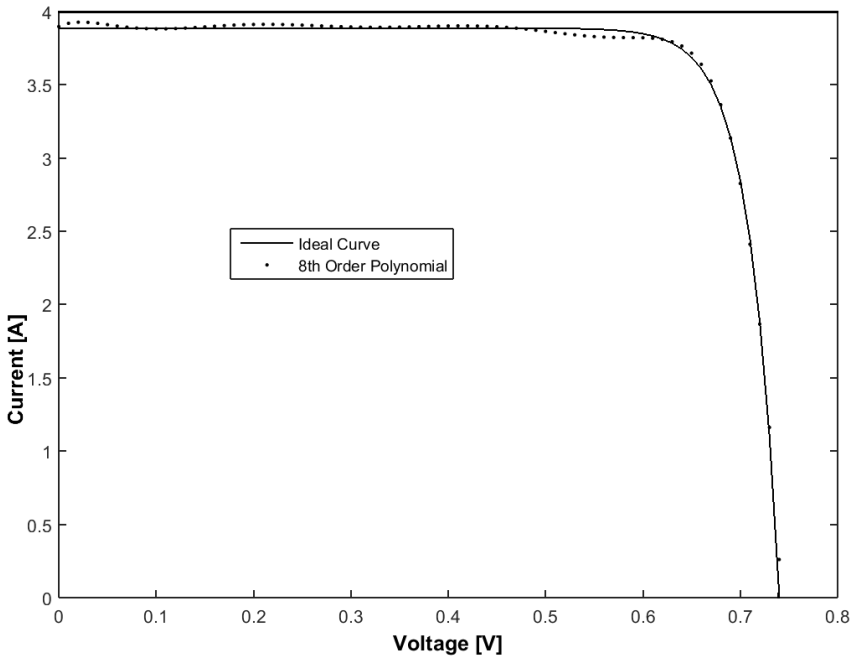

Figure 4.17: I-V curve with 8^{th} order polynomial.

The obtained I-V curve from measured data by using 8th order polynomial is presented in the figure 4.18.

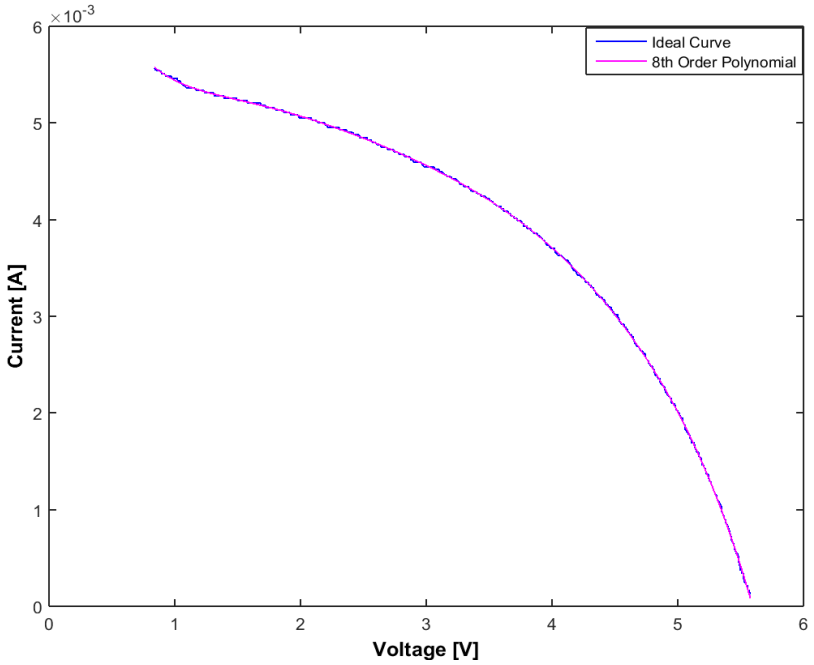

Figure 4.18: I-V curve with 8th order polynomial fitting.

The obtained P-V curve by using 8th order polynomial is presented in the figure 4.19.

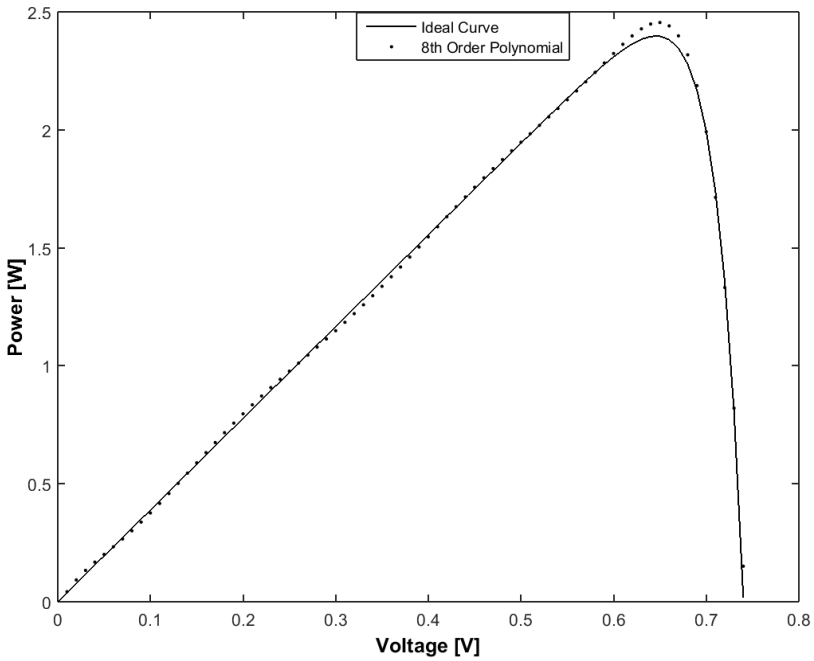

Figure 4.19: P-V curve with 8th order polynomial.

Figure 4.18 and figure 4.19 shows the current-voltage (I-V) and power-voltage (P-V) curve fitting approximation by using eighth order polynomial fitting. If we compare the both curves of fourth order fitting and eighth order fitting method then we will see some differences here. In eighth order fitting method it seems more stable then fourth order fitting approximation method.

In the next part we are going to see how it occurs with the real time data what we obtained from the laboratory measurement. We will observe the PV characteristics and fitting with eighth order polynomial. The obtained P-V curve from measured data by using 8^{th} order polynomial is:

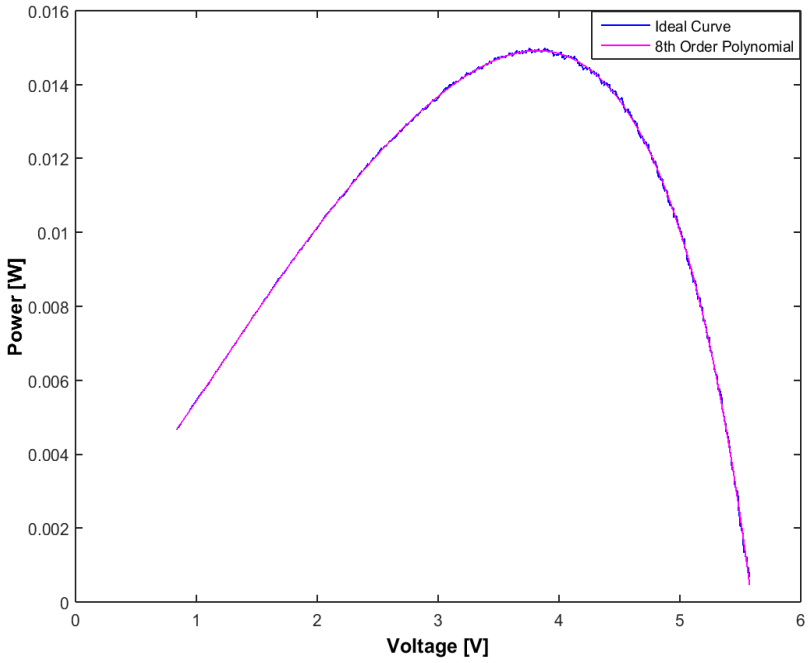

Figure 4.20: P-V curve with 8^{th} order polynomial fitting.

The above figure 4.20 shows the P-V curve with eighth order polynomial fitting by using experimental data. The blue curve is obtained by using the ideal data and the other curve is obtained by using polynomial fitting. We can see from the figure that both curves are almost overlapped each other. For the better fit we can use this method in the PV module curves.

In this section we observed the polynomial fitting by using fourth order and eighth order method. We used the method for current-voltage and power-voltage curve in the PV module. We used it for both simulated and measured data also. We analysed the characteristics for both method. We showed the fitted curve and ideal curve comparison by producing the curves in MATLAB.

4.3 NON-ITERATIVE MPPT ALGORITHM

The point at which PV module has the highest power that point is known as Maximum Power Point (MPP) of that module. For a PV array the tracking of that point is most important. Usually the essential part of a PV system is the maximum power point tracking (MPPT) [32]. But, the MPP varies with the internal and external parameters variation of a PV array.

By implementing a good algorithm technique we can make the best utilizations of the PV arrays [33]. There are many MPP tracking methods have been developed and implemented already. Normally the used method varies in accordance with the cost, complexity, convergence speed, sensors required, range of effectiveness and many other aspects [32].

We have developed an MPP tracking method by using MATLAB. Before describing the method we can first have a look on MPPT first by using simulation and measured data sets.

The obtained MPP curve by standard values is presented in the figure 4.21. [34]

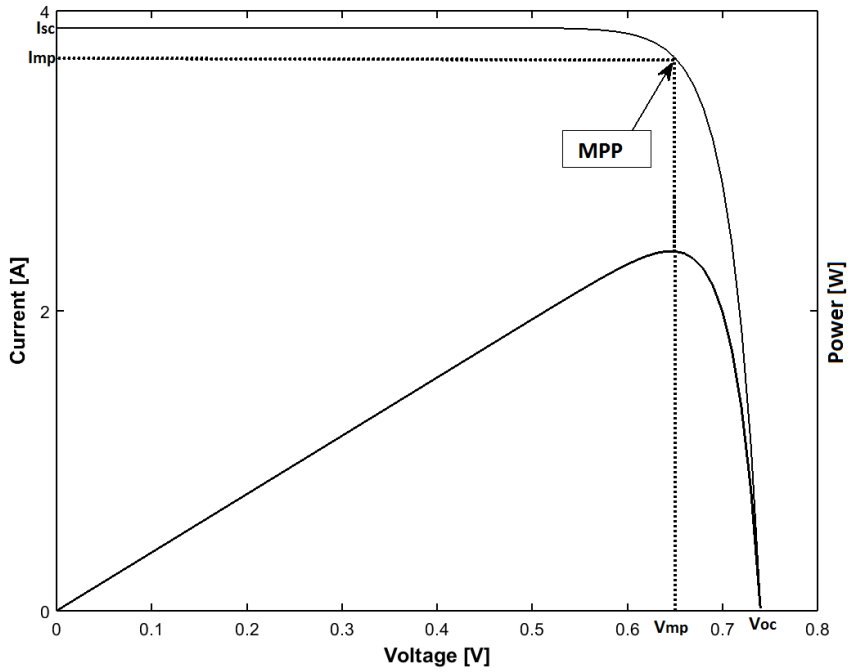

Figure 4.21: MPP curve of a PV cell.

Figure 4.21 shows the MPP curve of a PV cell. The curve is obtained by using MATLAB with the standard values from the industrial datasheets.

Now, we will see the MPP curve generated by MATLAB with the measured values. The objective is to see the behaviour for the MPP curve at real time simulation with experimental data sets.

The obtained curve from measured data is presented in the figure 4.22.

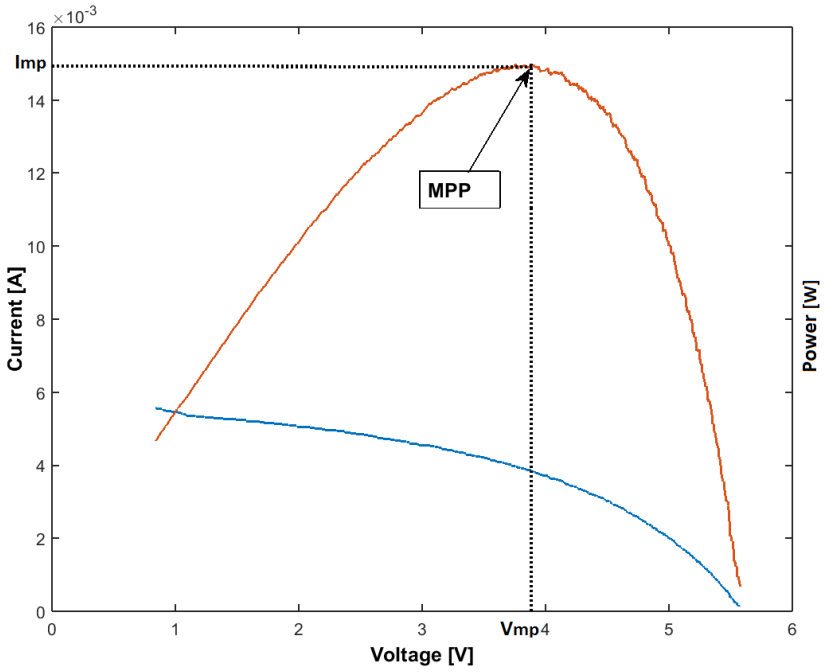

Figure 4.22: MPP curve of a PV cell from measured data.

The above maximum power point (MPP) curve contains current-voltage (I-V) and power-voltage curve (P-V). The MPP point is found and identified there. The blue curve signifies the current-voltage curve obtained from measured data.

The other curve shows the power-voltage (P-V) curve obtained from measured data too. From there, we obtained the MPP curve. The value of maximum power is found here 0.0150 W. And the current at maximum power point (Imp) is 0.0039 A and the voltage at maximum power point (Vmp) is 3.8850 V.

In the next part we are going to discuss about a newly developed non-iterative MPPT algorithm of MPPT method.

The five parameters model circuit of a PV cell is used to characterize and implement the maximum power point tracking (MPPT) algorithm. A numerical analysis with a standard method is considered in order to better estimation of the parameters variation. In here, MPPT is obtained by taking four samples from I-V curve.

The used method is shown in flowchart and described in the figure 4.23.

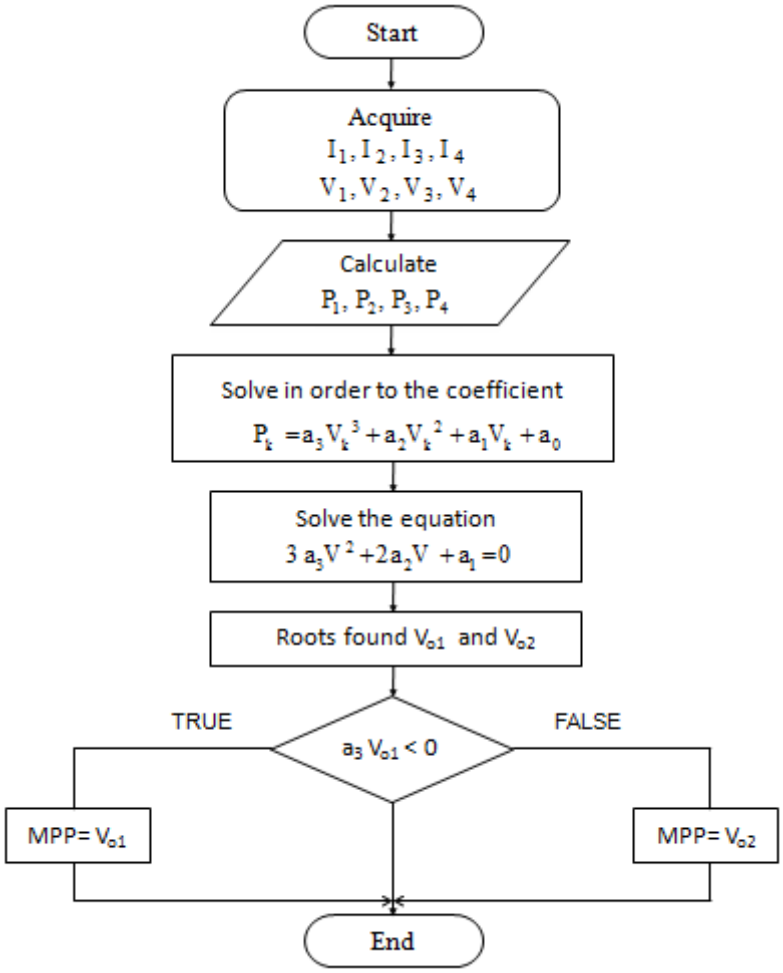

Figure 4.23: Flowchart of MPP non-iterative method.

In the first step, we acquire the voltage V_1, V_2, V_3, V_4 and the current I_1, I_2, I_3, I_4. Then it is obtained P_1, P_2, P_3, P_4 by calculating from I-V curve. We solved the systems in order to have the coefficients. The equation is as follows:

$$P_k = a_3 V_k^3 + a_2 V_k^2 + a_1 V_k + a_0 \quad (4.1)$$

It is solved the equations with the purpose of having roots. The solved equation is as follows:

$$3 a_3 V^2 + 2 a_2 V + a_1 = 0 \quad (4.2)$$

The found roots are V_{01} and V_{02}. We picked the root which is $3V_0 < 0$ and rejected the other one.

We considered third degree polynomial for fitting the power curve. From the polynom's coefficient we get the optimal power position. The samples are pointed in the ideal P-V curve in order to see how it fits in the curve [34].

The obtained MPP curve by non-iterative algorithm is presented in the figure 4.24. [34]

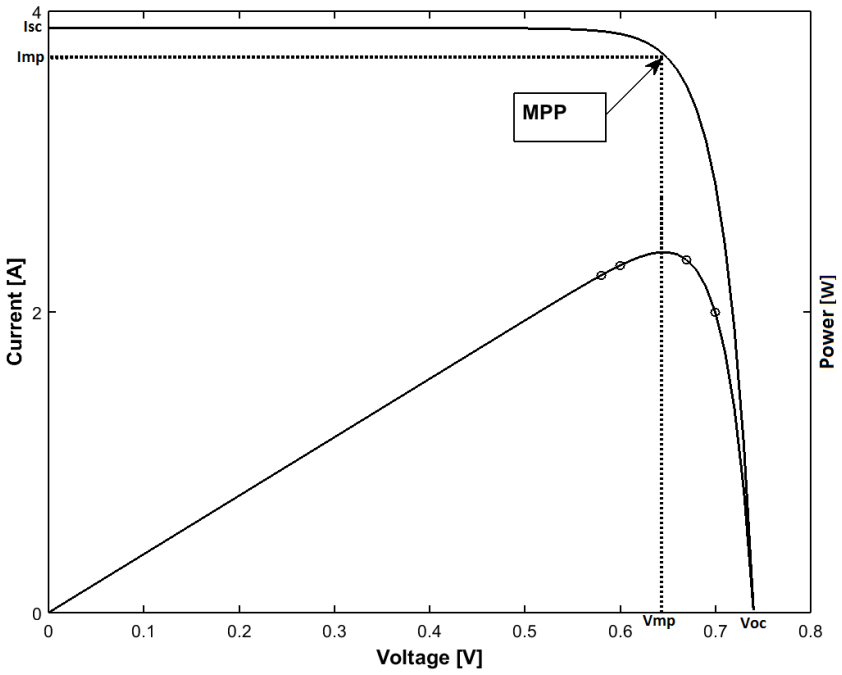

Figure 4.24: MPP curve of a PV cell obtained by non-iterative method.

The above figure 4.24 contains I-V curve, P-V curve and MPP obtained by a non-iterative method of MPPT algorithm. This algorithm is just an approximation though the tracking precision is higher in the algorithm. The obtained MPP by this algorithm is almost equal to the actual MPP of the curve. As it is an approximation there is a very little difference between the actual MPP and MPP obtained by the non-iterative method. If we look at the figure we can see that there are four samples in the P-V curve. Those samples are taken from the P-V curve and then we approximated the MPP by using the samples.

The figure 4.25 shown below is obtained by the measured data of a PV module by using non-iterative MPP algorithm. The blue curve in the figure shows the current-voltage curve obtained from measured data and the other curve shows the power-voltage curve obtained from measured data too. The four points in black in the P-V curve are the used samples from the measured data in order to obtain the maximum power point by using non-iterative algorithm. In result, we find that the obtained value is almost close to the actual value. The value may not be accurate because it is just an approximation. The four samples with third order polynomial fitting are used to obtain the MPP by this method. The obtained MPP curve by non-iterative algorithm from experimental data is presented in the figure 4.25.

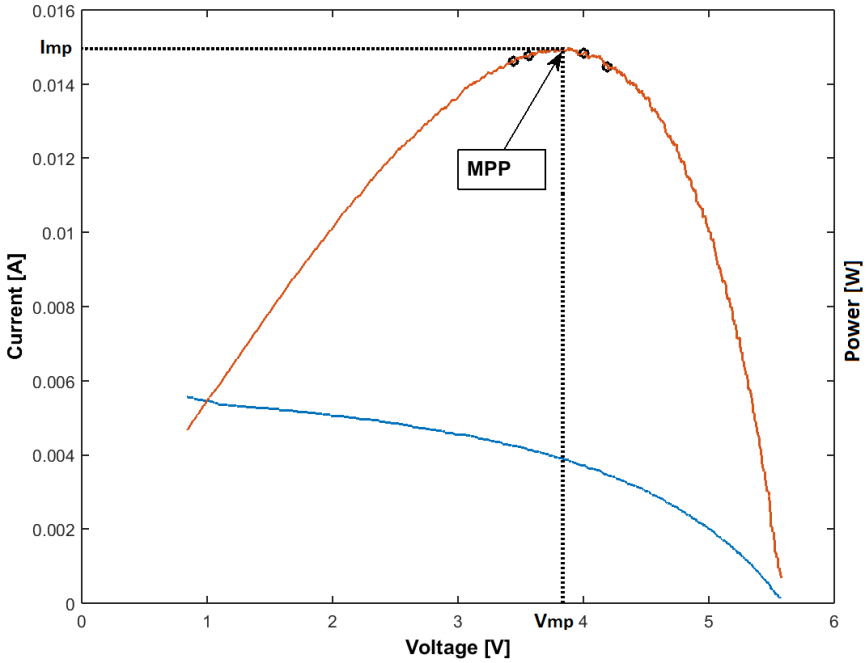

Figure 4.25: MPP curve of a PV cell obtained by non-iterative method.

It is already been told that it is an approximation so, in the next part we are going to see how it differs from the actual MPP point. We will show the curve obtained by simulation from industrial data and from the measured data. We will show the difference between the actual MPP and the obtained MPP by using our proposed method. The difference curve between both MPP obtained by simulation is presented in the figure 4.26. [34]

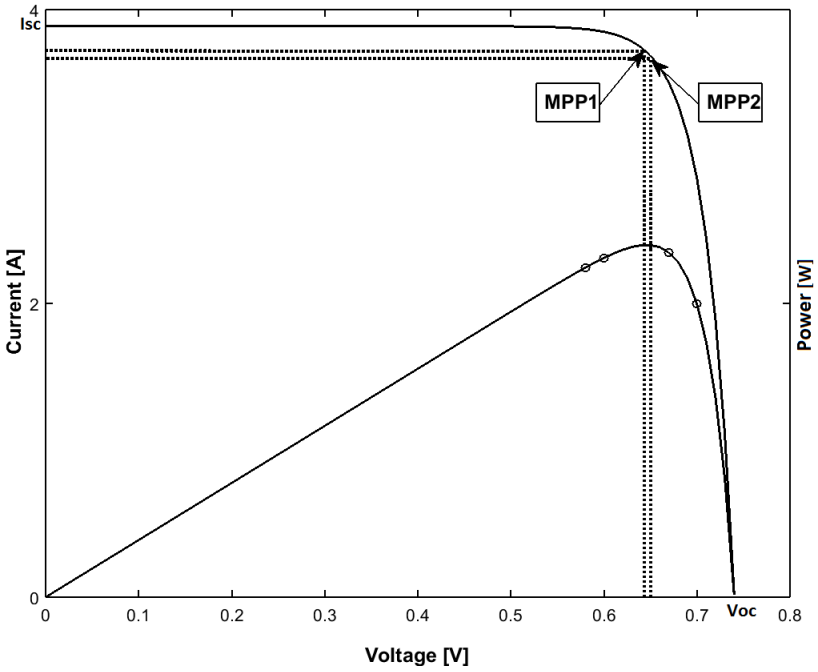

Figure 4.26: MPP comparison for both side values.

The figure 4.26 shows the MPP comparison for both side values. It is obtained by MATLAB simulation from industrial data. The MPP is also obtained in here. In the figure we can see that there are two MPP points indicated.

The MPPT2 is the actual MPP of this photovoltaic module. Here the value of maximum power point (MPP) is 2.3969 W. The value of voltage at maximum point (Vmp) is 0.65 V and the value of current at maximum point (Imp) is 3.6875 A.

In the figure, the MPPT1 is the MPP obtained by the proposed non-iterative algorithm. The found value of maximum power point (MPP1) by this algorithm is 2.3965 W. The voltage at maximum point (Vmp) is 0.6438 V and the current at maximum point (Imp) is 3.7224 A.

If we compare both MPP values then we find that the obtained actual MPP value and the value obtained by non-iterative algorithm are almost close. The difference is so small that it is ignorable. In the next part we are going to observe the same analyse for measured data.

The difference curve between both MPP obtained from measured data is presented in the figure 4.27.

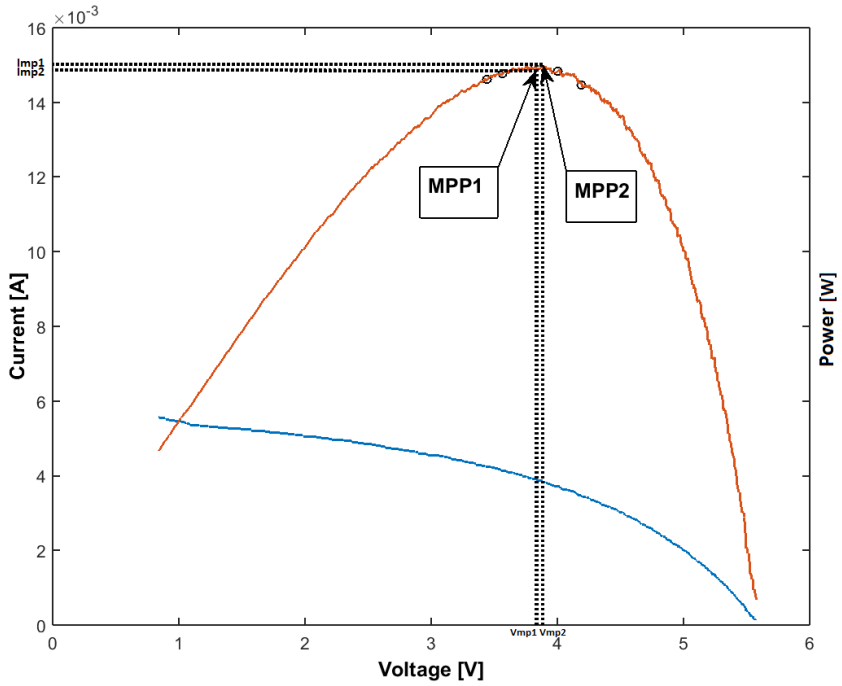

Figure 4.27: MPP comparison for both side measured values.

Figure 4.27 shows the MPP comparison for both side measured values. This figure is obtained by MATLAB simulation from measured data. The MPP is also obtained in here for both cases. In the figure we can see that there are two MPP points indicated.

The MPPT2 is the actual MPP of this photovoltaic module obtained from measured data. Here the value of maximum power point (MPP) is 0.0150 W. The value of voltage at maximum point (Vmp) is 3.8850 V and the value of current at maximum point (Imp) is 0.00386 A.

In the figure, the MPPT1 is the MPP obtained by the proposed non-iterative algorithm. The obtained value of maximum power point (MPP1) by this algorithm is 0.0148 W. The voltage at maximum point (Vmp) is 3.8356 V and the current at maximum point (Imp) is 0.00386 A.

If we compare both MPP values which are obtained from measured data then we find that the obtained actual MPP value and the value obtained by non-iterative algorithm are almost same. The difference is so small which can be ignored now.

In the last part the samples are taken from both sides of the actual MPP means the points before the MPP and the points after the MPP. In the next parts we are going to discuss the non-iterative MPP method by taking the samples from the points before the actual MPP point [34].

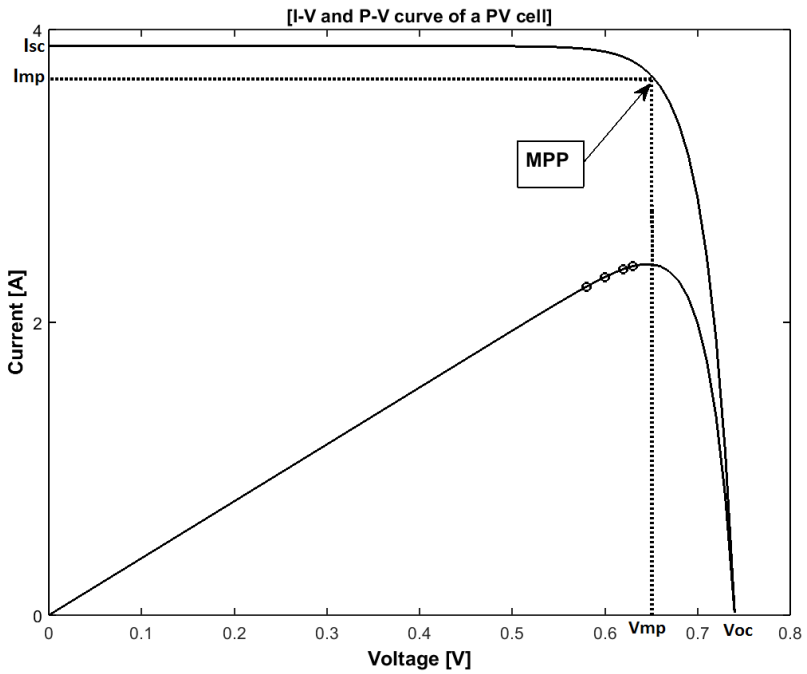

Figure 4.28: Obtained MPPT from left side points.

Figure 4.28 shows the MPPT tracking obtained by non-iterative algorithm from left side values of MPP point. To obtain the MPP curve and tracking it we used the samples from left side of the MPP point.

The obtained MPP here is 2.396930 W. The voltage at maximum power point (Vmp) is 0.65078 V and the current at maximum power point (Imp) is 3.6876 A.

The simulation for finding MPP by using the non-iterative method the standard values from the industry is used. In the next part we are going to see the same method by using the measured values from the PV panel.

The MPP from measured left side data points by using non-iterative algorithm is presented in the figure 4.29.

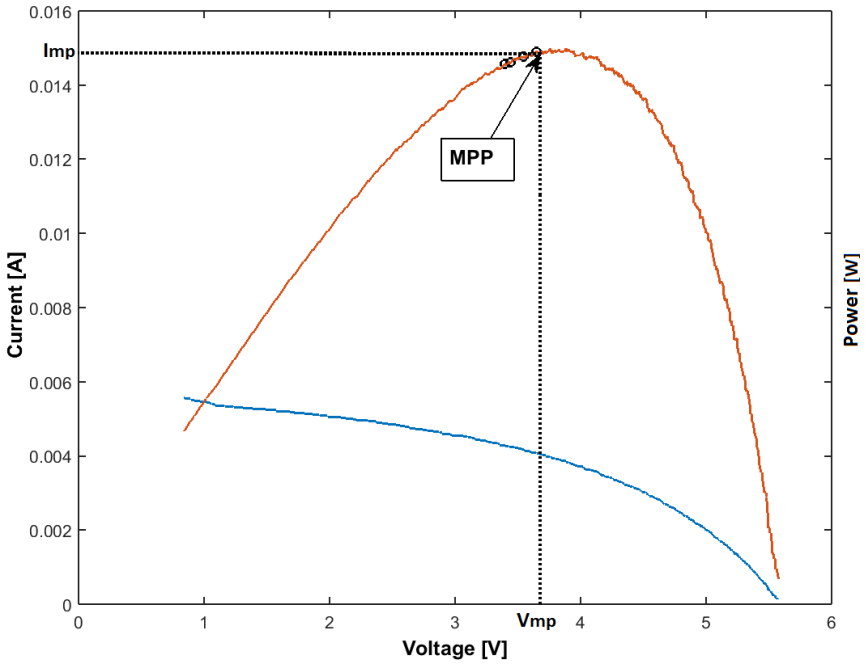

Figure 4.29: Obtained MPPT using left side points from measured data.

Figure 4.29 represents the MPPT tracking obtained by using non-iterative tracking algorithm from left side values of MPP using measured data. The blue curve signifies the current-voltage (I-V) curve of measured data and the other orange curve signifies the power-voltage (P-V) curve obtained from measured data too.

The obtained MPP here from measured data by using the non-iterative method is 0.0149 W. The voltage at maximum power point (Vmp) is 3.682 V and the current at maximum power point (Imp) is 0.0040 A.

For the simulation of non-iterative MPP by using this method we used the measured data. The data is obtained from the laboratory environment by using a PV module. In the next part we are going to see how far or close it is from the actual MPP value. And the difference between the actual MPP and the MPP obtained by our algorithm.

The curves obtained by differencing two MPP are shown in the figure 4.30. [34]

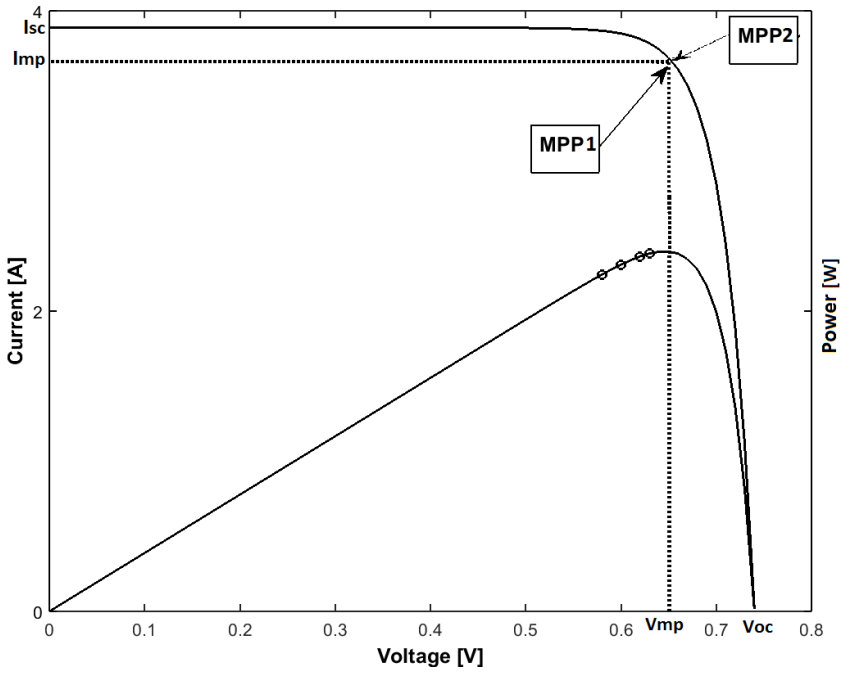

Figure 4.30: MPP comparison for left side values.

Figure 4.30 represents the MPP comparison for left side samples. This figure is obtained by MATLAB simulation from industrial data. In the figure we can see that there are two MPP points indicated which are for two different MPP values.

The MPPT2 is the actual MPP of this photovoltaic module. Here the value of maximum power point (MPP) is 2.3969 W. The value of voltage at maximum point (Vmp) is 0.65 V and the value of current at maximum point (Imp) is 3.6875 A.

In the figure 4.30, the MPPT1 is the MPP obtained by the proposed non-iterative algorithm. The found value of maximum power point (MPP1) by this algorithm is 2.39695 W. The voltage at maximum point (Vmp) is 0.6507 V and the current at maximum point (Imp) is 3.6836 A.

If we compare the both MPP values then we find that the obtained actual MPP value and the value obtained by non-iterative algorithm are almost close. But, the obtained MPP by non-iterative method using left side values is bit higher than the actual MPP value. But, the difference is so small that it is ignorable. In the next part we are going to observe the same analyse for measured data.

The difference curve between both MPP obtained from measured data is presented in the figure 4.31.

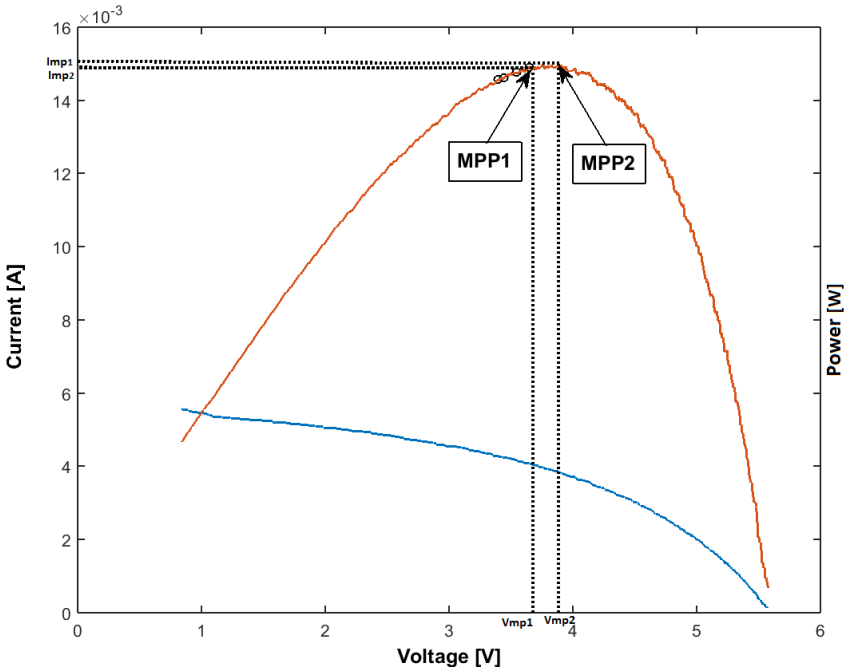

Figure 4.31: MPP comparison for left side measured values.

Figure 4.31 represents the MPP comparison for left side measured values. The figure is obtained by MATLAB simulation from measured data. The MPP is also obtained here for both cases. Obtained both MPP is indicated in the figure by naming MPPT1 and MPPT2.

The MPPT2 we can see in the figure is the MPP of this photovoltaic module obtained from measured data. The value for real maximum power point (MPP) is 0.0150 W. The value of voltage at maximum power point (MPP) is 3.8850 V and the value of current at maximum power point (Imp) is 0.0036 A.

The MPPT1 we can see in the figure is obtained by using proposed non-iterative MPPT algorithm from measured data. The obtained value of maximum power point (MPPT1) by this algorithm is 0.0148 W. The obtained voltage at maximum power point (Vmp) is 3.6763 V and the current at maximum power point (Imp) is 0.004037 A.

If we compare both MPP values which are obtained from measured data then we find that the obtained MPP value by our non-iterative method is lower. The real MPP value is 0.015 W and the MPP obtained by non-iterative algorithm is 0.0148 W.

We have made the experiments by taking both side samples, left side sample from real MPP. Now in the next part we will test for the samples from right side of the MPP. We will observe how it response and the position of MPP for this case.

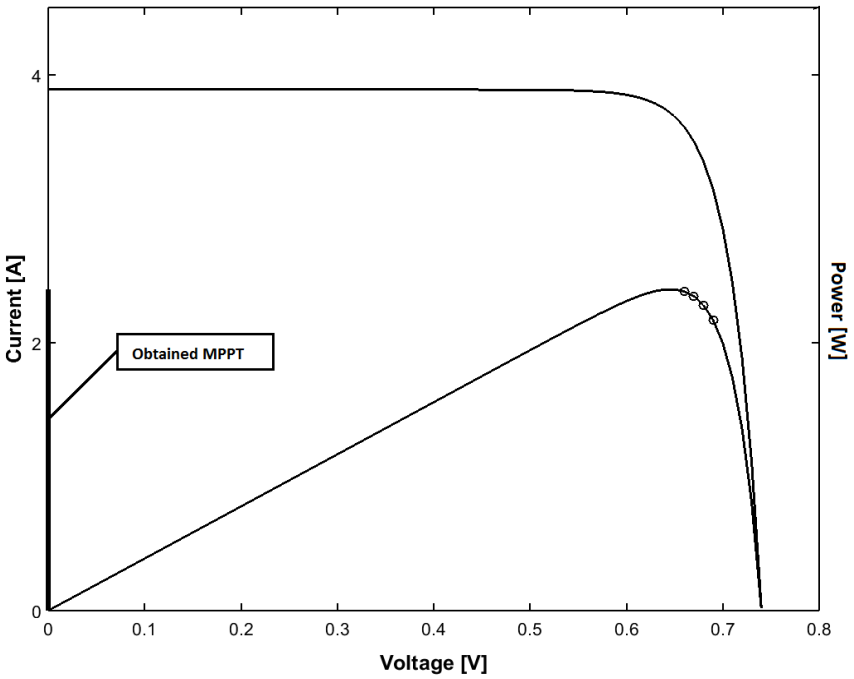

Figure 4.32: Obtained MPPT from right side points.

In the above figure 4.32, we can see that the curve shows the MPP at 0. MPP at 0 is not possible.

The reason is that while we take all the samples from right side of the real MPP there is not any MPP point to catch. And, the samples are decreasing and there is no MPP point in front of the samples.

As it does not find any MPP point then it goes to 0. If we look at the roots of the polynom we see that there is imaginary number in the result. For this imaginary number it cannot reach any result for us thus it goes to 0. That's why for this case there is no result found.

In the next part we are going to see the same method but by changing samples position. We will see if we can find any MPP by changing the samples.

To avoid the problem what is explained in the previous part we considered three samples from right side but one sample from left side. The output result is shown below:

The obtained curve by non-iterative algorithm is presented in the figure 4.33.

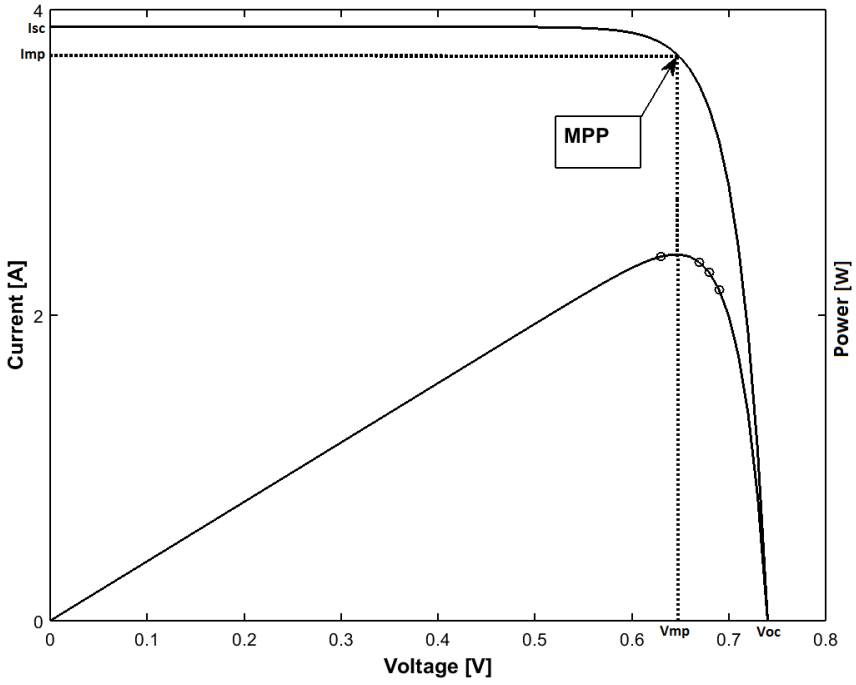

Figure 4.33: Obtained MPPT from modified right side points.

We used four samples and third order polynomial method for root finding and to reach the MPP. The samples are used from the industrial data. The three samples are taken from right side and one sample is taken from left side of the real MPP.

From the result we find that the value of voltage at maximum power point (V) is 0.6477 V and the current at maximum power point (Imp) is 3.7003 A. And, the obtained maximum power point at this stage is 2.3967 W.

If we compare with the real MPP and the MPP obtained by this method we find that the value of MPP is very close. There is no significant difference between both MPP in here.

In this part we will do the same observation but with the real measured data obtained from the photovoltaic module. The obtained curve from measured data is presented in the figure 4.34.

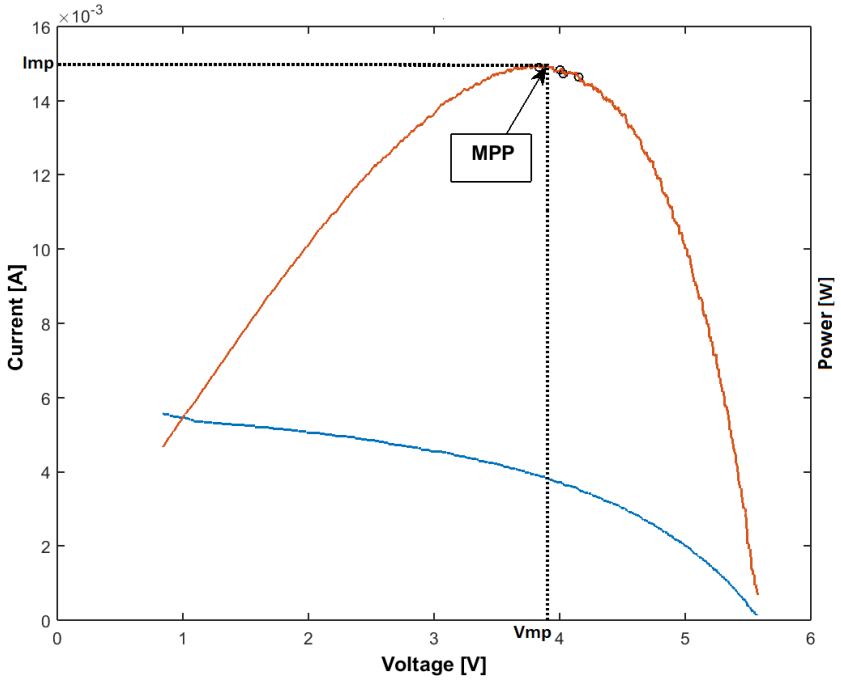

Figure 4.34: Obtained MPP from modified right side measured values.

The above figure shows the MPP curve obtained by using the non-iterative algorithm. The four samples are taken from measured data among them three are taken from the right side of MPP and another one is taken from left close side of MPP.

The obtained MPP by using this method is 0.0150 W. The voltage at maximum power point (Vmp) is 3.9030 V and the current at maximum power point (Imp) is 0.00384 A.

If we compare the result with the real MPP and the MPP obtained by this algorithm we find that the MPP is almost close in here. And, there is no significance difference between those two MPP.

We have analysed every possible cases in here by using our proposed algorithm though the development of this algorithm is going on. In future, we can find better solution with more precise output for MPPT finding non-iterative algorithm.

Chapter 5. CONCLUSION

Modelization and characterization are utterly important in solar photovoltaic systems. This work is composed of the analysis of PV module behaviour, its modeling, measurement and characterization. Curve fitting with noise analysis and a proposed non-iterative MPPT algorithm with simulation and experimental setup. Several articles, papers, books are studied related to that topic in order to get the closest and insight of the work.

Modeling of PV systems with solar cell technologies and working principles of solar cell is explained. The main purpose of modeling of PV cell/module is to predict and analyze the output behavior. Several types of semiconductor characteristics with classification are shown in details. A suitable PV cell model is considered for the characterization purpose after having a detailed examination of several models.

The model important parameters are photo current, cell temperature, diode ideality factor, diode reverse saturation current, and series resistance and shunt resistance. Different physical and mathematical models are investigated to forecast the accuracy of it. These models are analyzed to predict the power generated by monocrystalline PV panels. The studied physical models for analysis are PV cell ideal model, single diode simple model, single diode full model and the double diode model. It is found in the work that the single diode full model or five parameters model is more suitable as it is less complex, has high accuracy and has the capacity to simulate in a reasonable time.

The mathematical models for PV systems and corresponding determination methods were reviewed in detailed. In this study five parameters model was employed and solved the analytical and numerical methods leading to rapid convergence. The simulation and its results are obtained by MATLAB and the validation was carried out by comparing with the other related completed work.

PV cell's characteristics with parameters extraction are discussed. In the extraction procedure the impact of several parameters are also studied. Analysis of several parameters variation effects on the module are briefly implemented here. In that case, both external and internal parameters are considered with their effects on the cell output characteristics.

The current-voltage (I-V) and power-voltage (P-V) curve is obtained from generalized model by simulation. Among the external parameters the solar radiation variation effects and the cell temperature variation effects are studied.

For the variation of solar radiation it is found the increasing tendency of both I-V and P-V curve while it increases the irradiance level. That results in the increase of power output too. It also happens the opposite while the solar radiation is decreased. Another considered external parameter is cell temperature and it has significant impact on the PV cell/module. With the cell temperature increase there is decrease in I-V and P-V curve which results decrease in output power.

The other considered internal parameters are series resistance, shunt resistance, diode ideality factor and diode reverse saturation current. Series resistance increasing has negative impact on the PV cell that is decrease in power output. On the other side, the shunt resistance has positive impact on the PV cell. If the value of shunt resistance increases the I-V and P-V curve increases too which results increase in the power output. The increase of diode reverse saturation current value results the decrease in the output power of the cell. Another important model parameter is the diode ideality factor which has positive impact on the solar cell with its incremental value. It is seen that while we raise the ideality factor´s values from low to high then it increases the power output. And if we do the opposite then the power output reduces. The modelization proposed in this work can predict the power generated by PV panels with high accuracy.

In chapter 3 all the parameters variation effects are shown with the detailed analysis. The overall discussion is presented here is not shown in any other previous work. Another numerical method and parameters variation is shown to compare with the used method. No significant difference is found except in the optimization of convergence.

A simulink model with fixed power consumption analysis is shown. The generated I-V and P-V curve by simulink model has the similar characteristics of the curve obtained in the MATLAB model.

Measurement with data acquisition system (DAQ) is used. An experiment in laboratory environment is performed. The obtained curve without light and with light has difference in characteristics. The output curve from experiment can be used of the analysis of PV cell/module. Two sets of experimental data are considered to obtain I-V and P-V curve. The comparison between two I-V and P-V curve is also shown.

Noise effects on PV module and its related output characteristics are analysed. Both simulated and experimental data are used to observe the noise effects on the I-V and P-V curves. Two different percentages of noise are considered for the observation. Noise analysis is the implementation of practical I-V and P-V curve which can help us in better instrumentation. The noised data acquired by simulation and experimentation has no difference actually except in the characteristics.

Approximation of curve fitting with several polynomial methods is implemented for both simulated and measured data. Fourth and eighth order polynomial algorithm is used to fit the curve. The purpose is to fit the curve with a set of measured and simulated I-V and P-V values. In the fourth order polynomial I-V and P-V curve with simulated data has more deviation compared with the ideal curve. On the other hand, the curve obtained by measured data has not that significant deviation.

A non-iterative maximum power point tracking (MPPT) algorithm is proposed in order to track the maximum power point (MPP) of PV module output. Several tracking methods are performed to track MPP in this algorithm. The algorithm is tested for both simulated and measured data. The accuracy of the algorithm is very high in compare to other algorithm.

It can be concluded that the main contribution of this dissertation is the contribution in solar photovoltaic technology through characterizing and modelizing of PV module. It also includes the choice of better instrumentation which can give the appropriate choice of instruments. Furthermore, some modifications were made in order to reduce the complexity of the work which can be improved in the future work.

Optimization of photovoltaic panels requires high cost instrumentation devices and tools. The conception and modelization of a lost cost and high performance digital instrument with real time characterization will be the focus of future work. This dissertation will enable to help in producing high performance photovoltaic instrument in future.

Bibliography

[1] M. Zeman. Introduction to Photovoltaic Solar Energy, Delf University.

[2] "Global Energy Statistical Yearbook". Enerdata, Paris, 2016.

[3] B.Sai Pranahita, A. Sai Kumar, A. P. Babu. "A study on modelling and simlation of photovoltaic cells," *International Journal of Research in Engineering and Technology,* vol. 3, no. 11, pp. 2319-1163, Nov 2014.

[4] "China Tops Tables fro Renewables Investment". International Energy Partnership, Washington D.C. , 2013.

[5] "Renewables 2016: Global Status Report," REN 21, Paris, 2016.

[6] Valerio Lo Brano, G. Ciulla, M. Di Falco. "Artificial Neural Networks to Predict the Power Output of a PV Panel", *International Journal of Photoenergy,* vol. 2014, 2014.

[7] Tao Ma, H. Yang, L. Lu. "Solar photovoltaic system modeling and performance prediction", *Renewable and Sustainable Energy Reviews,* vol. 36, p. 304–315, 2014.

[8] D. Sera, "Real-time Modelling, Diagnostics and Optimised MPPT for Residental PV Systems", Aalborg Universitet, Aalborg, 2009.

[9] Tarek M. El-Sayed, F. H. Fahmy, A. E. A. Nafeh, H. K.M. Yousef. "PV Parameters Estimation using a Developed Iterative Method", *International Journal of Scientific Research Engineering Technology,* vol. 1, no. 1, pp. 2395-566X, Jan-2015.

[10] NCERT. "Semiconductor Electronics: Materials. Devices and Simple Circuits", NCERT.

[11] P. d. i. M. Zeman, "Semiconductor Materials For Solar cells", Open Education Consortium, Netherland, Feb 2016.

[12] Hu C.. "Electrons and Holes in Semiconductors," Feb 2009.

[13] W. Shockley, H. Queisser. "Detailed Balance Limit of Efficiency of p-n Junction Solar Cells", *Journal of Applied Physics,* vol. 32, no. 3, 1961.

[14] L.H. Lu. "Diodes" in *NTUEE Electronics*.

[15] H. Tian, F. M. David, K. Ellis, P. Jenkins. "A Detailed Performance Model for Photovoltaic Systems", *Solar Energy Journal,* pp. 5500-54601, 2012.

[16] G. M. Masters. Renewable and Efficient Electric Power Systems, Canada: JOHN WILEY & SONS,

INC., 2004.

[17] W. D. Soto, S. A. Klein, W. A. Beckman. "Improvement and validation of a model for photovoltaic array performance", *Solar Energy,* vol. 80, pp. 78-88, 2006.

[18] E.M.G. Rodrigues, E. Melicio, V.M.F Mendes, J.P.S Catalão. "Simulation of a solar cell considering single-diode equivalent circuit model", in *International Conference on Renewable Energies and Power Quality-ICREPQ'11*, PP. 1-5, Spain, 13-15 April 2011.

[19] A. Dolara, S. Leva, G. Manzolini. "Comparison of different physical models for PV power output prediction", *Solar Energy Elsevier,* vol. 119, pp. 83-99, September 2015.

[20] Md Tofael Ahmed, T. Gonçalves, Mo. Tlemçani. "Single Diode Model Parameters Analysis of Photovoltaic Cell", in *5th International Conference on Renewable Energy Research and Applications (ICRERA 2016)*, Birmingham, 2016.

[21] T. Salmi, M. Bouzguenda, A. Gastli, A. Masmoudi. "MATLAB/Simulink Based Modelling of Solar Photovoltaic Cell", *INTERNATIONAL JOURNAL of RENEWABLE ENERGY RESEARCH,* vol. 2, no. 2, 2012.

[22] Md Tofael Ahmed, T. Gonçalves, M. Tlemçani. "Different Parameters Variation Analysis of a PV Cell". in *International Conference for Students on Applied Engineering (ICSAE 2016)*, Newcastle, 2016.

[23] D. Sera, R. Teodorescu, P. Rodriguez. "PV panel model based on datasheet values", in *IEEE Xplore digital Library*.

[24] D. M. Tobnaghi, D. Naderi. "The Effect of Solar Radiation and Temperature on Solar cells Performance", *Extensive Journal of Applied Sciences,* vol. 3, no. 2, pp. 39-43, 2015.

[25] M. S. Salim, J. M. Najim, S. M. Salih. "Practical Evaluation of Solar Irradiance Effect on PV Performance", *Energy Science and Technology,* vol. 6, no. 2, pp. 36-40, 2013.

[26] M. N. Islam, M. Z. Rahman, S. M. Mominuzzaman. "The Effect of Irradiation on Different Parameters of Monocrystalline Photovoltaic Solar Cell", in *2014 3rd International Conference on the Developments in Renewable Energy Technology (ICDRET)*, Dhaka, 2014.

[27] R. Chenni, M. Makhçouf, T. Kerbache, A. Bouzid. "A detailed modeling method for photovoltaic cells", *Energy (Elsevier),* vol. 32, pp. 1724-1730, 2007.

[28] F. M. González-Longatt, "Model of Photovoltaic Module in Matlab™," in *2DO CONGRESO IBEROAMERICANO DE ESTUDIANTES DE INGENIERÍA ELÉCTRICA, ELECTRÓNICA Y COMPUTACIÓN (II CIBELEC 2005)*, 2005.

[29] K. Kachhiya, M. Lokhande, M. Patel. "MATLAB/Simulink Model of Solar PV Module and MPPT Algorithm", in *National Conference on Recent Trends in Engineering & Technology*, Gujrat, 2011.

[30] A. C. Foles, M. Tlemçani. "Convergence speed optimization of iterative methods for a Photovoltaic Cell simulation", in *Workshop On Earth Sciences*, Evora, 2016.

[31] Md Tofael Ahmed, T. Gonçalves, M. Tlemçani. "Noise Data Approximation and Curve Fitting of a PV cell", in *Workshop On Earth Sciences 2016*, Evora, 2016.

[32] T. Esram, P. L. Chapman, "Comparison of Photovoltaic Array Maximum Power Point Tracking Techniques", *IEEE TRANSACTIONS ON ENERGY CONVERSION,* vol. 22, no. 2, 2007.

[33] F.Z. Hamidon, P. D. Abd. Aziz, N. H, M. Yunus. "Photovoltaic Array Modelling with P&O MPPT Algorithm in MATLAB", in *Statistics in Science, Business, and Engineering (ICSSBE)*, Kedah, 2012.

[34] Md Tofael Ahmed, A. Albino, T. Gonçalves, M. Tlemçani. "Real Time Estimation of MPPT with Non-iterative Algorithm", in *The International conference on Advanced Materials for Photonics, Sensing and Energy AppliCAtions*, Agadir, 2017.

[35] G. Dzimano, "MODELING OF PHOTOVOLTAIC SYSTEMS," The Ohio State University, Columbus, 2008.

[36] Peter Y. Yu, Dres. h.c. Fundamentals of Semiconductors, Stuttgart: Springer, March 20110.

[37] V. Avrutin, N. Izyumskaya, H. Morkoç. "Semiconductor solar cells: Recent progress in terrestrial Applications", *Superlattices and Microstructures,* vol. 49, pp. 337-364, 2011.

[38] Zeman, "Solar Cell Operational Principles".

[39] R. U. d. Mayaguez, "Academicos," [Online]. Available: academic.uprm.edu/pcaceres/Courses/MatEng3045/EME5-1.pdf. [Accessed 06 February 2017].

[40] J. J. Rubin, "Julian's Science Experiments," June 2013. [Online]. [Accessed 22 February 2017].

[41] P. Hersch, H. Kenneth. "Basic Photovoltaic Principles and Methods", Technical Information Office , Colorado, 1982.

[42] "Emaze", [Online]. Available: https://www.emaze.com/. [Accessed 15 02 2017].

[43] "Phys Org", [Online]. Available: https://phys.org/news/2012-07-imec-industrial-level-silicon-solar-cells.html. [Accessed 20 02 2017].

[44] K. Jäger, O. Isabella, A. H. M. Smets, R. A. C. M. M. Swaaij, M. Seman. Solar Energy Fundamentals, Technology and Systems, Delft University of Technology, 2014.

[45] U. Eicker, Solar Technologies for Buildings, West Sussex: John Wiley & Sons Ltd, 2003.

[46] B. Mazhari, "An improved solar cell circuit model for organic solar cells," *Solar Energy Materials & Solar Cells,* vol. 90, pp. 1021-1033, 2006.

[47] M. Luque A. "Increasing the efficiency of ideal solar cells by photon induced transitions at intermediate levels", *Phys Rev Lett,* vol. 78, p. 5014–7, 1997.

[48] L. han, N. Koide, Y. Chiba, A. Islam, T. Mitate. "Modeling of an equivalent circuit for dye-sensitized solar cells", *Applied Physics Letters,* vol. 84, no. 13, p. 10.1063/1.1690495, March, 2004.

[49] S. Shrivastava, A. R. Saxena, A. K. Wadhwani. "MPPT Based Optimization of Photovoltaic System Using DC-DC Converter", *International Journal of Hybrid Information Technology,* vol. 8, no. 10, pp. 101-114, October 2015.

[50] D.S.H. Chan, J.C.H. Phang. "Analytical methods for the extraction of solar-cell single- and double-diode model parameters from I-V characteristics", *IEEE Transactions on Electron Devices,* vol. 34, no. 2, p. 286–293, March 1987.

[51] S. H. Antonio Luque, Handbook of Photovoltaic Science and Engineering, West Sussex: John Wiley & Sons Ltd, 2003.

[52] S. B. Dongue D. Njomo, J. G. Tamba, L. Ebengai. "Modeling of electrical response of illuminated crystalline photovoltaic modules using four- and five-parameter models", *International Journal of Emerging Technology and Advanced Engineering,* vol. 2, no. 11, pp. 2250-2459, November 2012.

[53] A. N. Celik, N. Acikgoz. "Modelling and experimental verification of the operating current of mono-crystalline photovoltaic modules using four- and five-parameter models", *Applied Energy,* vol. 84, pp. 1-15, January 2007.

[54] M. Karamirad, M. Omid, R. Alimardani, H. Mousazadeh, S. N. Heidari. "ANN based simulation and experimental verification of analytical four-and five-parameters models of PV modules", *Simulation Modelling Practice and Theory ,* vol. 34, pp. 86-98, May 2013.

[55] L. Fialho, R. Melicio, V.M.F. Mendes. "PV System Modeling by Five Parameters and in Situ Test," in *International Symposium on Power Electronics, Electrical Drives, Automation and Motion-SPEEDAM*, pp. 573-578, Ischia, Italy, 18-20 June, 2014.

[56] R.S. Anjos, R. Melicio, V.M.F. Mendes, H.M.I. Pousinho. "Crystalline Silicon PV Module under Effect of Shading Simulation of the Hot-Spot Condition", *Technological Innovation for Smart System, Springer,* pp. 479-487, May, 2017.

[57] J.A. Gow, C.D. Manning. "Development of a photovoltaic array model for use in power-electronics simulation studies", *IEE Proceedings - Electric Power Applications,* vol. 146, no. 2, pp. 193-200, April 1999.

[58] W. Shockley, "The theory of p-n junctions in semiconductors and p-n junction transistors," *Bell System Technical Journal,* vol. 28, p. 435–89, 1949.

[59] Md Tofael Ahmed, T. Gonçalves, M. Tlemçani. "Single Diode Model Parameters Analysis of photovoltaic cell" in *ICRERA 2016*, Birmingham, 2016.

[60] S. Lineykin, M. Averbukh, A. Kuperman. "Five-Parameter Model of Photovoltaic Cell Based on STC Data and Dimensionless", in *Electrical & Electronics Engineers in Israel (IEEEI)*, Eilat, 2012.

[61] H. Tsai, T. Cu-Siang, S. Yi-Jie. "Development of Generalized Photovoltaic Model Using MATLAB/SIMULINK", in *World Congress on Engineering and Computer Science 2008*, San Francisco, 2008.

[62] M. AZZOUZI, M. Stork. "MODELING AND SIMULATION OF A PHOTOVOLTAIC CELL CONSIDERING SINGLE-DIODE MODEL", *International Journal of Research in Engineering & Technology (IMPACT : IJRET),* vol. 2, no. 11, pp. 19-28, 2015.

[63] M. S. Hossain, N. K. Roy, Md. O. Ali. "Modeling of Solar Photovoltaic System Using MATLAB/Simulink", in *19th International Conference on Computer and Information Technology*, Dhaka, 2016.

[64] "Data Acquisition," [Online]. Available: http://www.ni.com/data-acquisition/what-is/.

[65] W. ABD EL-BASIT, A. M. ABD. El-Maksood, F. Abd. E. S. Soliman. "Mathematical Model for Photovoltaic Cells", *Leonardo Journal of Sciences,* pp. 13-28, 2013.

Annex I: List of Publications

Conferences

1. Conference Name:

5th Anniversary of ANSOLE (2011-2016): International Conference on Renewable Energy (INCORE2016) 3-6 February 2016, Sharm El-Sheikh, Egypt

Paper Name and Authors:

"Analysis of Five Parameters model of Photovoltaic cells**"**

Md Tofael Ahmed, Teresa Gonçalves and Mouhaydine Tlemcani

2. Conference Name:

International Conference for Students on Applied Engineering (ICSAE 2016), Newcastle, United Kingdom: 20th – 21st October 2016 at Great North Museum: Hancock, UK.

Paper Name and Authors:

"Different Parameters Variation Analysis of a PV Cell"

Md Tofael Ahmed, Teresa Gonçalves, Andre Albino, Masud Rana Rashel, Angela Veiga and Mouhaydine Tlemcani

DOI**:** 10.1109/ICSAE.2016.7810183

3. Conference Name:

5th International Conference on Renewable Energy Research and Applications (ICRERA 2016)

20th – 23rd November 2016, The National Exhibition Centre, Birmingham.

Paper Name and Authors:

"Single Diode Model Parameters Analysis of Photovoltaic Cell"

Md Tofael Ahmed, Teresa Gonçalves and Mouhaydine Tlemcani

DOI**:** 10.1109/ICRERA.2016.7884368

4. Conference Name:

International Conference for Students on Applied Engineering (ICSAE 2016), Newcastle, United Kingdom: 20th – 21st October 2016 at Great North Museum: Hancock, UK.

Paper Name and Authors:

"Comparison of Photovoltaic panel's standard and simplified models**"**

Masud Rana Rashel, Teresa Gonçalves, Andre Albino, Md Tofael Ahmed, Angela Veiga and Mouhaydine Tlemcani

DOI: 10.1109/ICSAE.2016.7810175

5. Conference Name:

International conference on Advanced Materials for Photonics, Sensing and Energy AppliCAtions (AMPSECA' 2017): 28th – 30th March 2017 at Palais des Roses Hotel, Agadir, Morocco organized by Moroccan Society of Advanced Materials Physics and their Applications (SMPM2A)

Paper Name and Authors:

"Real Time Estimation of MPPT with Non-iterative Algorithm"

Md Tofael Ahmed, André Albino,Teresa Gonçalves and Mouhaydine Tlemçani

Workshops

1. Name:

THE FIRST INTERNATIONAL WORKSHOP ON SUSTAINABILITY AND GREEN TECHNOLOGY

Co-located with the 1st European gLINK project meeting

13th January 2016, Bali, Indonesia

Paper Name and Authors:

"Conception and Characterization of Photovoltaic Cells"

Teresa Gonçalves, Md Tofael Ahmed, Masud Rana Rashel, Mouhaydine Tlemcani

2. Name:

Workshop On Earth Sciences 2016

ICT, University of Evora,

8-10 December 2016, Evora, Portugal

Paper Name and Authors:

"Noise data approximation and curve fitting of a PV cell"

Md Tofael Ahmed, Teresa Gonçalves and Mouhaydine Tlemcani

3. Name: 2nd International Workshop on Sustainability and Green Technologies

Held in conjunction with 3rd European EMA 2 gLINK Project Meeting, March 6-8, 2017

Danang, Vietnam

Paper Name and Authors:

"Analysis of noise with curve fitting method of a PV cell"

Md Tofael Ahmed, Teresa Gonçalves and Mouhaydine Tlemcani

*Invite to submit on the journal European Alliance for Innovation (EAI).